PRECLINICAL AND CLINICAL TARGETING OF INFLAMMATORY MEDIATORS IN TRIPLE NEGATIVE BREAST CANCER

A Dissertation

by

ANDREW CHUNG

Submitted to the Graduate and Professional School of
Texas A&M University
in partial fulfillment of the requirements for the degree of

DOCTOR OF PHILOSOPHY

Chair of Committee,	David Huston
Co-Chair of Committee,	Jenny Chang
Committee Members,	Ping-Ying Pan
	David Wink
Head of Program,	Van Wilson

May 2023

Major Subject: Medical Sciences

ABSTRACT

The incidence of breast cancer is the number one cause of cancer in women globally. Due to the complex heterogeneous diversity of this disease, certain classifications of breast cancer have developed targeted therapeutic strategies whereas other breast cancer classifications still remain without any effective therapies. Triple negative breast cancer (TNBC) is a pathology that currently relies on conventional chemotherapy and has historical poor prognosis due to chemo-resistance, distant metastasis, and patient relapse. This dissertation focuses on the results of preclinical and clinical studies inhibiting inflammatory mediators propagating chemo-resistance in TNBC. Previous work by our lab and others have established that IL-6 and inducible nitric oxide synthase (iNOS) are utilized by TNBC to resist chemotherapy by inducing cancer stem cells, cancer proliferation and metastasis. Clinical trials targeting IL-6 has not been thoroughly investigated in the context of breast cancer and previously it is not yet known which patients would benefit from anti IL-6 therapy. In experiment 1, we found that a specific molecular subtype of TNBC resisted chemotherapy by mitogen-activated protein kinase (MAPK) induced autocrine IL-6. In contrast, a different TNBC subtype had no MAPK activation following chemotherapy, which led to unaltered IL-6 production. Utilizing TNBC xenografts in female mouse models, we investigated the efficacy of tocilizumab, anti-IL-6R antagonist. Tocilizumab combined with chemotherapy provided significant tumor growth reduction compared to chemotherapy alone in mice with MAPK active TNBC xenografts. Conversely, the combinational regimen provided no benefit in mice with MAPK inactive TNBC xenografts. Our lab has previously investigated the durability of an iNOS inhibitor decreasing TNBC burden in mice xenograft studies. In experiment 2, we investigated a phase I/II trial on the safety and efficacy of the iNOS inhibitor in TNBC patients with local advanced or metastatic

disease. The inhibitor was well tolerated, and the objective response rate was 81.8% for local advanced patients and 15.4% for metastatic patients. We also observed that 86% of patients with progressive disease had detectable IL-6 in sera through two courses of iNOS therapy which may give rationale for exploring the efficacy of tocilizumab in combination with iNOS inhibition in future clinical trials.

DEDICATION

I dedicate this work to my mother, Candice, for her never ending love and support.

ACKNOWLEDGEMENTS

I would like to thank my committee chair, Dr. David Huston, and my committee members, Dr. Jenny Chang, Dr. Ping-Ying Pan, and Dr. David Wink, for their mentorship and dedication to my growth as a scientist. To my mentor, Dr. Chang, your mentorship and leadership made my graduate training possible and I am forever grateful. I would also like to thank the support and feedback from Dr. Chang's lab: Dr. Roberto Rosato, Anthony Kozielski, Wei Qian, Jianying Zhou, Ann Anselme. To Dr. Delphine Lee, you are my first mentor who got me started on my path as a physician scientist. Your mentorship and friendship will always be treasured. I would also like to thank Alfred Chan, from Dr. Lee's lab. I am also grateful for Dr. Pan and his lab for their support: Dr. Yitian Xu, Dr. Licheng Zhang.

My journey would not have been possible without the Texas A&M MD PhD program. A tremendous thank you to our program leadership: Dr. Julian Leibowitz and Dr. Carolyn Cannon.

I also like to thank my friends in the MD PhD program and back home in California for their never-ending support. Lastly, I wish to thank my entire family, especially my mother, for their never ending love.

CONTRIBUTORS AND FUNDING SOURCES

This work was supervised by a dissertation committee consisting of chair Dr. David Huston of the Texas A&M College of Medicine Department of Microbial Pathogenesis & Immunology; co-chair and advisor Dr. Jenny Chang of Houston Methodist Cancer Center; Dr. Ping-Ying Pan of Houston Methodist Cancer Center; and Dr. David Wink of the National Cancer Institute.

Data presented in Figures 2-1 A-C; 2-2A; 2-2C were analyzed by Dr. Delphine Lee and Alfred Chan at The Lundquist Institute, Torrance, Ca. Establishment of human tumor xenografts in live animal studies in data presented in Figures 2-11 C-E were assisted by Anthony Kozielski, Wei Qian, and Jianying Zhou of Houston Methodist Cancer Center. Data presented in Figure 2-12C was analyzed by Ann Anselme of Houston Methodist Cancer Center. Data presented in Figure 3-2 B-E was analyzed by Dr. Joe Ensor of Houston Methodist Cancer Center. Data presented in Figure 3-3 was analyzed by Dr. Kartik Anand of Houston Methodist Cancer Center. Data presented in Figure 3-4 were analyzed by Dr. Jenny Chang and Dr. Joe Ensor of Houston Methodist Cancer Center. Data presented in Figure 3-5 were analyzed by Dr. Jenny Chang of Houston Methodist Cancer Center and Dr. Mary Schwartz of Houston Methodist Department of Pathology. Data presented in Figures 3-6B and 3-7B were analyzed by Dr. Licheng Zhang of Houston Methodist Cancer Center. Data presented in figures 3-8, 3-9, 3-10 were analyzed by Dr. Licheng Zhang, Dr. Yitian Xu, Dr. Ping-Ying Pan, and Dr. Shu-Hsia Chen of Houston Methodist Cancer Center. For data shown in figures 3-11

and 3-12, technical assistance was given by Wei Qian of Houston Methodist Cancer Center.

All other work in the dissertation was completed by the student independently.

Funding Sources

This study was sponsored by the National Cancer Institute, Breast Cancer Research Foundation, the Moran Foundation, Causes for a Cure, and the Center for Drug Repositioning and Development Program awarded to Dr. Jenny Chang.

TABLE OF CONTENTS

Page

LIST OF FIGURES

Page

LIST OF TABLES

Page

1. INTRODUCTION

1.1. Introduction to Triple Negative Breast Cancer

Triple negative breast cancers (TNBC) account for 15-20% of all breast cancer cases and approximately one million new TNBC cases are diagnosed globally (*1*). Unfortunately, TNBC patients will not benefit from endocrine and growth factor receptor neutralizing therapies as they are receptor independent cancer cells. Because TNBC lacks any targeted therapies, the current standard of care is chemotherapy. TNBC remains a very difficult to treat cancer as they are chemotherapy-resistant, and most patients develop recurrence or distant metastasis (*2*). Indeed, metastatic TNBC patients have a grim overall survival of 9-12 months undergoing conventional therapies (*3*). Furthermore, the heterogeneity of TNBC results in numerous chemo-resistance pathways that are not yet fully delineated. This necessitates ongoing research to elucidate the cellular biology of TNBC to develop novel therapeutics to improve patient survival.

Previous molecular signaling pathway investigations by others identified that TNBC can be subdivided into distinct subtypes based on gene expression signatures (*4*); this TNBC subtyping model has been validated by an independent group (*5*). The basal-like 1 (BL1) subtype had genes enriched in cell cycle and division (*4*), and TNBC patients with BL1 tumors achieved the best pathologic complete response (pCR) rates (*5, 6*). In contrast, the mesenchymal stem-like (MSL) subtype had gene enrichment in hallmark cancer pathways: metastasis, angiogenesis, and stem cell (*4*). The MSL subtype also had genes enriched in the NF-kB pathway, but the relevance of this inflammatory pathway was not investigated (*4*). Moreover, patients with the MSL subtype achieved one of the worst clinical pCR rates (*5, 6*). Although this TNBC subtyping method is reproducible and early studies show that BL1 tumors are susceptible to antineoplastic agents, it is not yet clear what resistance mechanisms are utilized by MSL tumors in response to chemotherapy. Therefore, elucidating MSL chemo-resistance mechanisms

will allow integration of targeted therapies aimed to neutralize unique MSL pathways to complement conventional therapy.

The literature reports that numerous inflammatory cytokines have been shown to activate pro-tumor pathways in various cancers (*7-11*). It has also been established that various chemotherapy regimens correlate with elevated cytokine levels in cancer patients (*12-14*). Therefore, it is plausible that the resulting chemotherapy associated inflammatory cytokines may promote resistance mechanism in TNBC cells. Our lab has previously investigated that TNBCs rely on a tumor-produced inflammatory molecule (nitric oxide) to counter the efficacy of docetaxel, a frontline chemotherapy agent for TNBC (*15, 16*). It is thus possible that TNBCs may synthesize other inflammatory mediators to abrogate the effect of docetaxel. Given that MSL TNBC had gene enrichment in the inflammatory NF-kB pathway, we hypothesized that MSL TNBCs may resist docetaxel therapy with self-induced proinflammatory cytokines.
The paradigm of cancer cells producing autocrine inflammatory mediators has already been established in the literature. Indeed, several inflammatory products have been elucidated as cancer-promoting factors in the tumor microenvironment. To summarize, we begin our discussion with IL-6, a classical activator of the STAT3 pathway (*17-20*). IL-6/STAT3 activity has been reported to drive cancer stem cell induction, metastasis, and cancer cell proliferation. Abrogation of IL-6 in vitro led to increased TNBC cell death by chemotherapy as well as suppressed tumor growth in live animal models (*17*). These findings have been repeated by others and preliminary data suggests a rationale for targeting IL-6 in TNBC pre-clinical models (*21, 22*). Despite these advancements, the literature thus far does not provide any context into which TNBC patients may be the prime candidates for IL-6 targeted therapy.

GM-CSF is another cytokine that promotes a pro-tumor role in the tumor microenvironment. GM-CSF is widely provided as an immune adjuvant in cancer clinical trials (*23*) to activate antigen presenting cells and promote cell mediated immunity against tumors. However, there is growing literature that this immune stimulating cytokine can promote cancer cell proliferation and metastasis (*24, 25*). Although there is scientific reasoning to provide GM-CSF as an immune adjuvant, the possibility that this cytokine can directly stimulate cancer cells highlights the paramount importance of understanding the direct consequence of inflammatory mediators on the cancer target cells.

COX-2 has been established as a pro-tumor inflammatory mediator for several decades. COX-2 and its main metabolite, PGE2, have been found to correlate with poor prognoses in cancer and hypothesized to promote cancer proliferation and metastasis (*26-28*). In support, others have provided pre-clinical context for COX-2 inhibition therapy by decreased tumor growth in animal models (*29, 30*). Despite the clear evidence to target tumor derived COX-2, clinical trials investigating COX-2 inhibitors have been largely disappointing with no evidence of patient benefit (*31, 32*). This phenomenon could be explained by several hypotheses. Firstly, it could be rationalized that COX-2 inhibition would provide greatest benefit to patients with high COX-2 expressing tumors and modest to little benefit for patients with COX-2 independent tumors. Therefore, it would be of interest to perform retrospective analysis of patient biopsy samples to determine whether any benefit can be correlated based on COX-2 expression levels prior to therapy. Secondly, due to the plasticity of cancer cells, it may be possible that even with 100% neutralization of tumor derived COX-2, there may be other COX-independent pathways cancer cells may utilize to drive proliferation and metastasis.

NOS2 has been demonstrated to promote tumor progression in melanoma, glioma and various other cancers (*33-35*). Our lab and others have also demonstrated that TNBC utilize NOS2 by nitrosylating mediators of signaling pathways to promote chemo-resistance (*15, 29*). By utilizing a NOS2 inhibitor, L-NMMA, our previous study found that L-NMMA promoted endoplasmic reticulum stress and synergized with docetaxel to promote TNBC cell death. Our studies have consistently found that L-NMMA provided durable benefit in mice models with TNBC xenograft studies (*15, 16*). We therefore hypothesized whether L-NMMA may provide benefit to patients at a clinical level and initiated a phase I safety and phase II dose efficacy study.

In summary, this dissertation will examine the pre-clinical benefit of IL-6 targeted therapy against a specific molecular subtype of TNBC. This experiment will highlight the underlying pathway responsible for docetaxel induced autocrine IL-6 production and anti-IL-6 efficacy study with animal models of TNBC xenografts. Furthermore, this dissertation will also examine the clinical benefit of L-NMMA targeted therapy for TNBC patients. In closing, we will discuss future applications of translating targeted IL-6 therapy for clinical applications.

1.2. References

1. H. Yao, G. He, S. Yan, C. Chen, L. Song, T. J. Rosol, X. Deng, Triple-negative breast cancer: is there a treatment on the horizon? *Oncotarget* **8**, 1913-1924 (2017).
2. J. Collignon, L. Lousberg, H. Schroeder, G. Jerusalem, Triple-negative breast cancer: treatment challenges and solutions. *Breast Cancer (Dove Med Press)* **8**, 93-107 (2016).

3. P. Khosravi-Shahi, L. Cabezon-Gutierrez, S. Custodio-Cabello, Metastatic triple negative breast cancer: Optimizing treatment options, new and emerging targeted therapies. *Asia Pac J Clin Oncol* **14**, 32-39 (2018).

4. B. D. Lehmann, J. A. Bauer, X. Chen, M. E. Sanders, A. B. Chakravarthy, Y. Shyr, J. A. Pietenpol, Identification of human triple-negative breast cancer subtypes and preclinical models for selection of targeted therapies. *J Clin Invest* **121**, 2750-2767 (2011).

5. H. Masuda, K. A. Baggerly, Y. Wang, Y. Zhang, A. M. Gonzalez-Angulo, F. Meric-Bernstam, V. Valero, B. D. Lehmann, J. A. Pietenpol, G. N. Hortobagyi, W. F. Symmans, N. T. Ueno, Differential response to neoadjuvant chemotherapy among 7 triple-negative breast cancer molecular subtypes. *Clin Cancer Res* **19**, 5533-5540 (2013).

6. B. Jovanovic, I. A. Mayer, E. L. Mayer, V. G. Abramson, A. Bardia, M. E. Sanders, M. G. Kuba, M. V. Estrada, J. S. Beeler, T. M. Shaver, K. C. Johnson, V. Sanchez, J. M. Rosenbluth, P. M. Dillon, A. Forero-Torres, J. C. Chang, I. M. Meszoely, A. M. Grau, B. D. Lehmann, Y. Shyr, Q. Sheng, S. C. Chen, C. L. Arteaga, J. A. Pietenpol, A Randomized Phase II Neoadjuvant Study of Cisplatin, Paclitaxel With or Without Everolimus in Patients with Stage II/III Triple-Negative Breast Cancer (TNBC): Responses and Long-term Outcome Correlated with Increased Frequency of DNA Damage Response Gene Mutations, TNBC Subtype, AR Status, and Ki67. *Clin Cancer Res* **23**, 4035-4045 (2017).

7. F. Wu, J. Xu, Q. Huang, J. Han, L. Duan, J. Fan, Z. Lv, M. Guo, G. Hu, L. Chen, S. Zhang, X. Tao, W. Ma, Y. Jin, The Role of Interleukin-17 in Lung Cancer. *Mediators Inflamm* **2016**, 8494079 (2016).

8. L. M. Snell, T. L. McGaha, D. G. Brooks, Type I Interferon in Chronic Virus Infection and Cancer. *Trends Immunol* **38**, 542-557 (2017).

9. P. Ortiz-Montero, A. Londono-Vallejo, J. P. Vernot, Senescence-associated IL-6 and IL-8 cytokines induce a self- and cross-reinforced senescence/inflammatory milieu strengthening tumorigenic capabilities in the MCF-7 breast cancer cell line. *Cell Commun Signal* **15**, 17 (2017).

10. H. Kulbe, R. Thompson, J. L. Wilson, S. Robinson, T. Hagemann, R. Fatah, D. Gould, A. Ayhan, F. Balkwill, The inflammatory cytokine tumor necrosis factor-alpha generates an autocrine tumor-promoting network in epithelial ovarian cancer cells. *Cancer Res* **67**, 585-592 (2007).

11. A. S. Khazali, A. M. Clark, A. Wells, Inflammatory cytokine IL-8/CXCL8 promotes tumour escape from hepatocyte-induced dormancy. *Br J Cancer* **118**, 566-576 (2018).

12. L. Pusztai, T. R. Mendoza, J. M. Reuben, M. M. Martinez, J. S. Willey, J. Lara, A. Syed, H. A. Fritsche, E. Bruera, D. Booser, V. Valero, B. Arun, N. Ibrahim, E. Rivera, M. Royce, C. S. Cleeland, G. N. Hortobagyi, Changes in plasma levels of inflammatory cytokines in response to paclitaxel chemotherapy. *Cytokine* **25**, 94-102 (2004).

13. T. Eyob, T. Ng, R. Chan, A. Chan, Impact of chemotherapy on cancer-related fatigue and cytokines in 1312 patients: a systematic review of quantitative studies. *Curr Opin Support Palliat Care* **10**, 165-179 (2016).

14. J. A. Boyette-Davis, E. T. Walters, P. M. Dougherty, Mechanisms involved in the development of chemotherapy-induced neuropathy. *Pain Manag* **5**, 285-296 (2015).

15. D. Davila-Gonzalez, D. S. Choi, R. R. Rosato, S. M. Granados-Principal, J. G. Kuhn, W. F. Li, W. Qian, W. Chen, A. J. Kozielski, H. Wong, B. Dave, J. C. Chang,

Pharmacological Inhibition of NOS Activates ASK1/JNK Pathway Augmenting Docetaxel-Mediated Apoptosis in Triple-Negative Breast Cancer. *Clin Cancer Res* **24**, 1152-1162 (2018).

16. S. Granados-Principal, Y. Liu, M. L. Guevara, E. Blanco, D. S. Choi, W. Qian, T. Patel, A. A. Rodriguez, J. Cusimano, H. L. Weiss, H. Zhao, M. D. Landis, B. Dave, S. S. Gross, J. C. Chang, Inhibition of iNOS as a novel effective targeted therapy against triple-negative breast cancer. *Breast Cancer Res* **17**, 25 (2015).
17. Z. C. Hartman, G. M. Poage, P. den Hollander, A. Tsimelzon, J. Hill, N. Panupinthu, Y. Zhang, A. Mazumdar, S. G. Hilsenbeck, G. B. Mills, P. H. Brown, Growth of triple-negative breast cancer cells relies upon coordinate autocrine expression of the proinflammatory cytokines IL-6 and IL-8. *Cancer Res* **73**, 3470-3480 (2013).
18. E. J. Hillmer, H. Zhang, H. S. Li, S. S. Watowich, STAT3 signaling in immunity. *Cytokine Growth Factor Rev* **31**, 1-15 (2016).
19. D. E. Johnson, R. A. O'Keefe, J. R. Grandis, Targeting the IL-6/JAK/STAT3 signalling axis in cancer. *Nat Rev Clin Oncol* **15**, 234-248 (2018).
20. Z. Zhong, Z. Wen, J. E. Darnell, Jr., Stat3: a STAT family member activated by tyrosine phosphorylation in response to epidermal growth factor and interleukin-6. *Science* **264**, 95-98 (1994).
21. N. N. Alraouji, F. H. Al-Mohanna, H. Ghebeh, M. Arafah, R. Almeer, T. Al-Tweigeri, A. Aboussekhra, Tocilizumab potentiates cisplatin cytotoxicity and targets cancer stem cells in triple-negative breast cancer. *Mol Carcinog* **59**, 1041-1051 (2020).
22. D. Wang, J. Xu, B. Liu, X. He, L. Zhou, X. Hu, F. Qiao, A. Zhang, X. Xu, H. Zhang, M. S. Wicha, L. Zhang, Z. M. Shao, S. Liu, IL6 blockade potentiates the anti-tumor effects

of gamma-secretase inhibitors in Notch3-expressing breast cancer. *Cell Death Differ* **25**, 330-339 (2018).

23. S. Dai, D. Wei, Z. Wu, X. Zhou, X. Wei, H. Huang, G. Li, Phase I clinical trial of autologous ascites-derived exosomes combined with GM-CSF for colorectal cancer. *Mol Ther* **16**, 782-790 (2008).

24. I. S. Hong, Stimulatory versus suppressive effects of GM-CSF on tumor progression in multiple cancer types. *Exp Mol Med* **48**, e242 (2016).

25. S. Su, Q. Liu, J. Chen, J. Chen, F. Chen, C. He, D. Huang, W. Wu, L. Lin, W. Huang, J. Zhang, X. Cui, F. Zheng, H. Li, H. Yao, F. Su, E. Song, A positive feedback loop between mesenchymal-like cancer cells and macrophages is essential to breast cancer metastasis. *Cancer Cell* **25**, 605-620 (2014).

26. N. Hashemi Goradel, M. Najafi, E. Salehi, B. Farhood, K. Mortezaee, Cyclooxygenase-2 in cancer: A review. *J Cell Physiol* **234**, 5683-5699 (2019).

27. H. J. Hugo, C. Saunders, R. G. Ramsay, E. W. Thompson, New Insights on COX-2 in Chronic Inflammation Driving Breast Cancer Growth and Metastasis. *J Mammary Gland Biol Neoplasia* **20**, 109-119 (2015).

28. R. Solanki, N. Agrawal, M. Ansari, S. Jain, A. Jindal, COX-2 Expression in Breast Carcinoma with Correlation to Clinicopathological Parameters. *Asian Pac J Cancer Prev* **19**, 1971-1975 (2018).

29. D. Basudhar, S. A. Glynn, M. Greer, V. Somasundaram, J. H. No, D. A. Scheiblin, P. Garrido, W. F. Heinz, A. E. Ryan, J. M. Weiss, R. Y. S. Cheng, L. A. Ridnour, S. J. Lockett, D. W. McVicar, S. Ambs, D. A. Wink, Coexpression of NOS2 and COX2

accelerates tumor growth and reduces survival in estrogen receptor-negative breast cancer. *Proc Natl Acad Sci U S A* **114**, 13030-13035 (2017).

30. E. Bonavita, C. P. Bromley, G. Jonsson, V. S. Pelly, S. Sahoo, K. Walwyn-Brown, S. Mensurado, A. Moeini, E. Flanagan, C. R. Bell, S. C. Chiang, C. P. Chikkanna-Gowda, N. Rogers, B. Silva-Santos, S. Jaillon, A. Mantovani, E. S. C. Reis, N. Guerra, D. M. Davis, S. Zelenay, Antagonistic Inflammatory Phenotypes Dictate Tumor Fate and Response to Immune Checkpoint Blockade. *Immunity* **53**, 1215-1229 e1218 (2020).

31. S. Giacchetti, A. S. Hamy, S. Delaloge, E. Brain, F. Berger, B. Sigal-Zafrani, M. C. Mathieu, P. Bertheau, J. M. Guinebretiere, M. Saghatchian, F. Lerebours, C. Mazouni, O. Tembo, M. Espie, F. Reyal, M. Marty, B. Asselain, J. Y. Pierga, Long-term outcome of the REMAGUS 02 trial, a multicenter randomised phase II trial in locally advanced breast cancer patients treated with neoadjuvant chemotherapy with or without celecoxib or trastuzumab according to HER2 status. *Eur J Cancer* **75**, 323-332 (2017).

32. A. S. Hamy, S. Tury, X. Wang, J. Gao, J. Y. Pierga, S. Giacchetti, E. Brain, B. Pistilli, M. Marty, M. Espie, G. Benchimol, E. Laas, M. Lae, B. Asselain, B. Aouchiche, M. Edelman, F. Reyal, Celecoxib With Neoadjuvant Chemotherapy for Breast Cancer Might Worsen Outcomes Differentially by COX-2 Expression and ER Status: Exploratory Analysis of the REMAGUS02 Trial. *J Clin Oncol* **37**, 624-635 (2019).

33. E. Lopez-Rivera, P. Jayaraman, F. Parikh, M. A. Davies, S. Ekmekcioglu, S. Izadmehr, D. R. Milton, J. E. Chipuk, E. A. Grimm, Y. Estrada, J. Aguirre-Ghiso, A. G. Sikora, Inducible nitric oxide synthase drives mTOR pathway activation and proliferation of human melanoma by reversible nitrosylation of TSC2. *Cancer Res* **74**, 1067-1078 (2014).

34. P. Palumbo, F. Lombardi, G. Siragusa, S. R. Dehcordi, S. Luzzi, A. Cimini, M. G. Cifone, B. Cinque, Involvement of NOS2 Activity on Human Glioma Cell Growth, Clonogenic Potential, and Neurosphere Generation. *Int J Mol Sci* **19**, (2018).

35. D. D. Thomas, D. A. Wink, NOS2 as an Emergent Player in Progression of Cancer. *Antioxid Redox Signal* **26**, 963-965 (2017).

2. TOCILIZUMAB OVERCOMES CHEMOTHERAPY RESISTANCE IN MESENCHYMAL STEM-LIKE BREAST CANCER BY NEGATING AUTOCRINE IL-1A INDUCTION OF IL-6*

2.1. Abstract

Triple-negative breast cancer (TNBC) patients with mesenchymal stem-like (MSL) subtype have responded poorly to chemotherapy whereas patients with basal-like 1 (BL1) subtype achieved the best clinical response. In order to gain insight into pathways that may contribute to the divergent sensitivity to chemotherapy, we compared the inflammatory profile of the two TNBC subtypes treated with docetaxel. Cellular signaling analysis determined that docetaxel activated MAPK pathway in MSL TNBCs but not BL1 TNBCs. The subsequent MAPK pathway activation in MSL TNBCs led to an IL-1A mediated cascade of autocrine inflammatory mediators including IL-6. Utilizing the humanized IL-6R antibody, tocilizumab, our *in vitro* and *in vivo* data show that MSL TNBCs treated with tocilizumab together with chemotherapy results in delayed tumor progression compared to MSL TNBCs treated with docetaxel alone. Our study highlights a molecular subset of TNBC that may be responsive to tocilizumab therapy for potential translational impact.

2.2. Introduction

Triple-negative breast cancers (TNBC) account for 15-20% of all breast cancer cases and approximately one million new TNBC cases are diagnosed globally (*1, 2*). Unfortunately, TNBC patients do not benefit from endocrine and growth factor receptor neutralizing therapies as they are receptor-independent cancer cells. TNBC remains very difficult to treat and most patients develop recurrence or distant metastasis (*3, 4*). Indeed, metastatic TNBC patients have a

* Reprinted with permission from "Tocilizumab overcomes chemotherapy resistance in mesenchymal stem-like breast cancer by negating autocrine IL-1A induction of IL-6" by Andrew W Chung; Anthony J Kozielski; Wei Qian; Jianying Zhou; Ann C Anselme; Alfred A Chan; Ping-Ying Pan; Delphine J Lee; Jenny C Chang, 2022. *NPJ Breast Cancer*, Volume 8, Pages 30-39, Copyright 2022, The Authors.

grim overall survival of 9-12 months undergoing conventional therapies (*5, 6*). Furthermore, the heterogeneity of TNBC results in numerous chemoresistance pathways that are not yet fully delineated. This necessitates ongoing research to elucidate the cellular biology of TNBC to develop novel therapeutics to improve patient survival.

Previous molecular signaling pathway investigations by others identified that TNBC can be subdivided into distinct subtypes based on gene expression signatures (*7*). The basal-like 1 (BL1) subtype had genes enriched in cell cycle and division (*7*), and TNBC patients with BL1 tumors achieved the best clinical responses (*8, 9*). In contrast, the mesenchymal stem-like (MSL) subtype had gene enrichment in hallmark cancer pathways: metastasis, angiogenesis, and stem cell (*7*). Patients with MSL subtype are more chemoresistant and achieve one of the worst clinical response rates (*8, 9*). Although this TNBC subtyping method is reproducible and early studies show that BL1 tumors are susceptible to antineoplastic agents, it is not yet clear what resistance mechanisms are utilized by MSL tumors in response to chemotherapy. Therefore, elucidating MSL chemoresistance mechanisms will allow integration of targeted therapies aimed to neutralize unique MSL pathways to complement conventional therapy.

Numerous inflammatory cytokines have been shown to activate pro-tumor pathways in various cancers (*10-14*). It has also been established that various chemotherapy regimens correlate with elevated cytokine levels in cancer patients (*15-17*). Therefore, it is plausible that the resulting chemotherapy-associated inflammatory cytokines may promote resistance mechanisms in TNBC cells. Given that MSL TNBC had gene enrichment in the inflammatory NF-kB pathway (*7*), we hypothesized that MSL TNBCs may resist docetaxel therapy with self-induced proinflammatory cytokines.

As single agent taxanes are frontline therapy for TNBC patients (*18*), we investigated potential chemoresistant mechanisms by analyzing the inflammatory profile differences between MSL and BL1 TNBCs treated with docetaxel. Our results suggest that docetaxel treated MSL TNBCs initiate an autocrine IL-1A circuit to promote tumor production of IL-6. This mechanism is unique to MSL TNBCs and not observed in BL1 TNBCs. IL-6 is a well-established inducer of STAT3 signaling (*19, 20*), and STAT3 signaling mediates cancer proliferation (*21-23*). Therefore, targeting tumor-derived IL-6 with pharmacological inhibitors may negate chemoresistance pathways in docetaxel-treated MSL TNBCs. We tested our hypothesis by investigating the therapeutic efficacy of tocilizumab, a humanized anti-IL6R antibody with FDA approval for various auto-immune diseases (*24, 25*). This study aims to elucidate the upstream pathway promoting autocrine cytokine production in MSL TNBCs, and investigate the potential benefit of a novel regimen combining tocilizumab with docetaxel against different TNBC subtypes.

2.3. Results

2.3.1. Differential inflammatory gene expression in MSL vs BL1 TNBC cell lines

RNA sequencing was performed on four human MSL TNBC cell lines and four human BL1 TNBC cell lines that were untreated or treated with docetaxel. Gene expression profile differences were compared between untreated MSL vs BL1 TNBCs, and docetaxel-treated MSL vs. BL1 TNBCs. Ingenuity Pathway Analysis (IPA) demonstrated that MSL TNBCs had a higher inflammatory gene signature compared to BL1 TNBCs (*7*).

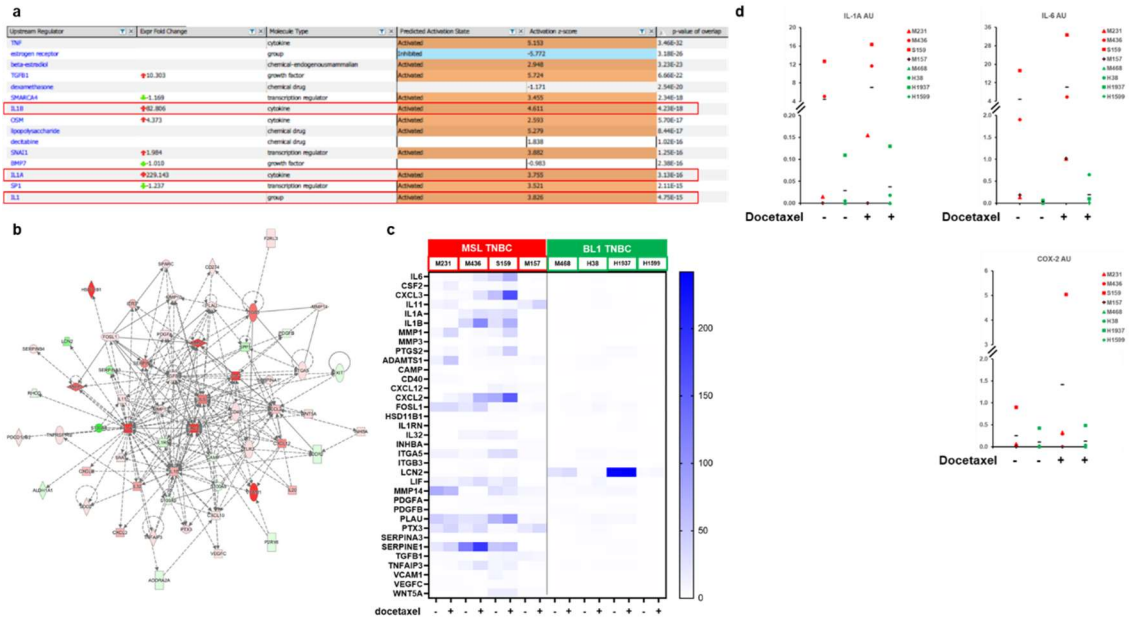

Figure 2-1. RNA sequencing predicts higher expression of immune molecules in MSL TNBCs compared to BL1 TNBCs.

Four MSL TNBC and four BL1 TNBC cell lines were treated in presence or absence of docetaxel (4 ng/ml) for 48 hours and RNA sequencing was performed. **(A)** IPA upstream regulator analysis of fold change ratio (cutoff value of 5 or -5) comparing averaged RPKM from four untreated MSL TNBC to averaged RPKM from four untreated BL1 TNBC. **(B)** IPA pathway builder of IL1A upstream regulator network overlayed with dataset from Fig. 2-1A (fold change ratio comparing averaged MSL untreated to averaged BL1 untreated samples). **(C)** Heat map expression of RPKM values from selection of genes shown in IL1A upstream regulator network from **Fig. 2-2B**. **(D)** Confirmatory qPCR for same samples used in RNA Seq experiment, shown are 2^-ΔCt values. Red represents MSL TNBC cell lines and green represents BL1 TNBC cell lines.

IPA predicted that the IL-1 cytokine family was upstream regulators in MSL TNBCs at baseline levels (**Fig. 2-1A**) and after docetaxel (**Fig. 2-2A**), which was missing in the BL1

TNBC cell lines. IL-1A and IL-1B are both potent inflammatory cytokines with multi-faceted roles in homeostasis, immunity, and inflammatory diseases (*26, 27*).

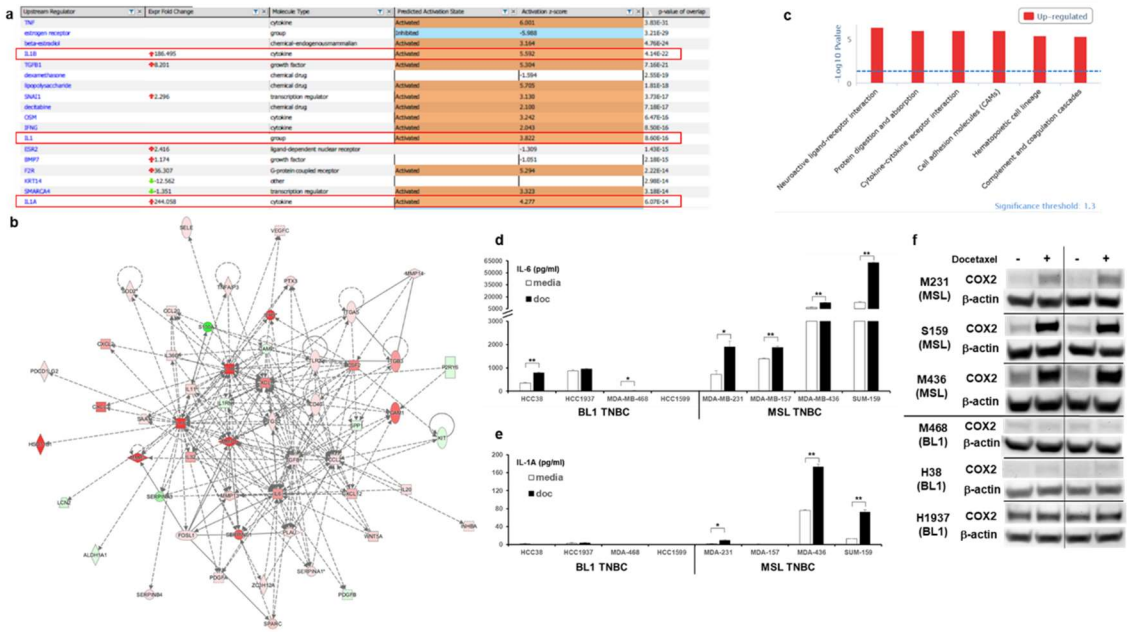

Figure 2-2. MSL TNBCs have predicted IL-1A mediated signaling, which is absent in BL1 TNBCs.

Four MSL TNBC and four BL1 TNBC cell lines were treated in presence or absence of docetaxel (4 ng/ml) for 48 hours and RNA sequencing was performed. **(A)** IPA upstream regulator analysis of fold change ratio (cutoff value of 5 or -5) comparing averaged RPKM from four docetaxel treated MSL TNBC to averaged RPKM from four docetaxel treated BL1 TNBC. **(B)** IPA pathway builder of IL1A upstream regulator network overlayed with dataset from **Fig. 2-2A** (fold change ratio comparing averaged MSL docetaxel treated to averaged BL1 docetaxel treated samples). **(C)** InnateDB analysis of aggregate 16 samples (four MSL media, four BL1 media, four MSL doc and four BL1 doc) with a permutation test comparing MSL to BL1 (p-value < 0.05 and log2FC > 4). Shown are pathways upregulated in MSL TNBCs compared to BL1 TNBCs. **(D)** IL-6 and **(E)** IL-1A average ± SEM ELISA results from supernatants collected 48 hours from each indicated human TNBC cell lines treated in presence or absence of docetaxel at 4ng/ml. Each cell line was tested with three biological replicates and results are

representative of at least two independent experiments. **(F)** Each cell line was treated in the presence or absence of docetaxel (4ng/ml), and whole cell lysate was collected after 48 hours and western blot for COX-2 and b-actin was performed for all indicated samples. Results are representative of at least two independent experiments. Statistical analysis performed with unpaired t-test: * $p < 0.05$; ** $p < 0.01$.

Pathogen mediated activation is required for mature IL-1B and given that our model is in the context of "sterile" inflammation with the absence of microbial antigens, we hypothesized that upregulation of the IL-1B transcript would not result in biologically active IL-1B. We confirmed that all TNBC cell lines did not produce any detectable levels of mature IL-1B protein (data not shown). Next, we investigated the inflammatory network regulated by IL-1A in MSL TNBCs. IPA network pathway results showed that MSL TNBC gene expression profiles had an IL-1A regulated interaction with other inflammatory mediators such as IL-6, IL-8, CSF2, CXCL2, CXCL3, IL-32, IL-11 at both baseline levels (**Fig. 2-1B**) and after docetaxel treatment (**Fig. 2-2B**). Given that we observed an upregulated cytokine network in MSL TNBCs, analysis was performed on a database for innate immune signaling pathways (InnateDB). Results indicated that MSL TNBCs had a significant upregulation of cytokine-cytokine receptor interaction compared to BL1 TNBCs ($p < 0.05$, **Fig. 2-2C**). In addition, heatmap analysis of the RNA sequencing results confirmed that MSL TNBCs had higher gene expression of various inflammatory mediators compared to their BL1 counterparts (**Fig. 2-1C**), which were validated by confirmatory RT-PCR of select target genes (**Fig. 2-1D**). Cumulatively, these data suggest that MSL TNBCs had an inflammatory gene expression profile that may be regulated by IL-1A in a mechanism that is absent in BL1 TNBCs.

2.3.2. Docetaxel induces inflammatory mediators in MSL TNBCs and not BL1 TNBCs

Next, we confirmed our RNA sequencing results by measuring select inflammatory mediators following docetaxel treatment *in vitro* by examining protein induction. Docetaxel treatment-induced statistically significant levels of IL-6 in MSL TNBCs ranging from approximately 2-63 ng/ml (**Fig. 2-2D**), whereas docetaxel induced IL-6 inconsistently from BL1 TNBCs ranging from not detectable to 1 ng/ml. Similarly, docetaxel treatment mediated statistically significant production of mature IL-1A in three out of four MSL TNBC cell lines (**Fig. 2-2E**) compared to a complete absence of detectable extracellular IL1A in BL1 TNBCs. COX-2 was also upregulated following docetaxel treatment in MSL TNBCs (**Fig. 2-2F**), which did not occur in BL1 TNBCs. As both mature and full-length forms of IL-1A are biologically active (*26, 27*), we determined the expression of pro IL-1A by western blot in the representative TNBC cell lines. In alignment with the extracellular IL-1A data (**Fig. 2-2E**), docetaxel induced pro IL-1A only in the surveyed MSL TNBCs compared to virtual absence in BL1 TNBCs (**Fig. 2-3**).

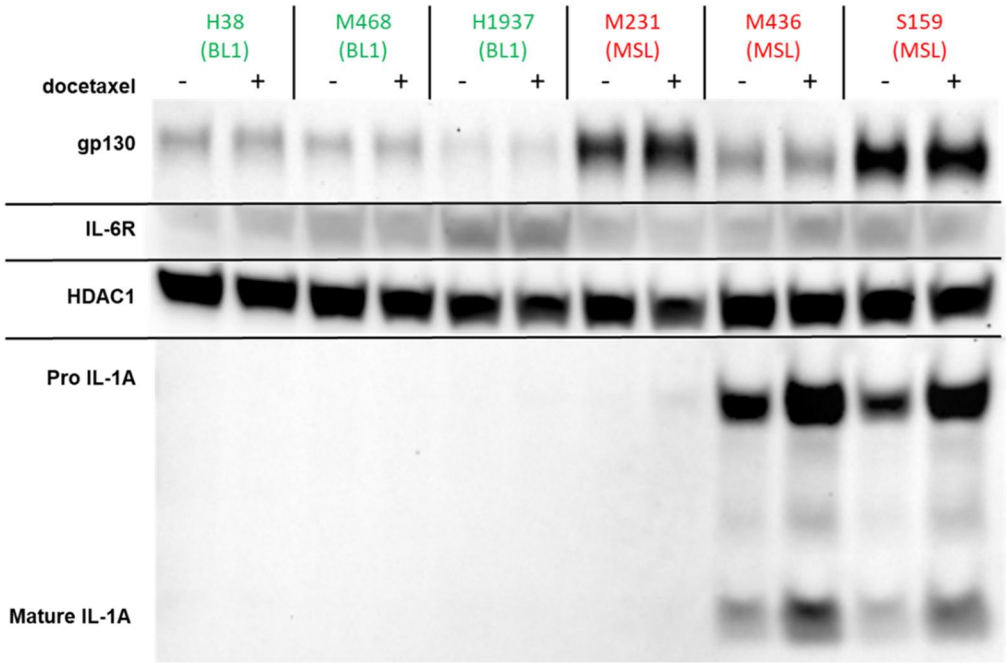

Figure 2-3. MSL TNBCs produce pro IL-1A in response to docetaxel, but not BL1 TNBCs.

MSL TNBC cell lines and BL1 TNBC cell lines treated with or without docetaxel (4 ng/ml) for 48 hours, western blot was performed for indicated proteins.

Because IL-6 is a well-characterized cytokine that is utilized for the benefit of various cancers (*21-23*), we explored the biological relevance of this cytokine in TNBCs. The signaling component of IL-6 requires both the IL-6R and gp130 as the downstream signal transducer for subsequent Jak/STAT activation (*28*). Although we found that all TNBC cell lines had ubiquitous expression of IL-6R (**Fig. 2-3**), we also found that MSL TNBCs had a trend of higher expression of the gp130 signal transducer in comparison to BL1 TNBCs. Docetaxel however did not alter the expression of the IL-6 signaling component in any TNBC cell line. These data confirms that docetaxel augments an inflammatory cytokine profile unique to MSL TNBCs which is notably absent in BL1 TNBCs.

2.3.3. MAPK pathway mediated IL-1A promotes the inflammatory cascade in MSL TNBCs

As our previous results indicated that IL-1A is an upstream in MSL TNBCs (**Fig. 2-2A**), we investigated whether elimination of IL-1A would diminish the inflammatory profile in MSL TNBCs. Two representative MSL TNBC cell lines, SUM-159 and MDA-MB-436, were treated with docetaxel in the presence or absence of IL-1A neutralizing antibody. IL-1A neutralizing antibody resulted in 72-77% reduction of docetaxel mediated production of IL-6 in the MSL TNBC cell lines versus isotype control ($p < 0.001$ in both cell lines, **Fig. 2-4A** and **Fig. 2-5A**).

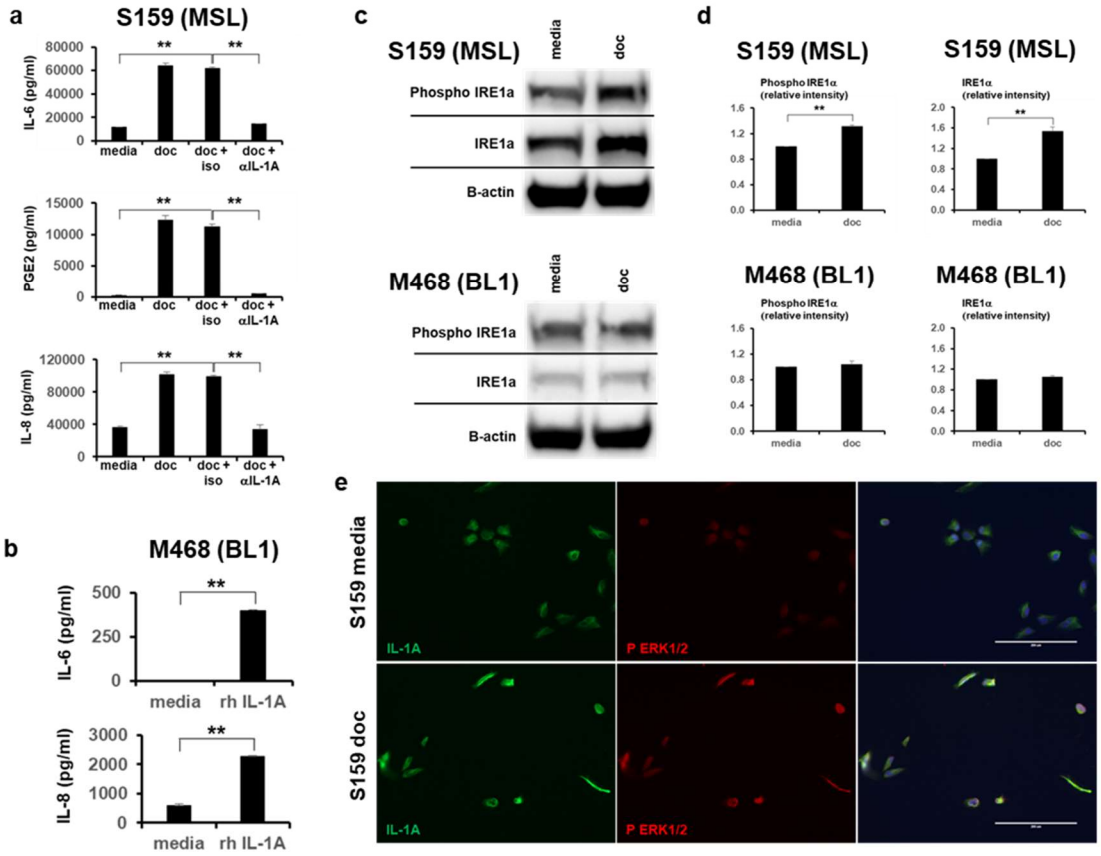

Figure 2-4. IL-1A is the upstream cytokine that promotes docetaxel mediated inflammation.

(A) IL-6, PGE2, and IL-8 ELISA results from supernatants collected from human TNBC cell line treated 48 hrs in presence or absence of docetaxel (doc) at 4ng/ml, NA/LE IL-1A mAb (1μg/ml) or NA/LE isotype mIgG2a (1μg/ml). **(B)** BL1 TNBC treated in presence or absence of recombinant human (rh) IL-1A (2ng/ml) for 48 hrs and supernatants analyzed for IL-6 and IL-8 ELISAs. **2-4A** and **2-4B** show average ± SEM from n=3 biological replicates. **(C)** Indicated TNBCs were treated in the presence or absence of doc (4 ng/ml) for 48 hrs. WB from whole cell lysates was performed, shown are representative images. **(D)** Average ± SEM densitometry analysis is from n=3. **(E)** Shown are representative 20X images (n=3 biological replicates) from S159 (MSL) cells cultured 48 hrs in chambered slides with or without doc (4 ng/ml). Immunofluorescence staining for IL-1A (Alexa Fluor 488) and Phospho ERK1/2 (Alexa 546) was performed. Statistical analysis performed with unpaired t-test: * $p < 0.05$; ** $p < 0.01$. All indicated experiments are representative of at least two independent experiments.

IL-1A neutralizing antibody also resulted in virtual elimination of PGE2, the main metabolite of COX-2 (*29*), following docetaxel treatment in the MSL TNBC cell lines ($p < 0.05$ for MDA-MB-436 and $p < 0.001$ for SUM-159, **Fig. 2-4A** and **Fig. 2-5A**).

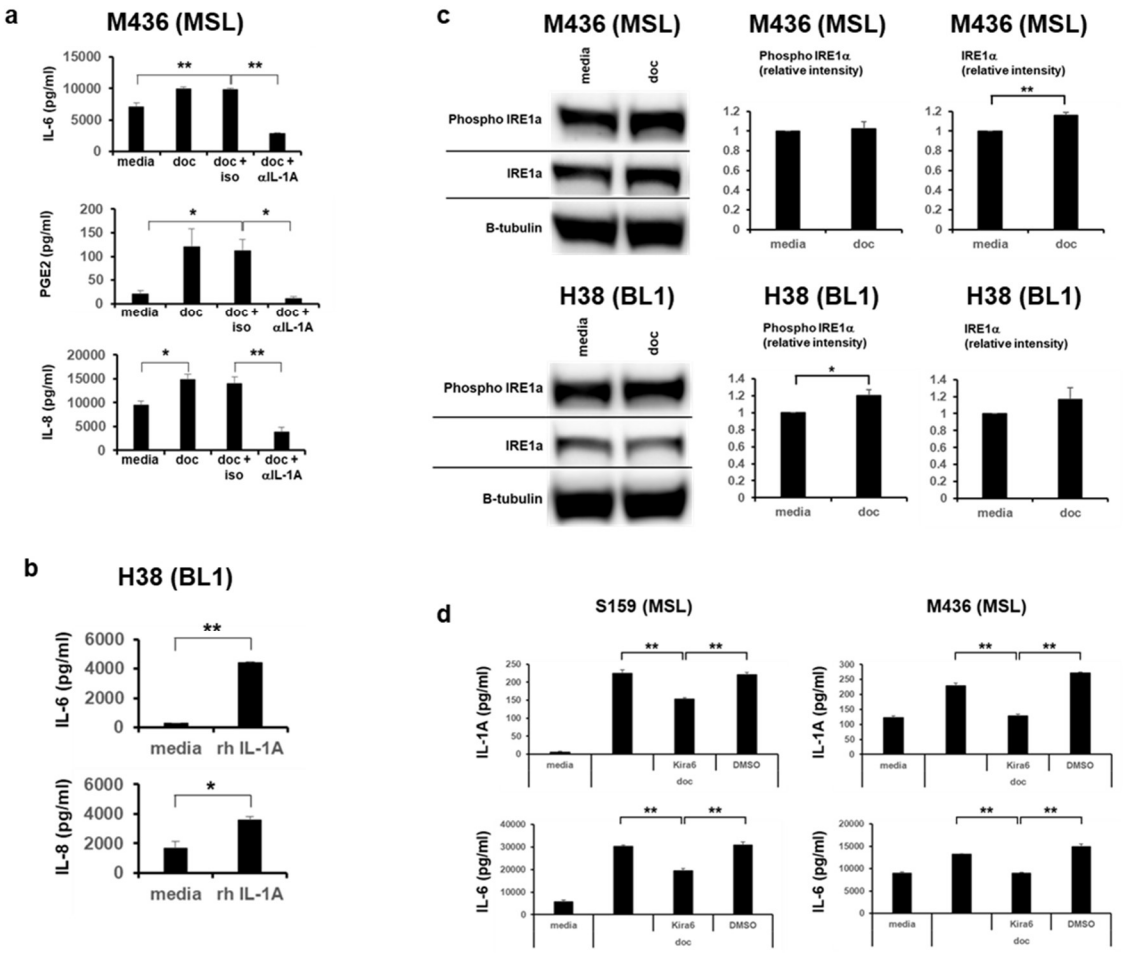

Figure 2-5. IL-1A promotes docetaxel mediated inflammation in MSL TNBCs, and not BL1 TNBCs.

(A) Shown are IL-6, PGE2, and IL-8 ELISA results from supernatants collected 48 hrs from human TNBC cell line treated in presence or absence of docetaxel (doc) at 4ng/ml, NA/LE IL-1A mAb (1μg/ml) or NA/LE isotype mIgG2a (1μg/ml). **(B)** BL1 TNBC treated in presence or absence of recombinant human (rh) IL-1A (2ng/ml) for 48 hrs and ELISAs analyzed supernatants for IL-6 and IL-8. Shown are average ± SEM from n=3 biological replicates. **(C)** TNBCs were treated in the presence or absence of doc (4 ng/ml) for 48 hrs. WB from whole cell lysates was performed, shown are representative images. Average ± SEM densitometry analysis is from n=3. **(D)** Kira6 is an IRE1 inhibitor. MSL TNBC was treated for 48 hrs at the indicated conditions (doc=4 ng/ml and Kira6=0.3μM) and supernatant was analyzed for IL-1A and IL-

6. Shown are average ± SEM ELISA results representative from n=3 biological replicates. Statistical analysis performed with unpaired t-test: * $p < 0.05$; ** $p < 0.01$. All indicated experiments are representative of at least two independent experiments.

Because IL-6 and IL-8 are often reported in tandem to promote TNBC growth, metastasis, and chemoresistance (*21, 30, 31*), we also evaluated if IL-1A neutralization diminished docetaxel mediated production of IL-8. Indeed, IL-1A neutralization resulted in 66-73% reduction of IL-8 in the MSL TNBC cell lines ($p < 0.01$ for MDA-MB-436 and $p < 0.001$ for SUM-159, **Fig. 2-4A** and **Fig. 2-5A**). We have previously shown that BL1 TNBCs do not produce IL-1A (**Fig. 2-2E**). We, therefore, investigated whether BL1 TNBCs are capable of downstream IL-1 signaling by treating two representative BL1 TNBC cell lines, MDA-MB-468 and HCC38, with recombinant human IL-1A. Treatment of BL1 TNBCs with recombinant human IL-1A resulted in significant production of IL-6 and IL-8 (**Fig. 2-4B** and **Fig. 2-5B**) indicating that BL1 TNBCs are capable of downstream IL-1 signaling and only lacking in endogenous production of IL-1.

Next, we and others have previously shown that taxane therapy induces endoplasmic reticulum (ER) stress (*32-34*). Surprisingly, docetaxel treatment increased the ER stress sensor IRE1α in MSL TNBCs, whereas BL1 TNBCs had no change after therapy (**Fig. 2-4C**, **2-4D** and **Fig. 2-5C**). Due to inconsistent findings with phosphorylated IRE1α between MSL and BL1 TNBCs, we verified docetaxel mediated inflammation was downstream of IRE1 with Kira6. Kira6 is an established IRE1 inhibitor (*35, 36*), and we found consistent abrogation of docetaxel induced IL-1A and IL-6 by Kira6 in both MSL TNBCs **Fig. 2-5D**. Furthermore, ER stress has been well-characterized for activation of MAPK pathway (*37-39*). In alignment with previous

reports, we observed that docetaxel treatment of MSL TNBC showed a correlative increase in both ERK1/2 phosphorylation and IL-1A (**Fig. 2-4E**). Cumulatively, our data show that docetaxel induces ER stress and inflammation in MSL TNBCs which is not observed in BL1 TNBCs.

To investigate the potential relevance of asymmetrical MAPK pathway activation in the two TNBC subtypes, we found docetaxel treatment resulted in the phosphorylation of MEK1/2 in MSL cell lines SUM-159 and MDA-MB-436 (**Fig. 2-6A** and **Fig. 2-7A**), whereas docetaxel did not activate MEK1/2 in BL1 cell lines MDA-MB-468 and HCC38.

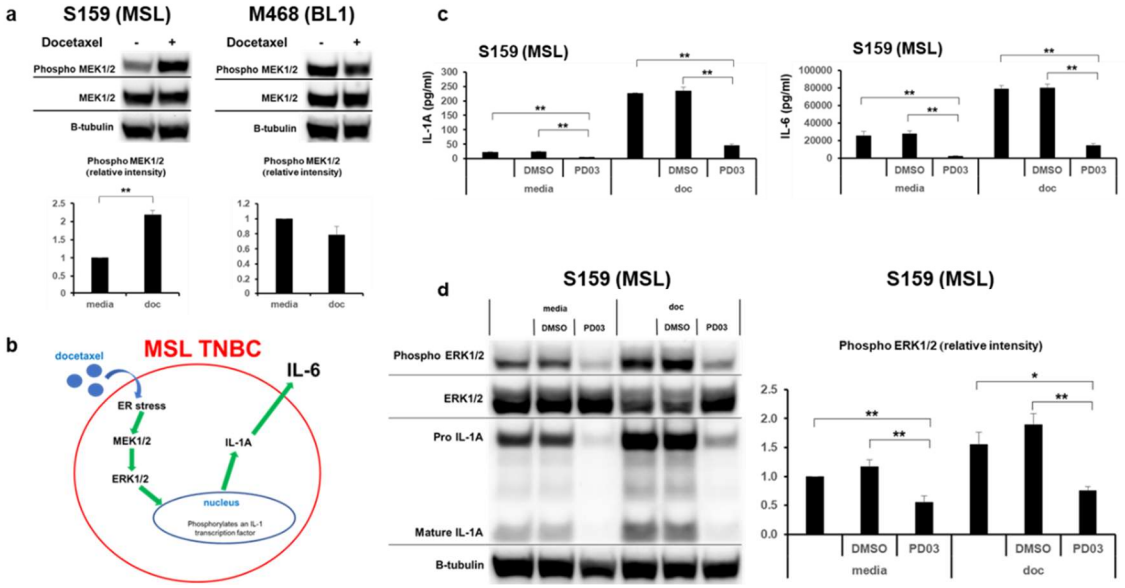

Figure 2-6. Docetaxel induced MAPK activity promotes autocrine IL-1A/IL-6 production in MSL TNBCs.

(A) TNBCs were treated in the presence or absence of docetaxel (doc) at 4ng/ml for 48 hrs. WB from whole cell lysates was performed, shown are representative images. Average ± SEM densitometry analysis is from n=3 biological replicates. **(B)** Cartoon representation of MAPK mediated induction of IL-1A/IL-6. **(C)** PD 0325901 (PD03) is a MEK inhibitor. MSL TNBC was treated for 48 hrs at the indicated conditions (doc=4 ng/ml and PD03=1μM), supernatants were measured for IL-1A and IL-6. Shown are

average ± SEM ELISA results from n=4 biological replicates. **(D)** WB from paired whole cell lysates to supernatant samples from **Fig. 2-6C**, shown is a representative image. Average ± SEM densitometry analysis is from n=4. Statistical analysis performed with unpaired t-test: * $p < 0.05$; ** $p < 0.01$. All indicated experiments are representative of at least two independent experiments.

To confirm the relevance of the MAPK pathway, MSL TNBC cell lines were treated in the presence or absence of docetaxel with MEK inhibitor PD 0325901 (*40*). MEK inhibition led to a statistically significant reduction of IL-1A both at baseline levels ($p < 0.001$) and after docetaxel treatment ($p < 0.001$, **Fig. 2-6C** and **Fig. 2-7B**) in both MSL TNBC cell lines.

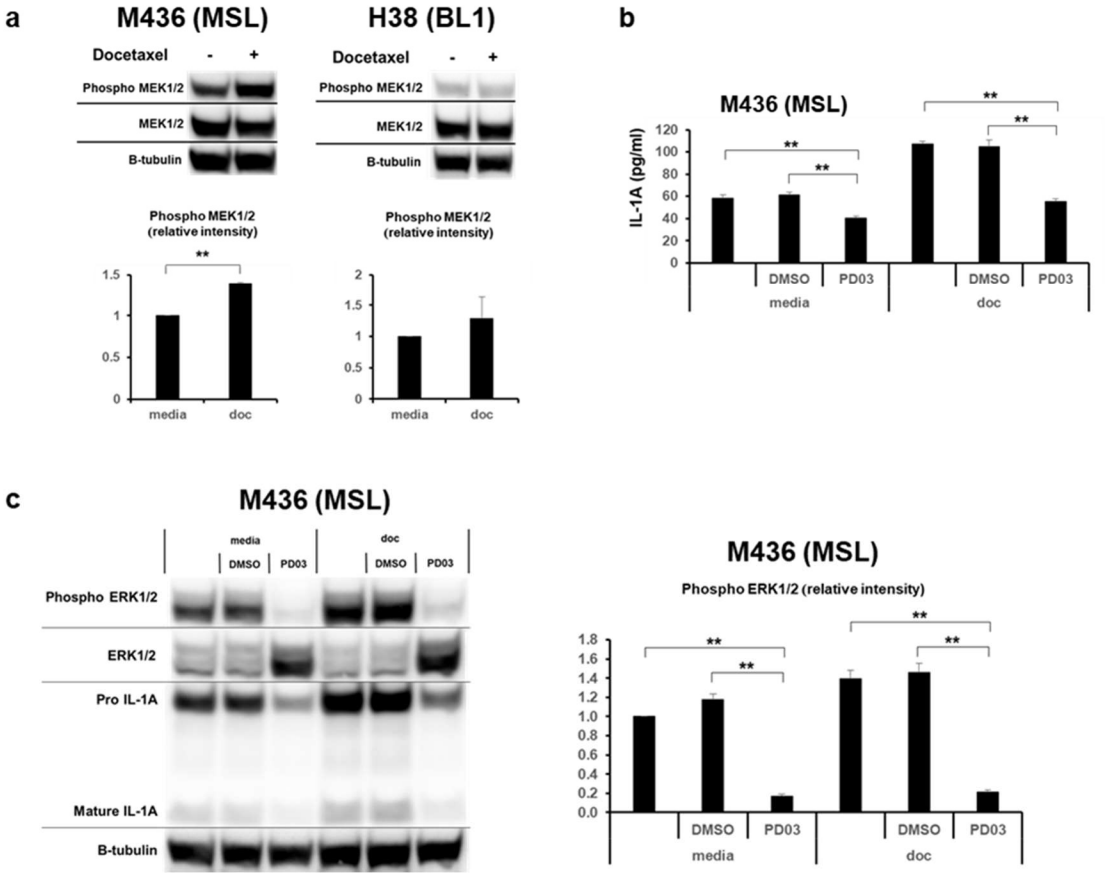

Figure 2-7. Docetaxel mediated MAPK/IL-1A/IL-6 signaling observed in MSL TNBCs, and not BL1 TNBCs.

(A) Indicated cell lines were treated in the presence or absence of docetaxel (doc) at 4ng/ml for 48 hrs. WB from whole cell lysates was performed, shown are representative images. Average ± SEM densitometry analysis is from n=3 biological replicates. **(B)** PD 0325901 (PD03) is a MEK inhibitor. MSL TNBC was treated for 48 hrs at the indicated conditions (doc=4 ng/ml and PD03=1μM) and supernatant was analyzed for IL-1A. Shown are average ± SEM ELISA results from n=4 biological replicates. **(C)** WB from paired whole cell lysates as supernatant samples from **Fig. 2-7B**, shown is a representative image. Average ± SEM densitometry analysis is from n=4. Statistical analysis performed with unpaired t-test: * $p < 0.05$; ** $p < 0.01$. All indicated experiments are representative of at least two independent experiments.

Furthermore, the reduction of IL-1A likewise led to decreased production of the downstream cytokine IL-6 in SUM-159 ($p < 0.001$, **Fig. 2-6C**). We next investigated the phosphorylation of downstream targets ERK1/2 to validate that the effect of PD 0325901 was the result of MEK inhibition (*41*). We confirmed that PD 0325901 significantly reduced ERK1/2 phosphorylation both in the absence and presence of docetaxel ($p < 0.01$, **Fig. 2-6D** and **Fig. 2-7C**) for both MSL TNBC cell lines. In addition, we also determined that MEK inhibition resulted in a clear reduction of pro-IL-1A (**Fig. 2-6D** and **Fig. 2-7C**) which aligned with the extracellular IL-1A reduction results as in **Fig. 2-6C** and **Fig. 2-7B**. These results indicate that docetaxel mediates activation of the MAPK pathway to initiate the IL-1A driven inflammation in MSL TNBCs (**Fig. 2-6B**). This mechanism does not occur in BL1 TNBCs as the MAPK pathway remains unchanged following docetaxel treatment. Furthermore, we found that MSL TNBCs responded dose-dependently to MEK inhibition by PD 0325901 (**Fig. 2-8A**).

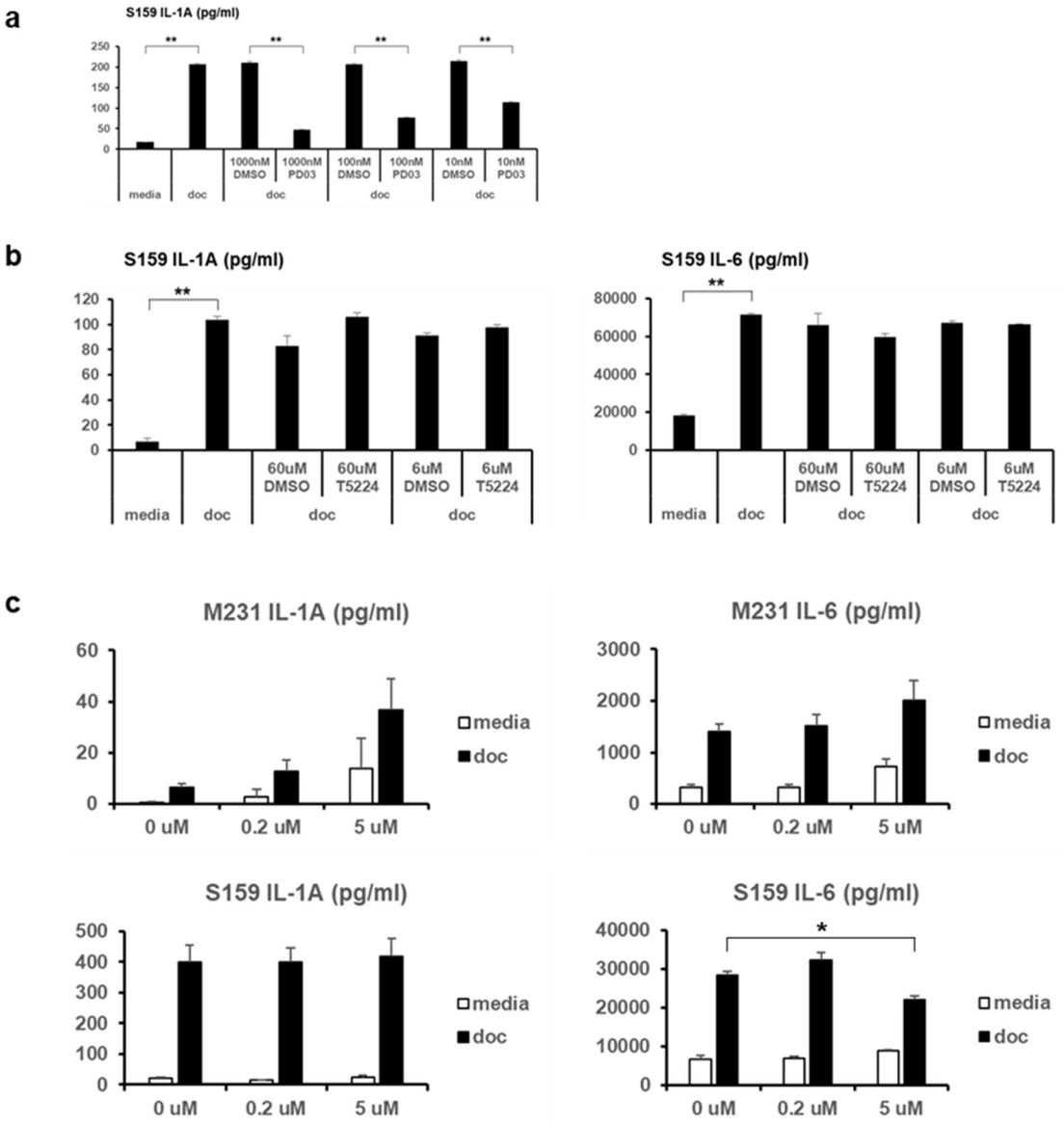

Figure 2-8. Dose dependent response of MEK1/2 inhibition against docetaxel treated MSL TNBCs.

Shown are supernatant analysis from ELISA after 48 hour culture. MSL TNBC cell lines were treated with docetaxel (4 ng/ml) and the following inhibitors: **(A)**PD03 (PD 0325901) is a MEK inhibitor and shown is average technical replicates ± SEM, representative from two independent experiments. **(B)** T5224 is an AP-1 inhibitor and shown is average technical replicates ± SEM, representative from two independent experiments. **(C)** SC75741 is a NFkB inhibitor and shown is average ± SEM from two

independent experiments with n=3 biological replicates. Statistical analysis performed with unpaired t-test: * $p < 0.05$; ** $p < 0.01$.

Cumulatively, our data aligns with previous reports that MAPK pathway activates transcription factors that bind to the IL-1A promoter in tumorigenesis (*42*). As IL-1A can be produced through MEK independent pathways (*43, 44*), we investigated the role of other reported pathways that can induce IL-1A. Inhibition of AP-1 resulted in no reduction of IL-1A and IL-6 in MSL TNBC cell lines (**Fig. 2-8B**), whereas inhibition of NF-kB resulted in inconsistent reduction of IL-6 in MSL TNBC cell lines (**Fig. 2-8C**). This suggests that NF-kB does not contribute to the MAPK/IL-1A axis, yet may play a minor independent role in IL-6 production. Cumulatively, these results show that docetaxel activates the MAPK pathway in MSL TNBCs which triggers an autocrine IL-1A cascade for subsequent inflammation. This mechanism is virtually absent in BL1 TNBCs as docetaxel treatment results in no MAPK activation.

2.3.4. Docetaxel synergizes with IL-6 neutralization against MSL TNBCs in vitro

As IL-6 has a multi-factorial role in promoting cancer cell proliferation, metastasis, and cancer stem cell induction (*19-23*), we investigated *in vitro* the potential efficacy of neutralizing MSL TNBC autocrine IL-6 production in combination with docetaxel treatment. Dual treatment of MSL TNBC cell lines with docetaxel and an IL-6 neutralizing antibody led to a significant reduction in phosphorylation of STAT3, a potent transcription factor for cancer proliferation (**Fig. 2-9A** and **Fig. 2-10A**).

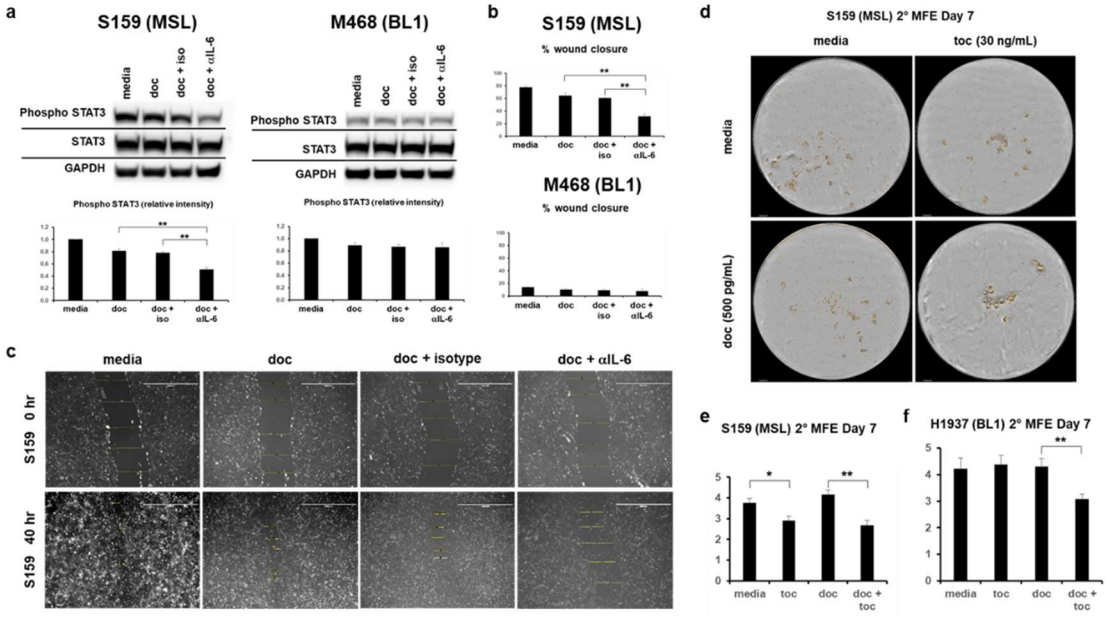

Figure 2-9. IL-6 neutralization in combination with docetaxel provides benefit against MSL TNBCs, but not BL1 TNBCs.

(A) The indicated TNBC cell lines were treated with docetaxel (4 ng/ml) with or without anti IL-6 neutralizing antibody (0.1 μg/ml) or isotype control for 24 hours, and then western blot was performed. Shown are representative western blot images and average ± SEM densitometry of phosphorylated STAT3 from n=3 biological replicates for both TNBC cell lines. **(B)** Scratch migration for TNBCs treated for 40-48 hours with or without docetaxel (4 ng/ml), anti IL-6 neutralizing antibody (1 μg/ml) and isotype control (1 μg/ml). Shown are average ± SEM % wound closure from n=5 biological replicates for all cell lines. **(C)** Representative (from **Fig. 2-9B**) scratch migration image for S159 at t=0hr and t=40hr. **(D)** Secondary mammospheres treated in the presence or absence of docetaxel (500 pg/ml) or tocilizumab (30 ng/ml). Mammospheres were counted on day 7 on Incucyte by threshold of cell area > 1256 um^2. Shown is a representative image from S159 (MSL) on day 7. **(E)** Shown are average ± SEM mammosphere formation efficiency (MFE) from n=8 biological replicates of S159 (MSL). **(F)** Shown are average ± SEM MFE from n=8 biological replicates of BL1 TNBC. Statistical analysis performed with unpaired t-

test: * $p < 0.05$; ** $p < 0.01$. All indicated experiments are representative of at least two independent experiments.

In contrast, IL-6 inhibition resulted in inconsistent reduction of STAT3 phosphorylation in BL1 TNBCs. We then determined whether IL-6 neutralization reduced TNBC cell migratory capability. Scratch migration assays showed that docetaxel in combination with IL-6 neutralizing antibody led to a significant decrease in wound closure in MSL TNBC cell lines and not BL1 TNBCs (**Fig. 2-9B, 2-9C** and **Fig. 2-10B**).

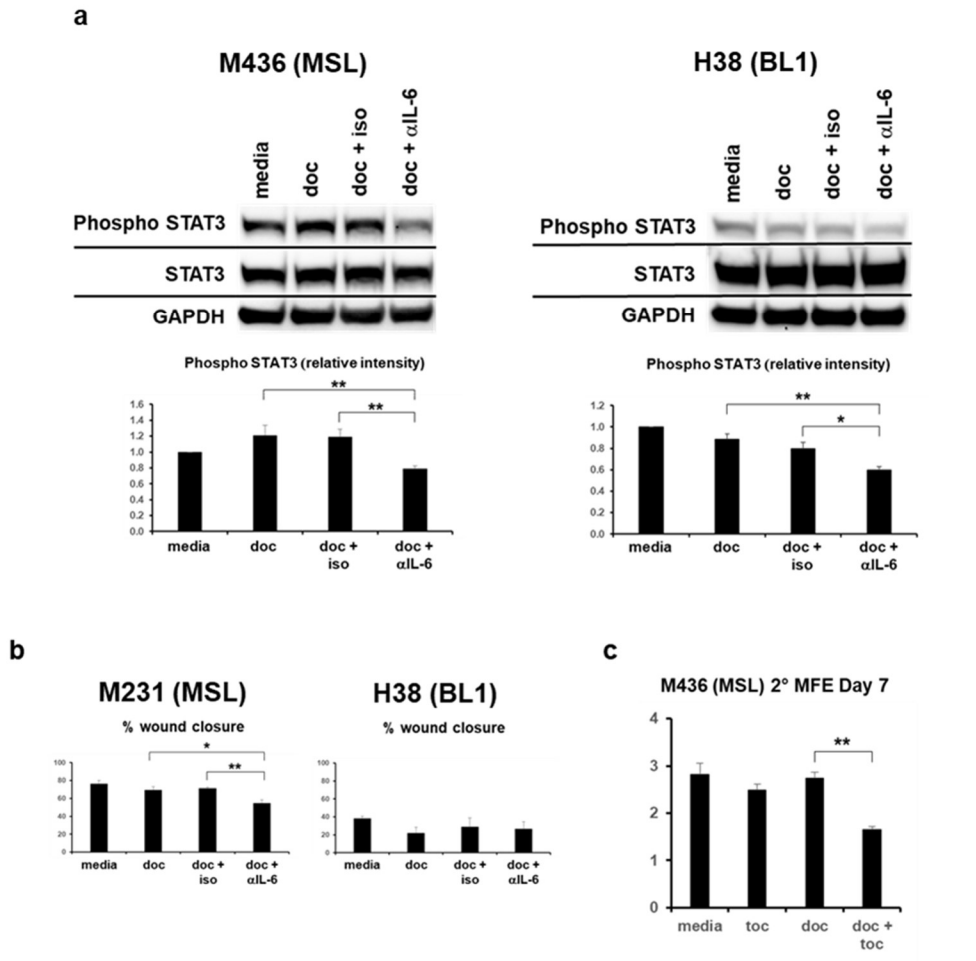

Figure 2-10. Docetaxel with IL-6 neutralizing antibody provides benefit against MSL TNBCs.

(A) Indicated TNBC lines were treated with docetaxel (4 ng/ml) with or without anti IL-6 neutralizing antibody (0.1 μg/ml) or isotype control for 24 hours, and then western blot was performed. Shown are representative western blot images and average ± SEM densitometry of phosphorylated STAT3 from n=3 biological replicates. **(B)** Scratch migration for TNBCs treated for 40-48 hours with or without docetaxel (4 ng/ml), anti IL-6 neutralizing antibody (1 □g/ml) and isotype control (1 μg/ml). Shown are average ± SEM % wound closure from n=5 biological replicates for all cell lines. **(C)** Secondary mammospheres treated in the presence or absence of docetaxel (500 pg/ml) or tocilizumab (30 ng/ml). Mammospheres

were counted on day 7 on Incucyte by threshold of cell area > 1256 um^2. Shown are average ± SEM mammosphere formation efficiency (MFE) from n=8 biological replicates of M436 (MSL). Statistical analysis performed with unpaired t-test: * $p < 0.05$; ** $p < 0.01$. All indicated experiments are representative of at least two independent experiments.

Tocilizumab is a humanized anti-IL6R antibody with FDA approval for arthritis but not yet for any cancer immunotherapy applications. As mammospheres are used as an *in vitro* surrogate for cancer stem cells(*45*), we investigated the efficacy of tocilizumab in abrogating mammosphere formation efficiency (MFE). MSL cell line SUM-159 had diminished secondary mammosphere colonies when co-treated with docetaxel and tocilizumab compared to chemotherapy alone (**Fig. 2-9D**). Although mono-therapy of tocilizumab resulted in decreased mammospheres in only one MSL TNBC cell line, combination therapy of docetaxel and tocilizumab led to a significant reduction of MFE in both MSL cell lines compared to docetaxel treatment alone (**Fig. 2-9E** and **Fig. 2-10C**). Surprisingly, docetaxel combined with tocilizumab also led to a significant reduction of MFE in a BL1 TNBC cell line (**Fig. 2-9F**). Despite these unexpected results, our cumulative data clearly shows a consistent benefit of IL-6 targeted therapy against MSL TNBCs compared to inconsistent benefit against BL1 TNBCs *in vitro*.

2.3.5. Tocilizumab combined with docetaxel has efficacy against MSL and not BL1 xenografts

To validate the relevance of docetaxel induced MAPK activity *in vivo*, we implanted cell line xenografts into NSG female mice. Concurrent with our *in vitro* data, docetaxel treatment led to significant phosphorylation of MEK1/2 in MSL xenografts and not BL1 xenografts (**Fig. 2-11A**).

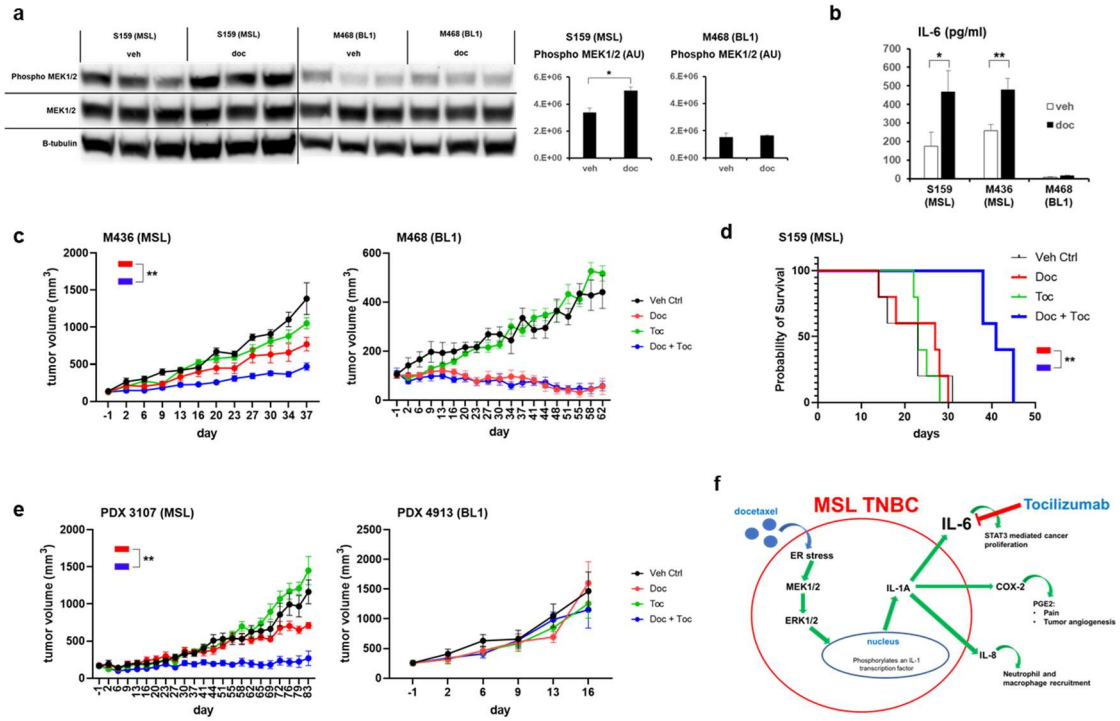

Figure 2-11. Tocilizumab in combination with docetaxel provides benefit against MSL TNBCs *in vivo*, and not against BL1 TNBCs.

(A) Female NSGs were implanted with human TNBC cell lines and treated for two days with vehicle (veh) or docetaxel (doc) 20 mg/kg. WB was performed from primary tumor and shown are average ± SEM densitometry (n=3 pairs for both cell line xenografts). The six indicated MSL samples were performed on one membrane and the six BL1 samples were performed on a separate membrane. **(B)** Female NSGs were implanted with human TNBC cell lines and treated with veh or doc (20 mg/kg). Two days later, serum was collected and human IL-6 average ± SEM was determined by ELISA. S159 = 10 pairs, M436 = 8 pairs, M468 = 6 pairs. **2-11A** and **2-11B** significance was determined by unpaired t-test. **(C)** Shown are average tumor volumes ± SEM from cell line xenograft studies. M436 animals (n=6 per group) received 5 cycles of therapy. M468 animals (n=6 per group) received 4 cycles of therapy, however cycle 2 lacked any tocilizumab treatment for applicable groups. Tumor volume significance was determined by 2-way ANOVA. **(D)** Kaplan-Meier (KM) survival from S159 xenografts (n=5 per group), animals received 4 cycles of therapy. **(E)** Shown are average tumor volumes ± SEM from PDX studies.

4913 animals (n=5 per group) received 2 cycles of therapy. 3107 animals (n=6 per group) received 6 cycles of therapy. Tumor volume significance was determined by mixed effects analysis. **(F)** Model figure of MSL TNBC resisting chemotherapy mediated by MAPK induction of IL-1A/IL-6. For all statistical analysis: * $p < 0.05$; ** $p < 0.01$.

Furthermore, docetaxel increased human IL-6 production in mice bearing MSL TNBC xenografts and not BL1 xenografts (**Fig. 2-11B**). Although we found inconsistent induction of IL-1A in MSL xenografts, we confirmed virtually no detectable IL-1A in BL1 xenografts (**Fig. 2-12A and 2-12B**).

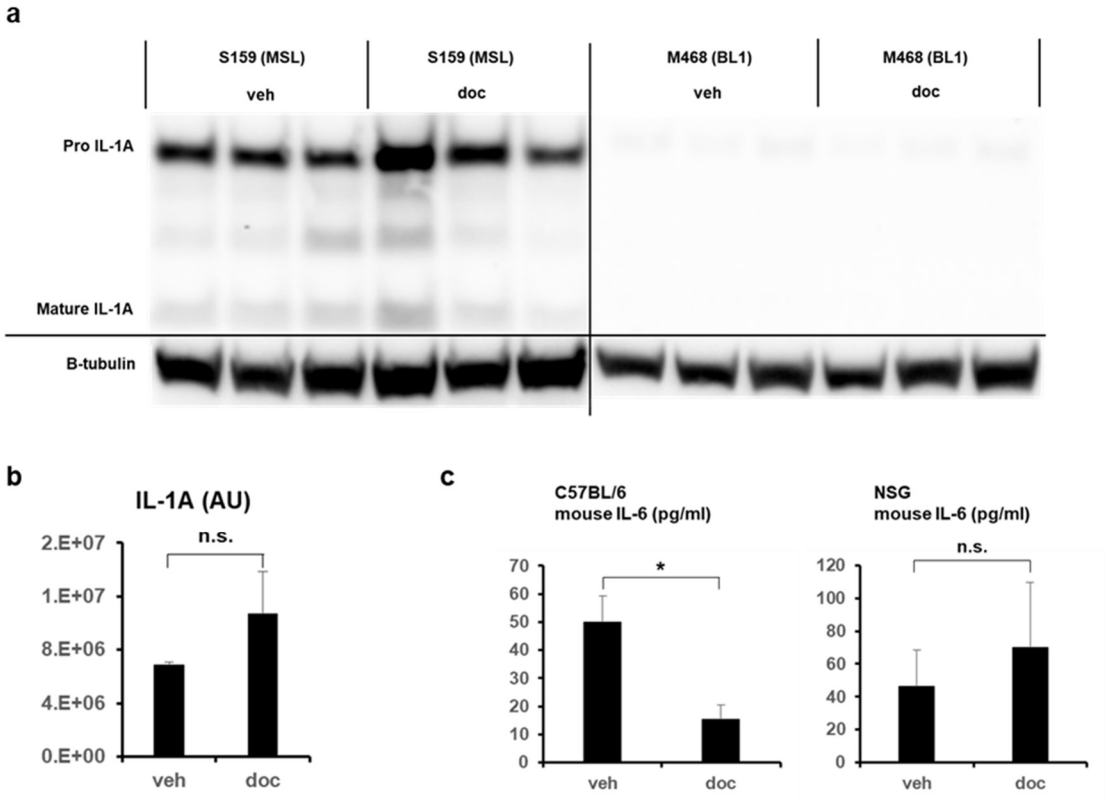

Figure 2-12. Docetaxel mediated induction of IL-6 is specific for human MSL TNBCs and not host murine IL-6 production.

(A) Female NSG mice were implanted with indicated human TNBC cell lines. On day zero, mice were treated with vehicle (veh) or docetaxel (doc) 20 mg/kg. On day two, mice were sacrificed and primary tumors were collected. Protein was isolated from tumor lysates and WB was performed. Shown are results from n=3 pairs of mice from both cell line xenografts. The six indicated MSL samples were performed on one membrane and the six BL1 samples were performed on a separate membrane. **(B)** S159 cell line xenograft IL-1A densitometry average ± SEM comparing 3 pairs of animals. **(C)** Female mice of indicated strains were treated with veh or doc (20 mg/kg). Two days later, serum was collected and circulating mouse IL-6 average ± SEM was measured by BD Bio mouse IL-6 ELISA kit. Both strains included four pairs of animals. Statistical analysis performed with unpaired t-test: * $p < 0.05$; ** $p < 0.01$.

Next to investigate the efficacy of tocilizumab *in vivo*, we distributed mice bearing MSL or BL1 xenografts into groups receiving mono-therapy of docetaxel, tocilizumab, or dual therapy. MDA-MB-436 (MSL) bearing animals had a statistically significant delayed tumor growth when receiving dual therapy compared to chemotherapy alone ($p < 0.001$), whereas dual therapy provided no benefit for MDA-MB-468 (BL1) bearing animals (**Fig. 2-11C**). Furthermore in a second MSL (S159) xenograft model, animals receiving docetaxel in combination with tocilizumab had a median increase in survival of two weeks ($p < 0.01$) compared to animals receiving chemotherapy alone (**Fig. 2-11D**). Our lab has previously characterized TNBC patient-derived xenografts (PDX) as MSL and BL1 subtypes (*46*). We, therefore, investigated the efficacy of our anti-inflammatory regimen in mice bearing MSL and BL1 PDXs. Similar to our cell line xenografts data, animals bearing MSL PDX benefited when receiving docetaxel with tocilizumab ($p < 0.001$) as compared to chemotherapy alone (**Fig. 2-11E**) and the benefit of dual therapy did not occur for animals bearing BL1 PDX. Although host murine IL-6 will not bind to human IL-6R(*47*), we validated that docetaxel induction of IL-6 was unique for a TNBC subtype rather than a broad cellular response to chemotherapy. Both immunocompromised NSG and immunocompetent C57BL/6 animals had no statistical induction of mouse IL-6 after chemotherapy (**Fig. 2-12C**).

2.4. Discussion

TNBC patients currently lack specific targeted therapeutics and have shown marginal benefit to immune checkpoint blockade therapy. It has previously been shown by others that high expression of IL-1A and IL-6 both correlate with poor prognosis for breast cancer patients (*21, 42*). And other preclinical studies have investigated the efficacy of tocilizumab against breast cancers broadly without necessarily delineating which TNBC patients would benefit the

most from tocilizumab (*48-50*). Here, we provide evidence that a molecular subset of TNBC resists conventional chemotherapy by a MAPK mediated autocrine IL-1A/IL-6 axis (**Fig. 2-11F**). Furthermore, our data potentially identifies a population of TNBC patients that may benefit from supplementing chemotherapy with tocilizumab to eliminate autocrine tumor production of IL-6. Currently, tocilizumab is not FDA approved for any tumor malignancies. Previous clinical trials have found that targeted IL-6 therapies provided no benefit in hematological malignancies, renal, and prostate cancer (*51, 52*). To the best of our knowledge, no clinical trial has completed an investigation of the potential efficacy of tocilizumab for TNBC patients.

We hypothesize that differential benefit from IL-6 blockade may be due to a gradient physiological effect of IL-6. BL1 TNBCs produce quantifiable levels of IL-6 both *in vitro* and *in vivo*, but to a lesser extent compared to MSL TNBCs. Neutralization of BL1 autocrine IL-6 provided no benefit in reducing tumor cell proliferation *in vivo*. In contrast, MSL TNBCs producing substantial IL-6 were effectively targeted with tocilizumab possibly providing insight that a gradient effect from autocrine IL-6 is necessary to promote tumor resistance. Therefore, our model demonstrates that tocilizumab will not be beneficial universally for TNBC patients. This novel therapeutic regimen will likely only improve the outcome for patients with chemoresistant tumors driven by MAPK induced IL-6.

This study identified MAPK activity-induced expression of other inflammatory mediators that may also be candidates for targeted therapy against MSL tumors. Although COX-2 has been well characterized to promote tumor angiogenesis and downregulate anti-tumor immunity, TNBC clinical trials targeting COX-2 have been largely unsuccessful (*53-55*). Our data shows that only a subset of TNBCs undergo MAPK induced expression of COX-2 after

docetaxel therapy, which may indicate that COX-2 inhibitors may not provide benefit for all TNBC patients. We, therefore, hypothesize that upon subtyping TNBC patients and performing a retrospective analysis of completed clinical trials investigating COX-2 inhibitors, there may be a differential response rate to COX-2 inhibitors based on tumor subtypes and MAPK activity of patient tumors.

IL-8 is a chemokine that recruits macrophages and neutrophils into the tumor microenvironment, and tumor-associated macrophages and neutrophils have been demonstrated to favor a pro-tumor niche (*56*). We identified IL-8 as another downstream inflammatory mediator produced by docetaxel resistant MAPK active tumor cells. IL-8 anti-biologic therapy has already been established to be safe in phase I trials against metastatic tumors and is currently under investigation in several phase II studies (*57*). Cumulatively, we endeavor to provide a rationale for a clinical trial that identifies TNBC patients with chemo-refractory tumors driven by MAPK activity. In essence, these patients may benefit from supplementing conventional chemotherapy with targeted therapies against MAPK driven production of IL-6, COX-2, and IL-8.

The chief limitation of our study is the absence of immune cellular contribution in the context of IL-6 blockade *in vivo*. Although we acknowledge that IL-6 has a broad cellular effect and is produced by diverse cell types, we provide clear evidence that docetaxel mediated MAPK/IL-6 activity is specific for a subtype of TNBCs. This is evident as docetaxel failed to induce host mouse IL-6 in both immunocompromised and immune-competent animals. Finally, tocilizumab will neutralize IL-6 signaling by antagonizing IL-6R regardless of the cellular source of IL-6 in the tumor microenvironment.

It should be noted that while we have consistently completed two representative MSL cell lines vs. two representative BL1 cell lines (i.e., S159 and M436 vs. M468 and H38), there were two notable exceptions: 1. Scratch migration (**Fig. 2-10B**), M436 did not migrate during the indicated time conditions. We, therefore, substituted with M231 as a second MSL TNBC for scratch migration. 2. Mammospheres (**Fig. 2-9F**), we failed to initiate mammospheres with M468 after two months. Published literature confirmed that M468 does not form mammospheres. We could not find evidence that others established successful H38 mammospheres. H1937 was the only BL1 TNBC cell line that others established mammospheres; we, therefore, investigated only H1937 as the sole BL1 cell line for mammospheres.

Although BL1 TNBCs can produce autocrine IL-6, tocilizumab provides no benefit against two BL1 xenografts *in vivo*. Due to inconsistent benefit of neutralizing IL-6 against BL1 tumors *in vitro* (**Fig. 2-9F** and **Fig. 2-10A**), we acknowledge that tocilizumab may possibly provide benefit for some non-MSL TNBC patients. However, our principal hypothesis is that tocilizumab therapy may provide greater efficacy against tumors with MAPK-driven IL-6 production. To investigate our hypothesis, we would design a phase 2 clinical trial screening 100 to 200 TNBC patients by RNA sequencing for sufficient enrollment of MSL patients as MSL is representative of 10-19% of TNBC patients (*8, 9*). All enrolled MSL trial patients would receive taxane therapy in combination with tocilizumab and evaluated for regimen efficacy. In addition, baseline tissue analysis for MAPK expression between responders and non-responders will be evaluated as potential predictive biomarkers for tocilizumab therapy.

Our investigation potentially identifies a population of TNBC patients that may benefit from supplementing conventional chemotherapy with a novel anti-inflammatory cocktail

regimen to negate MAPK-driven autocrine cytokines. In addition, our results may also apply to other cancer pathologies reliant on MAPK pathway for therapy resistance. Ultimately, it is a paramount objective to improve the identification of cancer patients for targeted therapy regimens.

2.5. Methods

2.5.1. Cell culture, reagents, and antibodies

The following human MSL and BL1 TNBC cell lines were used for this study (*7*): SUM-159, MDA-MB-436, MDA-MB-231, MDA-MB-157, MDA-MB-468, HCC38, HCC1937, and HCC1599. Cell lines were purchased from ATCC, authenticated, and regularly tested for mycoplasma. All cell lines were cultured in DMEM (HyClone- Logan, Utah) supplemented with 10% fetal bovine serum (FBS), Antibiotic-Antimycotic (GenDepot- Katy, Texas), and L-glutamine (Corning- Manassas, Virginia) in a 5% CO_2 incubator at 37°C. For the indicated *in vitro* conditions, the following tissue culture reagents were used at following concentrations unless noted differently: docetaxel (NovaPlus, 4 ng/ml from Ebewe Pharma, Austria), human IL-1A neutralizing antibody (R&D clone 4414, 1 μg/ml), mouse IgG_{2A} isotype control antibody (R&D clone 20102, 1 μg/ml), recombinant human IL-1A (R&D 200-LA, 2 ng/ml), DMSO (Sigma D2650), PD 0325901 (R&D 4192, 1μM), human IL-6 neutralizing antibody (BD Biosciences clone MQ2-13A5, 0.1 μg/ml), rat IgG_1 isotype control antibody (BD Biosciences clone R3-34, 0.1 μg/ml), tocilizumab (Roche, 30 ng/ml from San Francisco, CA), and Kira6 (Cayman Chemical 19151 from Ann Arbor, MI).

Anti-human antibodies used for ELISAs: IL-1A capture and detection (R&D clone 4414 and catalog# BAF200, respectively), IL-6 capture and detection (BD Biosciences clones MQ2-

13A5 and MQ2-39C3, respectively), IL-8 capture and detection (BD Biosciences clones G265-5 and G265-8, respectively). R&D items from Minneapolis, MN; Sigma items from St. Louis, MO; BD Biosciences items from San Jose, Ca.

The following Cell Signaling Technology (Danvers, MA) anti-human antibodies were used for western blots: COX2 (12282), β-actin (4970), GP130 (3732), β-tubulin (2146), ERK1/2 (4695), phospho-ERK1/2 (9101), MEK1/2 (4694), phospho-MEK1/2 (9154), GAPDH (5174), STAT3 (9139), IRE1α (3294), and phospho-STAT3 (9145). Abcam (Cambridge, MA) anti-human IL-1A (ab206410), anti-human phosphor-IRE1 (ab124945) and anti-human IL-6R (ab128008) were also used for western blots.

2.5.2. RNA sequencing analysis

Human TNBC cell lines were treated in the presence or absence of docetaxel (4 ng/ml) for 48 hours and RNA was extracted with RNeasy Plus Mini Kit (Qiagen from Hilden, Germany). Genomic DNA was removed with gDNA eliminator spin columns and total RNA purification was done according to manufacturer's instructions. cDNA library preparation and RNA Sequencing was performed by the Genome Sequencing Facility of Greehey Children's Cancer Research Institute at the University of Texas Health San Antonio as previously described (*58*). RNA sequencing data processing and analysis of RPKM values were done as previously described (*59*). In brief, RNAseq reads were quality filtered using Trimmomatic (doi: 10.1093/bioinformatics/btu170) and aligned to the human reference genome assembly GRCh38.p12 using HISAT2. Next, HTSeq was used to determine how many reads mapped to each features (doi: 10.1093/bioinformatics/btu638). Differential gene expression was performed using a permutation test for linear models. A total of 921 out of 24850 ENTREZ gene ID passed a fold-change cutoff of 4 and a p-value cutoff of 0.05 for pathway analysis on InnateDB (doi:

10.1093/nar/gks1147). Pathway over-representation analysis was performed using hypergeometric distribution test and Benjamini-Hochberg false discovery rate correction.

2.5.3. Ingenuity Pathway Analysis (IPA)

One RNA sequencing dataset analyzed fold change ratio of averaged RPKM gene expression from untreated MSL TNBCs compared to averaged RPKM gene expression from untreated BL1 TNBCs. The other dataset analyzed fold change ratio of averaged RPKM gene expression from docetaxel treated MSL TNBCs compared to averaged RPKM gene expression from docetaxel treated BL1 TNBCs. Fold change ratio cut-off of 5 or -5 was utilized for both datasets and the "Core Analysis" function on IPA was utilized for upstream analysis of uploaded datasets. Estimated RPKM values were used to visualize heatmaps.

2.5.4. Western blot analysis

Human TNBC cell lines were treated under the indicated conditions and whole-cell lysates were collected with RIPA buffer (Sigma), 1% protease inhibitor, and 1% phosphatase inhibitor. In brief, cells were washed with cold phosphate-buffered saline (PBS) twice and lysed with complete RIPA buffer. Culture wells were then scraped with cell scrapers, lysate solutions were collected and incubated on ice for 20 min. Following centrifugation at 4°C max speed for 10 min, whole-cell lysates were collected for western blot. Protein gel electrophoresis was performed on Bolt™ 4-12% Bis-Tris Plus Gels (ThermoFisher- Carlsbad, CA) followed by transfer onto 0.2 □m PVDF membranes. After 1 hr blocking in 5% milk, blots were stained overnight with previously listed primary antibodies at 4°C in 5% BSA.

All primary antibodies for WB were diluted 1:1000, except anti-human IL-6R (ab128008) was diluted at 1:500. Following overnight incubation, blots were developed with Cell Signaling Technology secondary antibodies anti-rabbit IgG HRP-linked (#7074, 1:2000

dilution) or anti-mouse IgG HRP-linked (#7076, 1:2000 dilution). Blot signals were detected with the BioRad XRS+ and densitometry analysis was performed with BioRad's Image Lab software. After development of phosphorylated targets, blots were stripped with Restore™ Western Blot Stripping Buffer (ThermoFisher) and re-probed with relevant total protein antibody. All indicated western blots are from the same membrane except Figure 1F, Figure 5A and Supplementary Figure 7A (see individual figure legends for more details).

2.5.5. ELISA analysis

Cultured supernatants from TNBC cell lines treated under indicated conditions were collected after 48 hrs. Human IL-1A, IL-6, and IL-8 ELISAs were performed with previously listed paired capture and detection antibodies according to the manufacturer's instructions. Human prostaglandin E2 (PGE2) ELISA was performed according to the manufacturer's instructions (Cayman 514010- Ann Arbor, MI).

For *in vivo* analysis of human IL-6 in mice implanted with human cell lines, serum was collected after two days of treatment with vehicle or docetaxel. Mouse sera were analyzed with the previously listed human-specific ELISA antibodies for human TNBC produced IL-6 *in vivo*.

2.5.6. RT-PCR

Human TNBC cell lines were cultured in the presence or absence of docetaxel (4 ng/ml) for 48 hrs, and RNA was isolated with Qiagen RNeasy Mini Kit (74104) according to manufacturer's instructions. cDNA synthesis was performed with BioRad's iScript cDNA synthesis kit (1708891) and real-time PCR (RT-PCR) was performed with BioRad's iQ SYBR Green Supermix (1708882) following the manufacturer's instructions on BioRad's CFX96. BioRad items are from Hercules, CA. Primers are listed under **Table 2-1**.

Table 2-1. RT-PCR primer sequences.

primer	Sequence 5' -> 3'
Human IL-1A Forward	CGCCAATGACTCAGAGGAAGA
Human IL-1A Reverse	AGGGCGTCATTCAGGATGAA
Human IL-6 Forward	CAAATTCGGTACATCCTCGACGGC
Human IL-6 Reverse	GGTTCAGGTTGTTTTCTGCCAGTGC
Human COX-2 Forward	TGCATTCTTTGCCCAGCACT
Human COX-2 Reverse	AAAGGCGCAGTTTACGCTGT
Human TBP Forward	TTGGGTTTTCCAGCTAAGTTCT
Human TBP Reverse	CCAGGAAATAACTCTGGCTCA

2.5.7. Mammosphere formation efficiency

TNBC cell lines were cultured as primary mammospheres with MammoCult medium (Stem Cell Tech #05620) supplemented with heparin (Stem Cell Tech #07980) and hydrocortisone (Stem Cell Tech # 07925) according to manufacturer's instructions. Stem Cell Tech items are from Cambridge, MA. Cells were seeded at 24,000 cells per well in 2 mL of complete MammoCult medium in 6-well ultra-low attachment plates. Every two-three days, 1 mL of fresh MammoCult medium was added to the wells. After eight to eleven days, cells were collected with 0.05% trypsin and neutralized with 10% FBS for secondary mammosphere assays. The cells were then re-suspended in complete MammoCult medium and seeded at 8,000 cells per well in 24-well ultra-low attachment plates. Secondary mammospheres were treated under the presence or absence of docetaxel (500 pg/ml) and tocilizumab (30 ng/ml) on day zero. On day three, cells were re-fed with complete MammoCult medium and tocilizumab (30 ng/ml final) was re-added to applicable wells. On day seven, mammospheres were quantified with Incucyte Live-Cell Imaging System and its bundled software. Quantification included a minimum cell area of 1256 μm^2 and mammosphere formation efficiency was calculated as follows: (number of

spheres / 8,000) x 100%. Mammosphere assays were repeated with eight replicates for each treatment group.

2.5.8. Scratch migration assay

TNBC cell lines were seeded overnight in 6-well culture plates and grown to 60-90% confluence. The cell monolayer was then scratched with a p200 pipette tip, and the monolayer was washed with PBS. The monolayer was then left untreated or treated with docetaxel (4 ng/ml) in the presence or absence of IL-6 neutralizing antibody or isotype control antibody (1 μg/ml). The scratch widths were then captured on the EVOS brightfield microscope (ThermoFisher) at 2X magnification for time = 0 hr. Cells were incubated for 40-48 hrs, and then the scratch widths were re-captured at 2X magnification. At all time points, average scratch widths were determined from n = 5 measurements. Percent wound closure was calculated as follows: 100 x [(scratch width at T = 0 hr) – (scratch width at T = final hr)] / (scratch width at T = 0 hr).

2.5.9. Immunofluorescence

SUM-159 cell lines were cultured overnight in eight chambered cell culture slides (Corning 354118) pre-coated with Poly-L-lysine (Sigma P1399). Cells were then treated in the presence or absence of docetaxel (4 ng/ml) for 48 hours and then stained for immunofluorescence. In brief, cells were fixed with 4% paraformaldehyde and permeabilized with 100% methanol. After blocking, cells were stained for Phospho ERK1/2 (R&D MAB1018) overnight at 4C. The next day, cells were washed and stained with goat anti-rabbit Alexa Fluor 546 (ThermoFisher A-11035). Afterwards, cells were washed and stained for IL-1A (R&D MAB200) followed by goat anti-mouse Alexa Fluor 488 (ThermoFisher A-11001). Slides were

mounted with Vectashield (Vector Labs H-1200 from Burlingame, Ca) and sealed with coverslips. Slides were imaged on the EVOS FL Auto Imaging System.

2.5.10. *In vivo* experiments

The Houston Methodist Hospital Research Institute Animal Care and Use Review Office approved this study. All tumor models were developed orthotopically in the mammary fat pad of female NOD scid gamma (NSG) mice and handled as described previously (*58*). In brief, cell lines were injected into the right mammary fat pad of female NSGs: SUM-159 ($3x10^6$), MDA-MB-436 ($9x10^6$) and MDA-MB-468 ($2x10^6$). Patient derived xenografts (PDX) were derived and subtyped as MSL and BL1 as previously described (*46, 58*). After tumors were grown orthotopically to 100–200 mm^3 in volume, mice were randomized into groups of (i) vehicle control, (ii) docetaxel (20 mg/kg), (iii) tocilizumab (20 mg/kg), (iv) docetaxel and tocilizumab (both 20 mg/kg). All groups were treated intraperitoneally once every 2 weeks.
For *in vivo* analysis of murine IL-6 production following docetaxel therapy, female NSG and C57BL/6 mice were treated with vehicle or docetaxel (20 mg/kg). Sera were collected after two days and analyzed with mouse IL-6 ELISA kit (BD Biosciences 550950).

2.5.11. Statistical analysis

Statistical analyses were performed using two-tailed unpaired t-tests in Microsoft Excel. For all mice model experiments, outcomes of interest included tumor growth kinetics, biomarker expression and disease specific survival. Survival outcomes were compared using log-rank (Mantel-Cox) test and visualized using Kaplan-Meier curves. Two-way ANOVA and log-rank (Mantel-Cox) tests were performed using GraphPad Prism 8.

2.6. References

1. E. S. Stovgaard, D. Nielsen, E. Hogdall, E. Balslev, Triple negative breast cancer - prognostic role of immune-related factors: a systematic review. *Acta Oncol* **57**, 74-82 (2018).
2. H. Yao, G. He, S. Yan, C. Chen, L. Song, T. J. Rosol, X. Deng, Triple-negative breast cancer: is there a treatment on the horizon? *Oncotarget* **8**, 1913-1924 (2017).
3. J. Collignon, L. Lousberg, H. Schroeder, G. Jerusalem, Triple-negative breast cancer: treatment challenges and solutions. *Breast Cancer (Dove Med Press)* **8**, 93-107 (2016).
4. C. Denkert, C. Liedtke, A. Tutt, G. von Minckwitz, Molecular alterations in triple-negative breast cancer-the road to new treatment strategies. *Lancet* **389**, 2430-2442 (2017).
5. G. Bianchini, J. M. Balko, I. A. Mayer, M. E. Sanders, L. Gianni, Triple-negative breast cancer: challenges and opportunities of a heterogeneous disease. *Nat Rev Clin Oncol* **13**, 674-690 (2016).
6. P. Khosravi-Shahi, L. Cabezon-Gutierrez, S. Custodio-Cabello, Metastatic triple negative breast cancer: Optimizing treatment options, new and emerging targeted therapies. *Asia Pac J Clin Oncol* **14**, 32-39 (2018).
7. B. D. Lehmann, J. A. Bauer, X. Chen, M. E. Sanders, A. B. Chakravarthy, Y. Shyr, J. A. Pietenpol, Identification of human triple-negative breast cancer subtypes and preclinical models for selection of targeted therapies. *J Clin Invest* **121**, 2750-2767 (2011).
8. B. Jovanovic, I. A. Mayer, E. L. Mayer, V. G. Abramson, A. Bardia, M. E. Sanders, M. G. Kuba, M. V. Estrada, J. S. Beeler, T. M. Shaver, K. C. Johnson, V. Sanchez, J. M. Rosenbluth, P. M. Dillon, A. Forero-Torres, J. C. Chang, I. M. Meszoely, A. M. Grau, B. D. Lehmann, Y. Shyr, Q. Sheng, S. C. Chen, C. L. Arteaga, J. A. Pietenpol, A

Randomized Phase II Neoadjuvant Study of Cisplatin, Paclitaxel With or Without Everolimus in Patients with Stage II/III Triple-Negative Breast Cancer (TNBC): Responses and Long-term Outcome Correlated with Increased Frequency of DNA Damage Response Gene Mutations, TNBC Subtype, AR Status, and Ki67. *Clin Cancer Res* **23**, 4035-4045 (2017).

9. H. Masuda, K. A. Baggerly, Y. Wang, Y. Zhang, A. M. Gonzalez-Angulo, F. Meric-Bernstam, V. Valero, B. D. Lehmann, J. A. Pietenpol, G. N. Hortobagyi, W. F. Symmans, N. T. Ueno, Differential response to neoadjuvant chemotherapy among 7 triple-negative breast cancer molecular subtypes. *Clin Cancer Res* **19**, 5533-5540 (2013).

10. A. S. Khazali, A. M. Clark, A. Wells, Inflammatory cytokine IL-8/CXCL8 promotes tumour escape from hepatocyte-induced dormancy. *Br J Cancer* **118**, 566-576 (2018).

11. H. Kulbe, R. Thompson, J. L. Wilson, S. Robinson, T. Hagemann, R. Fatah, D. Gould, A. Ayhan, F. Balkwill, The inflammatory cytokine tumor necrosis factor-alpha generates an autocrine tumor-promoting network in epithelial ovarian cancer cells. *Cancer Res* **67**, 585-592 (2007).

12. P. Ortiz-Montero, A. Londono-Vallejo, J. P. Vernot, Senescence-associated IL-6 and IL-8 cytokines induce a self- and cross-reinforced senescence/inflammatory milieu strengthening tumorigenic capabilities in the MCF-7 breast cancer cell line. *Cell Commun Signal* **15**, 17 (2017).

13. L. M. Snell, T. L. McGaha, D. G. Brooks, Type I Interferon in Chronic Virus Infection and Cancer. *Trends Immunol* **38**, 542-557 (2017).

14. F. Wu, J. Xu, Q. Huang, J. Han, L. Duan, J. Fan, Z. Lv, M. Guo, G. Hu, L. Chen, S. Zhang, X. Tao, W. Ma, Y. Jin, The Role of Interleukin-17 in Lung Cancer. *Mediators Inflamm* **2016**, 8494079 (2016).

15. J. A. Boyette-Davis, E. T. Walters, P. M. Dougherty, Mechanisms involved in the development of chemotherapy-induced neuropathy. *Pain Manag* **5**, 285-296 (2015).

16. T. Eyob, T. Ng, R. Chan, A. Chan, Impact of chemotherapy on cancer-related fatigue and cytokines in 1312 patients: a systematic review of quantitative studies. *Curr Opin Support Palliat Care* **10**, 165-179 (2016).

17. L. Pusztai, T. R. Mendoza, J. M. Reuben, M. M. Martinez, J. S. Willey, J. Lara, A. Syed, H. A. Fritsche, E. Bruera, D. Booser, V. Valero, B. Arun, N. Ibrahim, E. Rivera, M. Royce, C. S. Cleeland, G. N. Hortobagyi, Changes in plasma levels of inflammatory cytokines in response to paclitaxel chemotherapy. *Cytokine* **25**, 94-102 (2004).

18. P. Schmid, S. Adams, H. S. Rugo, A. Schneeweiss, C. H. Barrios, H. Iwata, V. Dieras, R. Hegg, S. A. Im, G. Shaw Wright, V. Henschel, L. Molinero, S. Y. Chui, R. Funke, A. Husain, E. P. Winer, S. Loi, L. A. Emens, I. M. T. Investigators, Atezolizumab and Nab-Paclitaxel in Advanced Triple-Negative Breast Cancer. *N Engl J Med* **379**, 2108-2121 (2018).

19. E. J. Hillmer, H. Zhang, H. S. Li, S. S. Watowich, STAT3 signaling in immunity. *Cytokine Growth Factor Rev* **31**, 1-15 (2016).

20. Z. Zhong, Z. Wen, J. E. Darnell, Jr., Stat3: a STAT family member activated by tyrosine phosphorylation in response to epidermal growth factor and interleukin-6. *Science* **264**, 95-98 (1994).

21. Z. C. Hartman, G. M. Poage, P. den Hollander, A. Tsimelzon, J. Hill, N. Panupinthu, Y. Zhang, A. Mazumdar, S. G. Hilsenbeck, G. B. Mills, P. H. Brown, Growth of triple-negative breast cancer cells relies upon coordinate autocrine expression of the proinflammatory cytokines IL-6 and IL-8. *Cancer Res* **73**, 3470-3480 (2013).

22. D. E. Johnson, R. A. O'Keefe, J. R. Grandis, Targeting the IL-6/JAK/STAT3 signalling axis in cancer. *Nat Rev Clin Oncol* **15**, 234-248 (2018).

23. N. Kumari, B. S. Dwarakanath, A. Das, A. N. Bhatt, Role of interleukin-6 in cancer progression and therapeutic resistance. *Tumour Biol* **37**, 11553-11572 (2016).

24. G. Horneff, A. C. Schulz, J. Klotsche, A. Hospach, K. Minden, I. Foeldvari, R. Trauzeddel, G. Ganser, F. Weller-Heinemann, J. P. Haas, Experience with etanercept, tocilizumab and interleukin-1 inhibitors in systemic onset juvenile idiopathic arthritis patients from the BIKER registry. *Arthritis Res Ther* **19**, 256 (2017).

25. S. Karkhur, M. Hasanreisoglu, E. Vigil, M. S. Halim, M. Hassan, C. Plaza, N. V. Nguyen, R. Afridi, A. T. Tran, D. V. Do, Y. J. Sepah, Q. D. Nguyen, Interleukin-6 inhibition in the management of non-infectious uveitis and beyond. *J Ophthalmic Inflamm Infect* **9**, 17 (2019).

26. I. S. Afonina, C. Muller, S. J. Martin, R. Beyaert, Proteolytic Processing of Interleukin-1 Family Cytokines: Variations on a Common Theme. *Immunity* **42**, 991-1004 (2015).

27. A. Mantovani, C. A. Dinarello, M. Molgora, C. Garlanda, Interleukin-1 and Related Cytokines in the Regulation of Inflammation and Immunity. *Immunity* **50**, 778-795 (2019).

28. C. A. Hunter, S. A. Jones, IL-6 as a keystone cytokine in health and disease. *Nat Immunol* **16**, 448-457 (2015).

29. K. Echizen, O. Hirose, Y. Maeda, M. Oshima, Inflammation in gastric cancer: Interplay of the COX-2/prostaglandin E2 and Toll-like receptor/MyD88 pathways. *Cancer Sci* **107**, 391-397 (2016).

30. S. Fu, J. Lin, Blocking Interleukin-6 and Interleukin-8 Signaling Inhibits Cell Viability, Colony-forming Activity, and Cell Migration in Human Triple-negative Breast Cancer and Pancreatic Cancer Cells. *Anticancer Res* **38**, 6271-6279 (2018).

31. D. Samanta, D. M. Gilkes, P. Chaturvedi, L. Xiang, G. L. Semenza, Hypoxia-inducible factors are required for chemotherapy resistance of breast cancer stem cells. *Proc Natl Acad Sci U S A* **111**, E5429-5438 (2014).

32. D. Davila-Gonzalez, D. S. Choi, R. R. Rosato, S. M. Granados-Principal, J. G. Kuhn, W. F. Li, W. Qian, W. Chen, A. J. Kozielski, H. Wong, B. Dave, J. C. Chang, Pharmacological Inhibition of NOS Activates ASK1/JNK Pathway Augmenting Docetaxel-Mediated Apoptosis in Triple-Negative Breast Cancer. *Clin Cancer Res* **24**, 1152-1162 (2018).

33. P. C. Liao, S. K. Tan, C. H. Lieu, H. K. Jung, Involvement of endoplasmic reticulum in paclitaxel-induced apoptosis. *J Cell Biochem* **104**, 1509-1523 (2008).

34. N. M. Mhaidat, R. Thorne, X. D. Zhang, P. Hersey, Involvement of endoplasmic reticulum stress in Docetaxel-induced JNK-dependent apoptosis of human melanoma. *Apoptosis* **13**, 1505-1512 (2008).

35. R. Ghosh, L. Wang, E. S. Wang, B. G. Perera, A. Igbaria, S. Morita, K. Prado, M. Thamsen, D. Caswell, H. Macias, K. F. Weiberth, M. J. Gliedt, M. V. Alavi, S. B. Hari, A. K. Mitra, B. Bhhatarai, S. C. Schurer, E. L. Snapp, D. B. Gould, M. S. German, B. J. Backes, D. J. Maly, S. A. Oakes, F. R. Papa, Allosteric inhibition of the IRE1alpha

RNase preserves cell viability and function during endoplasmic reticulum stress. *Cell* **158**, 534-548 (2014).

36. M. Mahameed, T. Wilhelm, O. Darawshi, A. Obiedat, W. S. Tommy, C. Chintha, T. Schubert, A. Samali, E. Chevet, L. A. Eriksson, M. Huber, B. Tirosh, The unfolded protein response modulators GSK2606414 and KIRA6 are potent KIT inhibitors. *Cell Death Dis* **10**, 300 (2019).

37. M. R. de Galarreta, A. Navarro, E. Ansorena, A. G. Garzon, T. Modol, M. J. Lopez-Zabalza, J. J. Martinez-Irujo, M. J. Iraburu, Unfolded protein response induced by Brefeldin A increases collagen type I levels in hepatic stellate cells through an IRE1alpha, p38 MAPK and Smad-dependent pathway. *Biochim Biophys Acta* **1863**, 2115-2123 (2016).

38. J. A. Smith, Regulation of Cytokine Production by the Unfolded Protein Response; Implications for Infection and Autoimmunity. *Front Immunol* **9**, 422 (2018).

39. N. J. Darling, S. J. Cook, The role of MAPK signalling pathways in the response to endoplasmic reticulum stress. *Biochim Biophys Acta* **1843**, 2150-2163 (2014).

40. P. M. LoRusso, S. S. Krishnamurthi, J. J. Rinehart, L. M. Nabell, L. Malburg, P. B. Chapman, S. E. DePrimo, S. Bentivegna, K. D. Wilner, W. Tan, A. D. Ricart, Phase I pharmacokinetic and pharmacodynamic study of the oral MAPK/ERK kinase inhibitor PD-0325901 in patients with advanced cancers. *Clin Cancer Res* **16**, 1924-1937 (2010).

41. Y. Zhao, A. A. Adjei, The clinical development of MEK inhibitors. *Nat Rev Clin Oncol* **11**, 385-400 (2014).

42. S. Liu, J. S. Lee, C. Jie, M. H. Park, Y. Iwakura, Y. Patel, M. Soni, D. Reisman, H. Chen, HER2 Overexpression Triggers an IL1alpha Proinflammatory Circuit to Drive

Tumorigenesis and Promote Chemotherapy Resistance. *Cancer Res* **78**, 2040-2051 (2018).

43. H. Kayama, M. Kohyama, D. Okuzaki, D. Motooka, S. Barman, R. Okumura, M. Muneta, K. Hoshino, I. Sasaki, W. Ise, H. Matsuno, J. Nishimura, T. Kurosaki, S. Nakamura, H. Arase, T. Kaisho, K. Takeda, Heme ameliorates dextran sodium sulfate-induced colitis through providing intestinal macrophages with noninflammatory profiles. *Proc Natl Acad Sci U S A* **115**, 8418-8423 (2018).

44. Y. Murakami, K. Watari, T. Shibata, M. Uba, H. Ureshino, A. Kawahara, H. Abe, H. Izumi, N. Mukaida, M. Kuwano, M. Ono, N-myc downstream-regulated gene 1 promotes tumor inflammatory angiogenesis through JNK activation and autocrine loop of interleukin-1alpha by human gastric cancer cells. *J Biol Chem* **288**, 25025-25037 (2013).

45. J. Manuel Iglesias, I. Beloqui, F. Garcia-Garcia, O. Leis, A. Vazquez-Martin, A. Eguiara, S. Cufi, A. Pavon, J. A. Menendez, J. Dopazo, A. G. Martin, Mammosphere formation in breast carcinoma cell lines depends upon expression of E-cadherin. *PLoS One* **8**, e77281 (2013).

46. T. P. Reddy, D. S. Choi, A. C. Anselme, W. Qian, W. Chen, J. Lantto, I. D. Horak, M. Kragh, J. C. Chang, R. R. Rosato, Simultaneous targeting of HER family pro-survival signaling with Pan-HER antibody mixture is highly effective in TNBC: a preclinical trial with PDXs. *Breast Cancer Res* **22**, 48 (2020).

47. A. Hammacher, L. D. Ward, J. Weinstock, H. Treutlein, K. Yasukawa, R. J. Simpson, Structure-function analysis of human IL-6: identification of two distinct regions that are important for receptor binding. *Protein Sci* **3**, 2280-2293 (1994).

48. N. N. Alraouji, F. H. Al-Mohanna, H. Ghebeh, M. Arafah, R. Almeer, T. Al-Tweigeri, A. Aboussekhra, Tocilizumab potentiates cisplatin cytotoxicity and targets cancer stem cells in triple-negative breast cancer. *Mol Carcinog* **59**, 1041-1051 (2020).

49. D. Wang, J. Xu, B. Liu, X. He, L. Zhou, X. Hu, F. Qiao, A. Zhang, X. Xu, H. Zhang, M. S. Wicha, L. Zhang, Z. M. Shao, S. Liu, IL6 blockade potentiates the anti-tumor effects of gamma-secretase inhibitors in Notch3-expressing breast cancer. *Cell Death Differ* **25**, 330-339 (2018).

50. Y. S. Weng, H. Y. Tseng, Y. A. Chen, P. C. Shen, A. T. Al Haq, L. M. Chen, Y. C. Tung, H. L. Hsu, MCT-1/miR-34a/IL-6/IL-6R signaling axis promotes EMT progression, cancer stemness and M2 macrophage polarization in triple-negative breast cancer. *Mol Cancer* **18**, 42 (2019).

51. N. C. Kampan, S. D. Xiang, O. M. McNally, A. N. Stephens, M. A. Quinn, M. Plebanski, Immunotherapeutic Interleukin-6 or Interleukin-6 Receptor Blockade in Cancer: Challenges and Opportunities. *Curr Med Chem* **25**, 4785-4806 (2018).

52. J. F. Rossi, Z. Y. Lu, M. Jourdan, B. Klein, Interleukin-6 as a therapeutic target. *Clin Cancer Res* **21**, 1248-1257 (2015).

53. E. P. Chen, E. M. Smyth, COX-2 and PGE2-dependent immunomodulation in breast cancer. *Prostaglandins Other Lipid Mediat* **96**, 14-20 (2011).

54. A. S. Hamy, S. Tury, X. Wang, J. Gao, J. Y. Pierga, S. Giacchetti, E. Brain, B. Pistilli, M. Marty, M. Espie, G. Benchimol, E. Laas, M. Lae, B. Asselain, B. Aouchiche, M. Edelman, F. Reyal, Celecoxib With Neoadjuvant Chemotherapy for Breast Cancer Might Worsen Outcomes Differentially by COX-2 Expression and ER Status: Exploratory Analysis of the REMAGUS02 Trial. *J Clin Oncol* **37**, 624-635 (2019).

55. C. Ruegg, O. Dormond, A. Mariotti, Endothelial cell integrins and COX-2: mediators and therapeutic targets of tumor angiogenesis. *Biochim Biophys Acta* **1654**, 51-67 (2004).

56. A. Yuan, J. J. Chen, P. L. Yao, P. C. Yang, The role of interleukin-8 in cancer cells and microenvironment interaction. *Front Biosci* **10**, 853-865 (2005).

57. M. Bilusic, C. R. Heery, J. M. Collins, R. N. Donahue, C. Palena, R. A. Madan, F. Karzai, J. L. Marte, J. Strauss, M. E. Gatti-Mays, J. Schlom, J. L. Gulley, Phase I trial of HuMax-IL8 (BMS-986253), an anti-IL-8 monoclonal antibody, in patients with metastatic or unresectable solid tumors. *J Immunother Cancer* **7**, 240 (2019).

58. R. R. Rosato, D. Davila-Gonzalez, D. S. Choi, W. Qian, W. Chen, A. J. Kozielski, H. Wong, B. Dave, J. C. Chang, Evaluation of anti-PD-1-based therapy against triple-negative breast cancer patient-derived xenograft tumors engrafted in humanized mouse models. *Breast Cancer Res* **20**, 108 (2018).

59. R. D. Lardone, A. A. Chan, A. F. Lee, L. J. Foshag, M. B. Faries, P. A. Sieling, D. J. Lee, Mycobacterium bovis Bacillus Calmette-Guerin Alters Melanoma Microenvironment Favoring Antitumor T Cell Responses and Improving M2 Macrophage Function. *Front Immunol* **8**, 965 (2017).

3. FIRST-IN-CLASS PHASE 1/2 CLINICAL TRIAL TARGETING NITRIC OXIDE IN TREATMENT OF CHEMORESISTANT TRIPLE-NEGATIVE BREAST CANCER PATIENTS*

3.1. Abstract

The inducible nitric oxide signaling (iNOS) pathway is associated with poor prognosis in triple-negative breast cancer (TNBC). Prior studies using *in vivo* models showed that the inhibition of the iNOS pathway by using the pan-NOS inhibitor NG-monomethyl-L-arginine (L-NMMA) reduced tumor growth and enhanced survival. Here, we report a first-in-class phase 1/2 trial of L-NMMA plus taxane for patients with chemorefractory locally advanced (LABC) or metastatic TNBC, as well as immune correlates to therapy response. A total of 35 TNBC patients were recruited (phase 1, n=15; phase 2, n= 24, including 4 recommended phase 2 dose (RP2D) patients from phase 1). In phase 2, 54.2% had metastatic TNBC (with 5 median prior lines of chemotherapy) and 45.8% had LABC (anthracycline-refractory). Overall response rate (ORR) was 45.8% (11/24); 81.8% (9/11) for LABC and 15.4% (2/13) for metastatic TNBC. Among the LABC patients, 3 patients had a pathological complete response (CR) at surgery (27.3%). Grade ≥3 toxicity was noted in 21% of patients; however, none was attributed to L-NMMA. Correlative data analyzed by imaging CyTOF showed that non-responders had a significantly higher expression of biomarkers associated with M2 macrophage polarization and levels of circulating IL-6 and IL-10, observations consistent with higher circulating M2 macrophages in non-responder peripheral blood mononuclear cell (PBMC). In contrast, responders may have decreased pro-tumor N2 neutrophils at end of therapy. This combination warrants further investigation in larger studies along with the evaluation of M2 macrophage and N2 neutrophil biomarkers as a potential predictor to iNOS targeted therapy.

* Reprinted with permission from "A phase 1/2 clinical trial of the nitric oxide synthase inhibitor L-NMMA and taxane for treating chemoresistant triple-negative breast cancer" by Andrew W Chung; Kartik Anand; Ann C Anselme; Alfred A Chan; Nakul Gupta; Luz A Venta; Mary R Schwartz; Wei Qian; Yitian Xu; Licheng Zhang; John Kuhn; Tejal Patel; Angel A Rodriguez; Anna Belcheva; Jorge Darcourt; Joe Ensor; Eric Bernicker; Ping-Ying Pan; Shu Hsia Chen; Delphine J Lee; Polly A Niravath; Jenny C Chang, 2021. *Science Translational Medicine*, Volume 13, Pages 1-11, Copyright 2021, The Authors.

3.2. Introduction

Triple-negative breast cancer (TNBC) constitutes 10-20% of all breast cancers and is characterized by the lack of expression of estrogen receptor (ER), progesterone receptor (PR), and human epidermal growth factor receptor 2 (HER2) (*1, 2*). Increased risk of metastases is one of the main reasons for increased mortality in TNBC patients (*2*). Conventional therapy may eliminate most of the tumor cells except breast cancer stem cells (BCSCs) which have tumor-initiating properties (*3*). Two previously identified putative genes, namely ribosomal protein L39 (RPL39) and myeloid leukemia factor 2 (MLF2), regulated by inducible nitric oxide signaling (iNOS, NOS2) pathway may play a role in BCSCs' self-renewal and metastasis (*4*). Robust published preclinical data have demonstrated that increased iNOS expression in various cancers, including TNBC, is associated with poor prognosis (*5-7*). We have previously published that NOS inhibition with the pan-NOS inhibitor NG-monomethyl-L-arginine (L-NMMA) decreased cell proliferation, migration, and mammosphere formation in vitro and significantly reduced tumor growth, lung metastases, tumor initiation, and self-renewal in TNBC patient-derived xenograft (PDX) models (*8*). Based on these data, we planned a first-in-class phase 1/2 trial of L-NMMA plus taxane for patients with chemorefractory locally advanced or metastatic TNBC. L-NMMA has been studied in the management of cardiogenic shock in an international, multicenter, phase 3 placebo-controlled trial and was well tolerated with a safe toxicity profile (*9*).

The primary objectives of the clinical trial were 1) to assess the maximum tolerated dose (MTD) of L-NMMA when combined with docetaxel in the treatment of refractory locally advanced or metastatic TNBC patients, and 2) to determine the efficacy of L-NMMA combined with a taxane, as assessed by the Response Evaluation Criteria in Solid Tumors (RECIST) 1.1. Secondary objectives were 1) to describe the dose-limiting toxicities (DLTs) and other toxicities

associated with L-NMMA when combined with taxane as assessed by the Common Terminology Criteria for Adverse Events (CTCAE) v4.03, and 2) to determine the recommended phase 2 dose (RP2D) of L-NMMA when combined with docetaxel/amlodipine. The exploratory objectives were 1) to study the plasma pharmacokinetics (PK) and pharmacodynamics (PD) of L-NMMA, 2) to measure circulating serum cytokines, 3) to describe changes in tumor immune microenvironment with 35 biomarkers evaluated using multiplex immunohistochemistry with Hyperion tissue imaging, and 4) to describe changes peripheral blood mononuclear cells (PBMCs) using CyTOF.

3.3. Results

3.3.1. Patient characteristics

From July 2016 to September 2020, 35 patients were enrolled in this phase 1/2 study -15 patients recruited into the dose-finding phase 1 portion (flow diagram description **Fig. 3-1A**), and a total of 24 patients (including 4 from phase 1) recruited for the phase 2 efficacy study (consort diagram **Fig. 3-1B**, **Table 3-1**). The median age of the whole cohort was 59 years (36-75 years). Sixty-nine percent of patients had metastatic disease and 31% of the patients had chemotherapy-refractory locally advanced breast cancer (LABC).

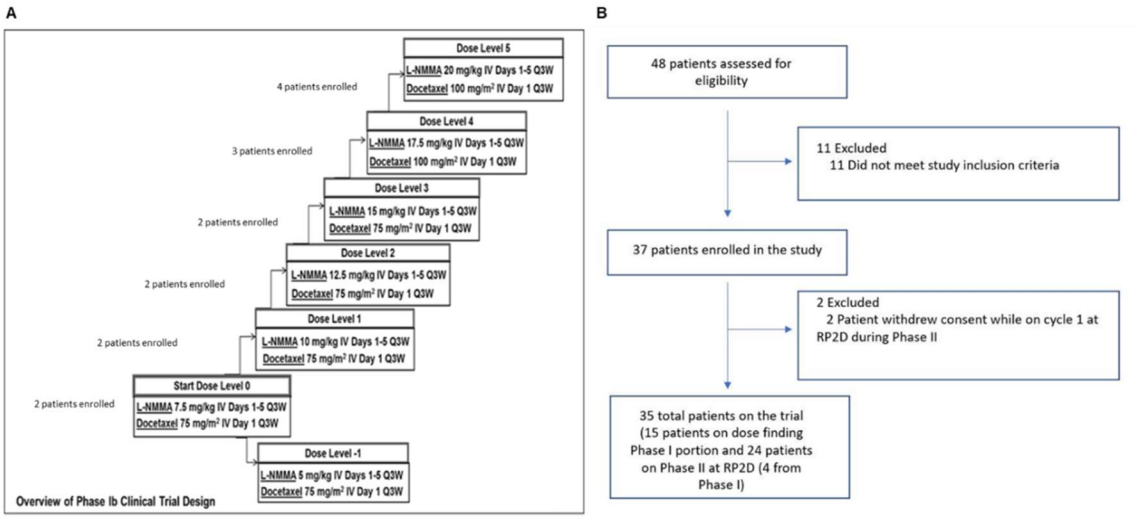

Figure 3-1. Overview of phase 1b recruitment to determine recommended phase II dose.

(**A**) Investigation of combination doses of docetaxel (two doses) and L-NMMA (seven doses) to determine recommended phase II dose (RP2D). (**B**) Consort diagram.

Table 3-1. Patient Characteristics

	Phase I (n=15)	Phase II (n=24; 4 from Phase I)	Total patients (n=35)
Median age, years (range)	62 (46-68)	58.5 (36-75)	59 (36-75)
Race			
Non-Hispanic Caucasian	6 (40%)	14 (58.3%)	19 (54.3%)
Hispanic Caucasian	2 (13.3%)	0 (0%)	2 (5.7%)
African American	6 (40%)	8 (33.3%)	12 (34.3%)

Asian	1 (6.7%)	2 (8.3%)	2 (5.7%)
Stage			
Metastatic breast cancer	13 (86.7%)	13 (54.2%)	24 (68.6%)
Locally advanced	2 (13.3%)	11 (45.8%)	11 (31.4%)
Median prior lines of chemotherapy (range)	4 (3-7)	5 (2-7)	4.5 (3-7)

In the phase 1 portion, 87% of patients had metastatic disease, while 13% had locally advanced breast cancer refractory to anthracycline-based chemotherapy (all locally advanced patients had doxorubicin plus cyclophosphamide as the first regimen). Of 24 patients enrolled in phase 2, 54% percent (13 patients) had metastatic disease with five median prior lines of chemotherapy, and 46% (11 patients) had chemorefractory LABC.

3.3.2. Pharmacodynamics and pharmacokinetics

To determine successful targeting of iNOS, we assayed patients' sera for the main metabolites of nitric oxide, namely serum nitrates and nitrites (*10*). The concentration of total

serum nitrates and nitrites decreased significantly in Cycle 1 from baseline (Day 1) mean of 22.3 uM to Day 2 mean of 13.6 uM ($p<0.0001$) (**Fig. 3-2A**).

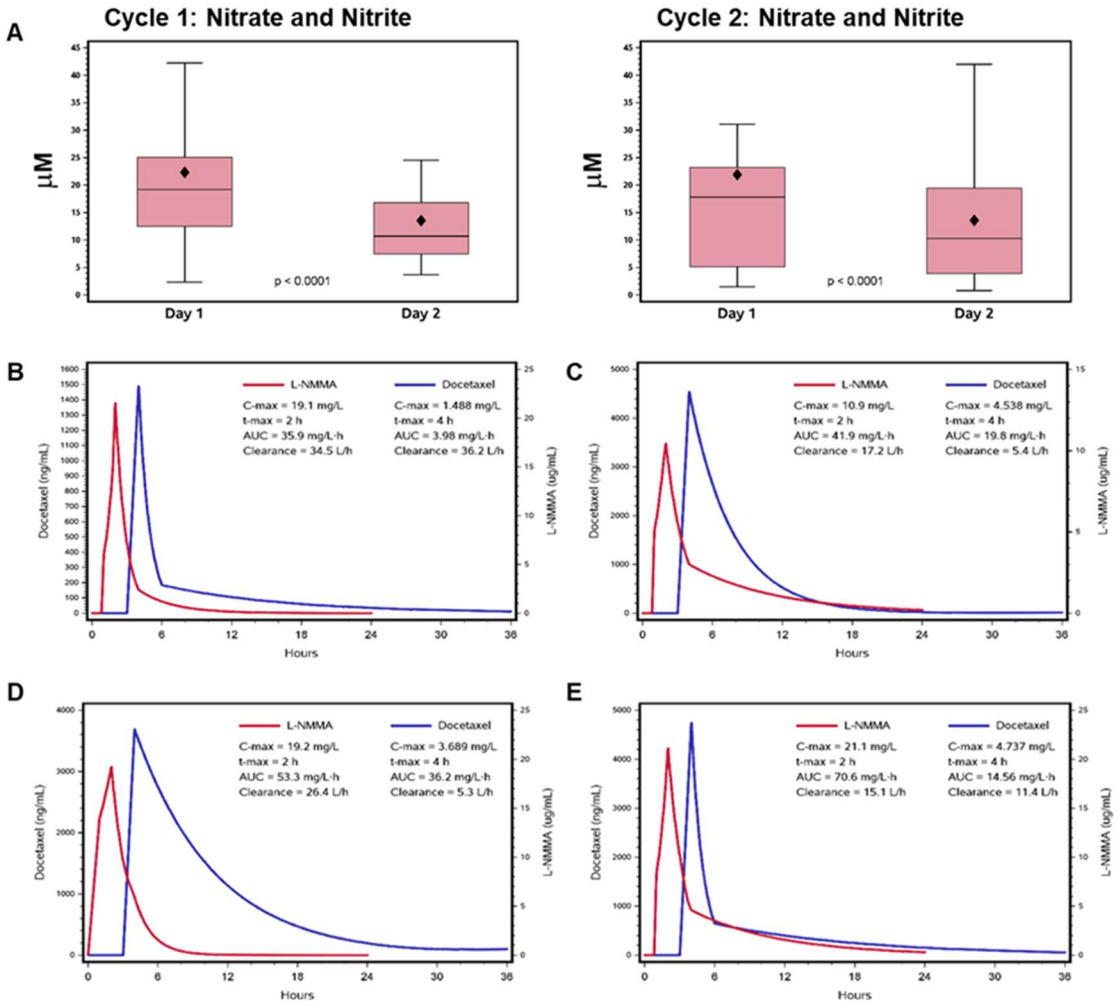

Figure 3-2. Pharmacodynamics from RP2D patients and pharmacokinetics analysis of docetaxel and L-NMMA.

(**A**) Shown are pharmacodynamics (PD) data by measurement of patients' sera for NO metabolites nitrates and nitrites. Median values for each time point were normalized to starting day for each cycle: Cycle 1 time points were normalized to Day 1; Cycle 2 time points were normalized to Day 22. Pharmacokinetics data of L-NMMA and docetaxel clearance are shown for patients (**B**) 100_010, (**C**) 100_013, (**D**) 100_015, and (**E**) 100_016. Friedman's test was performed to determine the significance of PD data comparing Day 2 to respective baseline Day 1 for each cycle.

Similarly, the concentration of total serum nitrates and nitrites significantly decreased in Cycle 2 from baseline (Day 1) mean of 21.9 uM to Day 2 mean of 13.6 uM ($p<0.0001$). This pharmacodynamics (PD) data indicates successful on-target suppression of the iNOS pathway in the trial participants. Next, to determine the pharmacokinetics (PK), we assayed the sera from two patients receiving 15 mg/kg L-NMMA and 75 mg/m^2 docetaxel (**Fig. 3-2B and 3-2C**) and two patients receiving 17.5 mg/kg L-NMMA and 100 mg/m2 docetaxel (**Fig. 3-2D and 3-2E**). For all patients regardless of dosage, we observed rapid clearance of both drugs as Tmax for L-NMMA was 2 hours and Tmax for docetaxel was 4 hours, consistent with the reported rapid clearance of both agents (*11, 12*). Cumulatively, our PD and PK data show effective targeting of iNOS and reproducible clearance of both agents.

3.3.3. Phase I dose-limiting toxicities

Of the 15 patients that were recruited, one patient had treatment-associated syncope at 17.5 mg/kg L-NMMA which resolved rapidly with intravenous fluids, and one patient had arterial thrombosis at 20 mg/kg which was successfully treated with thrombectomy and anticoagulation.

3.3.4. Phase 2 toxicities

While 83.3% of patients experienced any grade toxicity, only 20.8% of the patients had documented Grade ≥ 3 toxicity. None of the Grade ≥3 toxicity was attributed to L-NMMA (**Table 3-2**).

Table 3-2. Phase II Toxicities

Toxicity	Grade 1 or 2 79.2% (19/24)	Grade ≥3 20.8% (5/24)	Any Grade 83.3% (20/24)	Likely attributed to L-NMMA	Likely attributed to Taxane
Constitutional	10 (41.7%)	1 (4.2%)	11 (45.8%)	No	Yes
Gastrointestinal	10 (41.7%)	0 (0%)	10 (41.7%)	No	Yes
Peripheral neuropathy	7 (29.2%)	1 (4.2%)	8 (33.3%)	No	Yes
Dermatological	7 (29.2%)	1 (4.2%)	8 (33.3%)	No	Yes
Musculoskeletal	5 (20.8%)	0	5 (20.8%)	No	Yes
Hematological	5 (20.8%)	0	5 (20.8%)	No	Yes
Mucositis	4 (16.7%)	0	4 (16.7%)	No	Yes
Pulmonary	4 (16.7%)	0	4 (16.7%)	Yes	No
Infectious	0	2 (8.3%)	2 (8.3%)	No	Yes

Cardiovascular	2 (8.3%)	0	2 (8.33%)	Yes	No
Renal	0	1 (4.16%)	1 (4.16%)	No	Yes
Elevation AST /ALT	0	1 (4.16%)	1 (4.16%)	No	Yes
Dehydration	0	1 (4.16%)	1 (4.16%)	No	Yes
Electrolyte imbalance	1 (4.16%)	0	1 (4.16%)	No	Yes
Hypotension	1 (4.16%)	0	1 (4.16%)	Yes	No
Neurological	1 (4.16%)	0	1 (4.16%)	No	Yes
Sinus tachycardia	1 (4.16%)	0	1 (4.16%)	Yes	No

Two patients were counted as treatment failure as they were taken off study due to adverse events (AEs) prior to the first restaging scan post Cycle 2 - one patient had thrombectomy for right common carotid arterial thrombosis, and the second patient had pneumonia with Cycle 2. Adverse events possibly attributed to L-NMMA included four patients with pulmonary symptoms - grade 1 cough (n=2), and grade 1 dyspnea (n=1), grade 2 dyspnea (n=2); 2 patients with chest pain that resolved without any intervention; one patient with sinus tachycardia which resolved without any intervention; and one patient with hypotension which resolved with oral hydration. Systolic and

diastolic BP was measured before the first dose of L-NMMA on Cycle 1, and at the end of Cycle 2. Twenty-two patients received 2 complete cycles of L-NMMA and docetaxel; two discontinued early due to toxicity. Mean systolic BP for the 21 evaluable patients marginally increased from 117.7 (95% CI 108.4, 127.1) at baseline to 133.0 (95% CI 121.6,144.4) at end of Cycle 2. Mean diastolic BP increased from 62.5 (95% CI 57.7, 67.2) at baseline to 73.2 (95% CI 67.9, 78.5) (See **Table 3-3** and **Fig. 3-3**).

Table 3-3. Change in Mean and Median blood pressure from baseline to end of cycle 2 for 21 patients who had at least 2 cycles of L-NMMA and docetaxel.

Blood Pressure	Time Period	N	Mean	95% CI Bounds for Mean		Std Dev	Median	95% CI Bounds for Median		Min	Max	p-value	
												Paired *t*-test	Signed-rank
Systolic	Baseline	21	117.7	108.4	127.1	20.5	113.0	102	135	92	159	0.0002	< 0.0001
	Remeasure	21	133.0	121.6	144.4	25.0	131.0	109	154	102	185		
Diastolic	Baseline	21	62.5	57.7	67.2	10.4	61.0	55	67	48	87	< 0.0001	< 0.0001
	Remeasure	21	73.2	67.9	78.5	11.7	74.0	70	76	53	99		

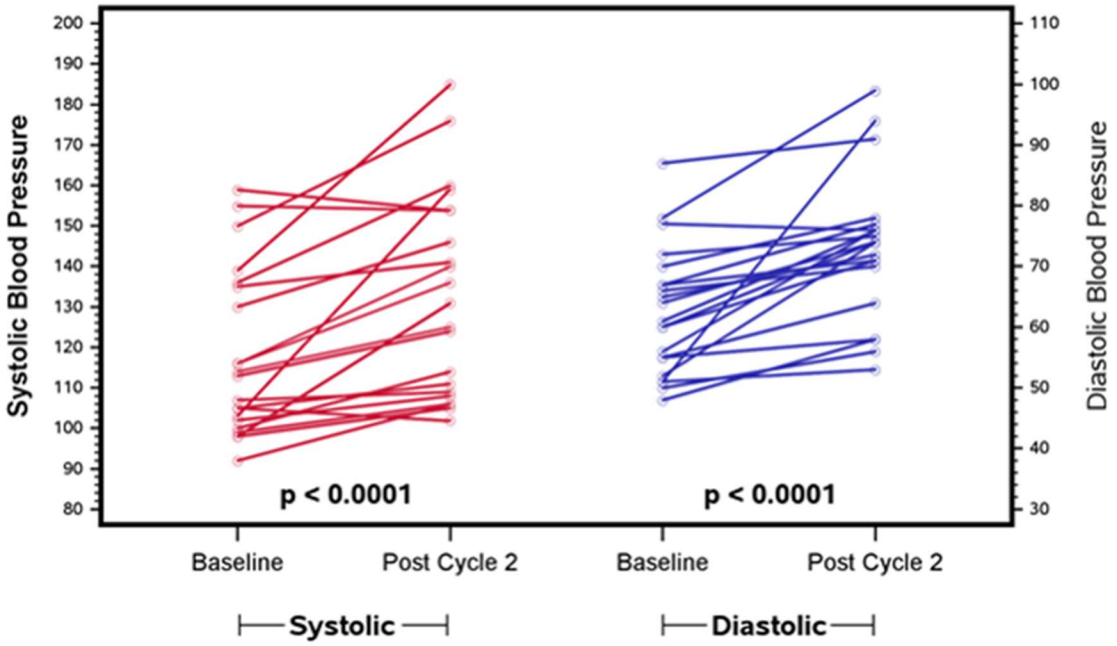

Figure 3-3. Changes in blood pressure comparing baseline to end of Cycle 2.
Significant changes in systolic and diastolic blood pressure in 21 patients comparing baseline to after 2 cycles of therapy were determined by paired t-test and signed-rank.

3.3.5. Phase 2 efficacy

Percent change in tumor sizes (**Fig. 3-4A)** suggested clinical durability of combining L-NMMA with chemotherapy in TNBC patients.

A

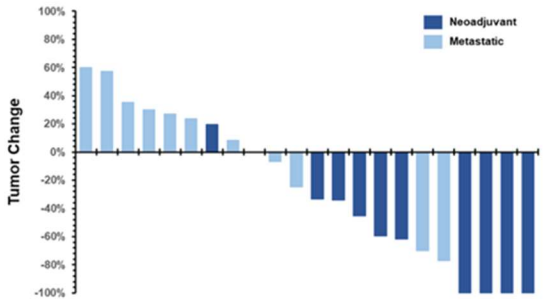

B

Phase 2 efficacy responses

Best Response	All patients (n=24)	Metastatic (n=13)	Chemorefractory LABC (n=11)
Overall Response	11 (45.8%)	2 (15.4%)	9 (81.8%)
CR	4 (16.7%)	0 (0%)	4 (36.4%)
PR	7 (29.2%)	2 (15.4%)	5 (45.5%)
SD	4 (16.7%)	3 (23.1%)	1 (9.1%)
PD	7 (29.2%)	6 (46.2%)	1 (9.1%)
Treatment failure	2 (8.3%)	2 (15.4%)	0 (0%)

Figure 3-4. Phase 2 efficacy of L-NMMA and taxane therapy in TNBC patients.
(**A**) Shown is a waterfall plot of tumor size changes from 22 TNBC patients treated at RP2D of L-NMMA. Two RP2D patients were withdrawn due to toxicity. (**B**) Shown are the phase 2 efficacy responses.

The overall response rate (ORR) for patients treated at RP2D was 45.8% (11/24). Among the patients with chemorefractory locally advanced disease (LABC), the overall response rate was 81.8% (9/11); 36.36% (4/11) complete response (CR), and 45.45% (5/11) partial response (PR). In patients with metastatic disease, the response rate was 15.4% (2/13). The median number of prior chemotherapy regimens for patients with metastatic disease was 5 lines (range, 2-7). Among four patients with chemorefractory LABC who had CR as per imaging, three were found to have a pathologic complete response (pCR) at surgery and one had residual cancer burden-II (RCB-II) at surgery. Thus, the pCR rate for chemorefractory LABC was noteworthy at 27.3% (3/11). **Fig. 3-5** (**A and B**) is from representative Patient #100-48 with advanced chemorefractory metaplastic breast cancer, a subtype of highly chemoresistant TNBC with the worst prognosis, comparing baseline (BL) and end of therapy (EOT) images.

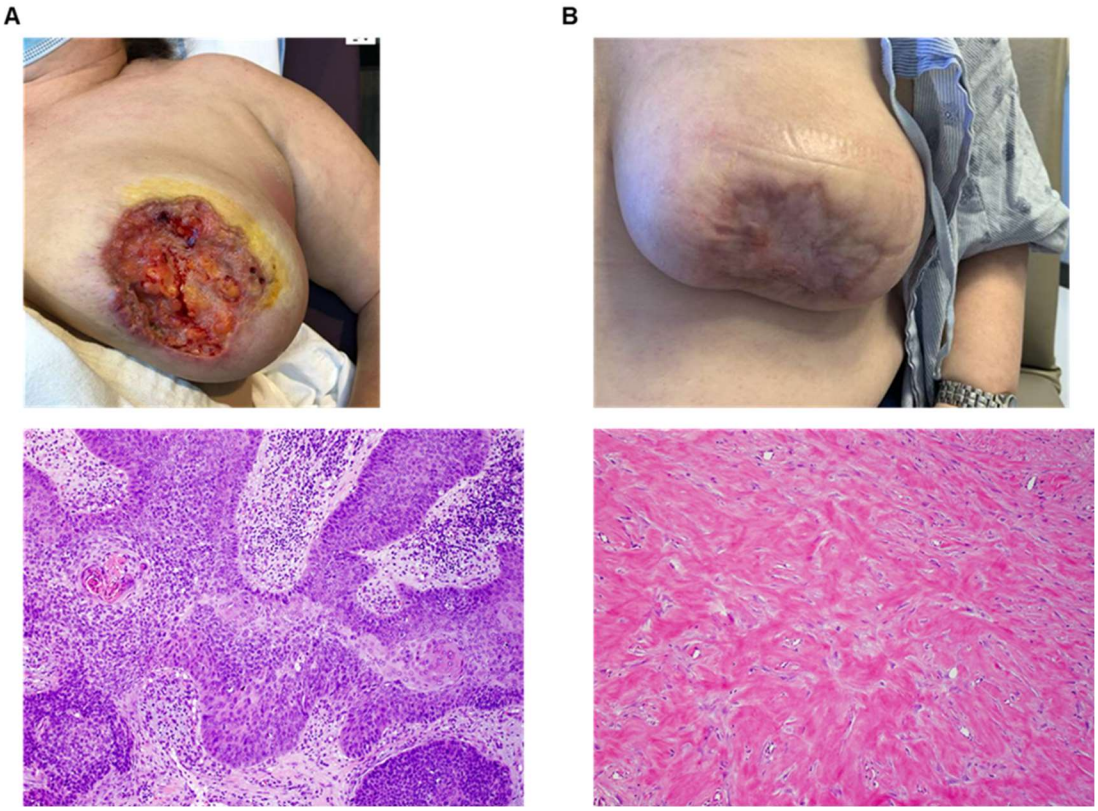

Figure 3-5. Response for patient 100-48 with chemorefractory LABC.
Patient 100-48 who had chemotherapy-refractory locally advanced metaplastic triple-negative breast cancer **(A)** at baseline, after having received 4 cycles of doxorubicin and cyclophosphamide, and before trial enrollment. **(B)** Pathologic complete response in breast post neoadjuvant chemotherapy with L-NMMA and docetaxel.

The skin ulceration and tumor mass responded to the study regimen despite no response to anthracyclines. At surgery, she was found to have pathologic complete response in her breast. The clinical benefit rate (CR, PR, and SD) for LABC was 90.9% (10/11) and 53.8% (7/13) for patients with metastatic disease (**Fig. 3-4B**).

3.3.6. Circulating cytokines

A panel of 38 circulating cytokines was determined by the Luminex assay at Day 1 (baseline), Day 2, and Day 5 of Cycles 1 and 2 for twenty patients (13 responders and 7 non-responders). Twenty-one cytokines increased over time in all patients, with the highest increase on Day 5 for both Cycles 1 and 2 (**Fig. 3-6A** and **Fig. 3-7A**).

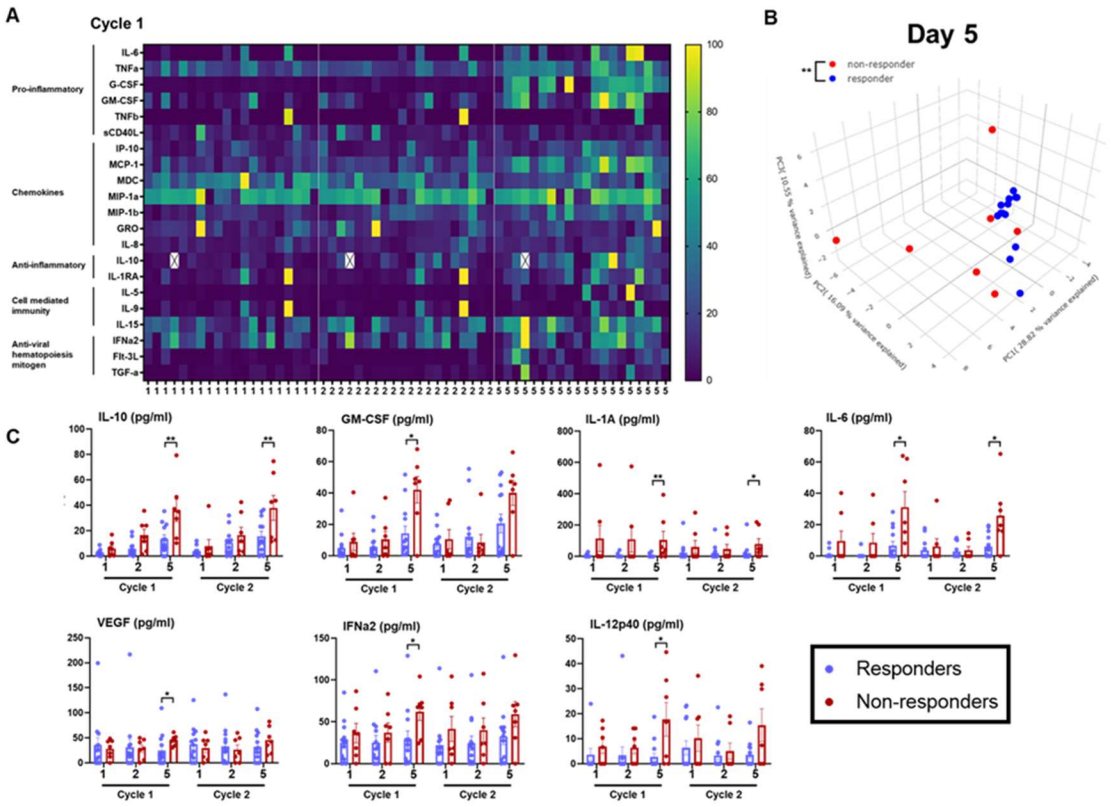

Figure 3-6. Circulating cytokines analysis in RP2D patients.

(A) Heat map of statistically significant circulating cytokines and chemokines during treatment from 20 patients treated at RP2D. For each cytokine, data was standardized to set the highest measured value as 100 by a constant. Next, each unique constant was multiplied to respective cytokines to normalize the expression scale from zero to 100, and significant changes on Days 2 and 5 in respect to baseline were determined by paired t-test. Shown are standardized cytokine values from cycle 1: Days 1, 2, and 5. (**B**) Principal component analysis between responders (13) versus non-responders (7) was performed on Day

5, significance was determined by PERMANOVA. (**C**) 20 patients' sera from indicated time points were analyzed by Luminex for 38 circulating cytokines/chemokines. Shown are the significant differential expression between responders (13) versus non-responders (7). Significance was determined with pairwise analysis by Wilcoxon Ranked-Sum test. For all statistical analysis: * $p < 0.05$; ** $p < 0.01$.

These cytokines represented diverse categories including pro-inflammatory cytokines, anti-inflammatory cytokines, chemokines, cell-mediated immune cytokines, hematopoiesis, mitogen, and anti-viral inflammatory markers. The heat map indicates increased circulating cytokines (*13-17*), including TNF-a, IL-10, IL-6, and IL-8 with treatment. Next, as exploratory analysis for predictive biomarkers, principal component analysis (PCA) showed that non-responder patients had significantly greater global changes vs. responder patients on Day 5 for both cycles (**Fig. 3-6B** and **Fig. 3-7B**).

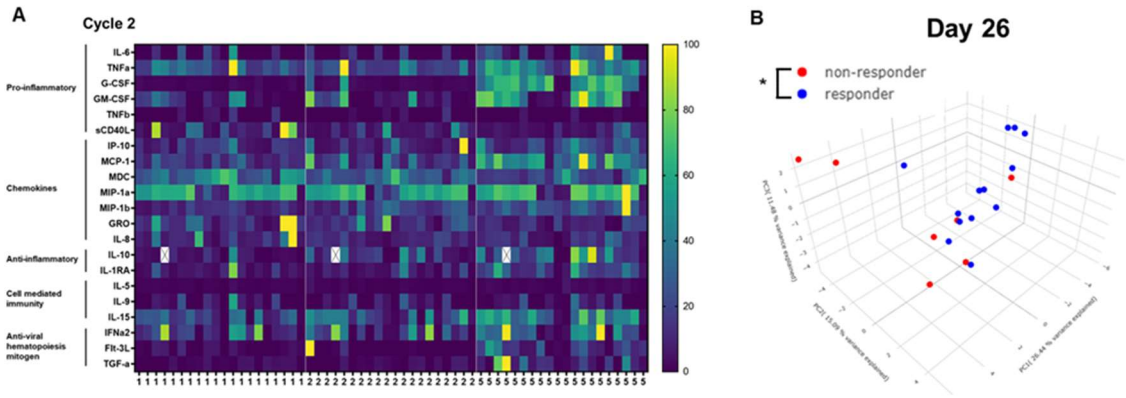

Figure 3-7. Cycle 2 sera cytokines analysis in RP2D patients.
(A) Heat map of statistically significant circulating cytokines and chemokines during treatment from 20 patients treated at RP2D. For each cytokine, data was standardized to set the highest measured value as 100 by a constant. Next, each unique constant was multiplied to respective cytokines to normalize the expression scale from zero to 100, and significant changes on Days 2 and 5 in respect to baseline were

determined by paired t-test. Shown are standardized cytokine values from Cycle 2: Days 1, 2, and 5. **(B)** Principal component analysis between responders (13) versus non-responders (7) was performed on Day 26, significance was determined by PERMANOVA. For all statistical analysis: * $p < 0.05$; ** $p < 0.01$.

By Wilcoxon ranked-sum test, non-responder patients had significantly higher levels of GM-CSF during Cycle 1 and increased IL-10, IL-1A, and IL-6 in both cycles (**Fig. 3-6C**). VEGF, IFNa2, and IL-12p40 were also significantly different between responders and non-responders, the physiological relevance of these findings will be investigated in follow-up clinical studies.

3.3.7. CyTOF

To profile circulating immune populations, we analyzed PBMC by CyTOF from two responders vs. two non-responders at baseline, Day 17 (during Cycle 1) and Day 38 (during Cycle 2). Log2 fold change analysis during Cycle 1 and 2 in respect to baseline for cell percentage over CD45+ was performed on each patient. During Cycle 1 (Day 17), we observed a trend that responders have higher CD4 and CD8 populations compared to non-responders, whereas non-responders have a higher representation of the monocyte family (**Fig. 3-8A**).

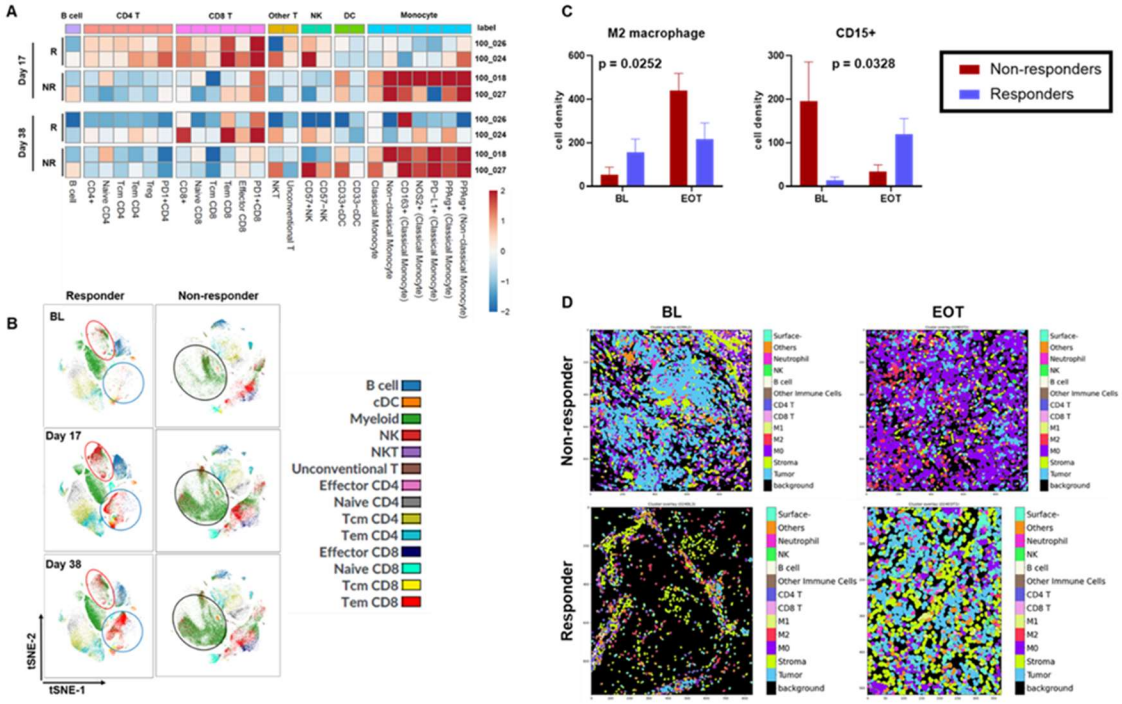

Figure 3-8. Peripheral blood and tissue analysis for cellular phenotyping in RP2D patients.

Two responder patients and two non-responder patients' baseline, day 17 and day 38 peripheral blood mononuclear cells were analyzed by CyTOF. (**A**) Heatmap expressing Log2 fold change of day 17 and day 38 in respect to baseline for all four patients for cell percentage over CD45+ population. (**B**) Shown are tSNE plots for one responder and one non-responder patient at indicated time points. (**C**) Three responder patients and three non-responder patients' paired baseline (BL) and end of treatment (EOT) tissue sections were analyzed by Imaging Mass Cytometry (IMC). Group analysis of CD15 and M2 macrophages comparing changes from BL to EOT between the responders vs. non-responders. Significance was determined by mixed model two-way ANOVA. (**D**) Shown are representative IMC metacluster overlays of one non-responder patient and one responder patient.

These trends were consistent during Cycle 2 (Day 38) except for no observable difference in CD4 populations between the two groups. The CyTOF cell percentage over CD45+ data is shown in **Fig. 3-9** for all four patients.

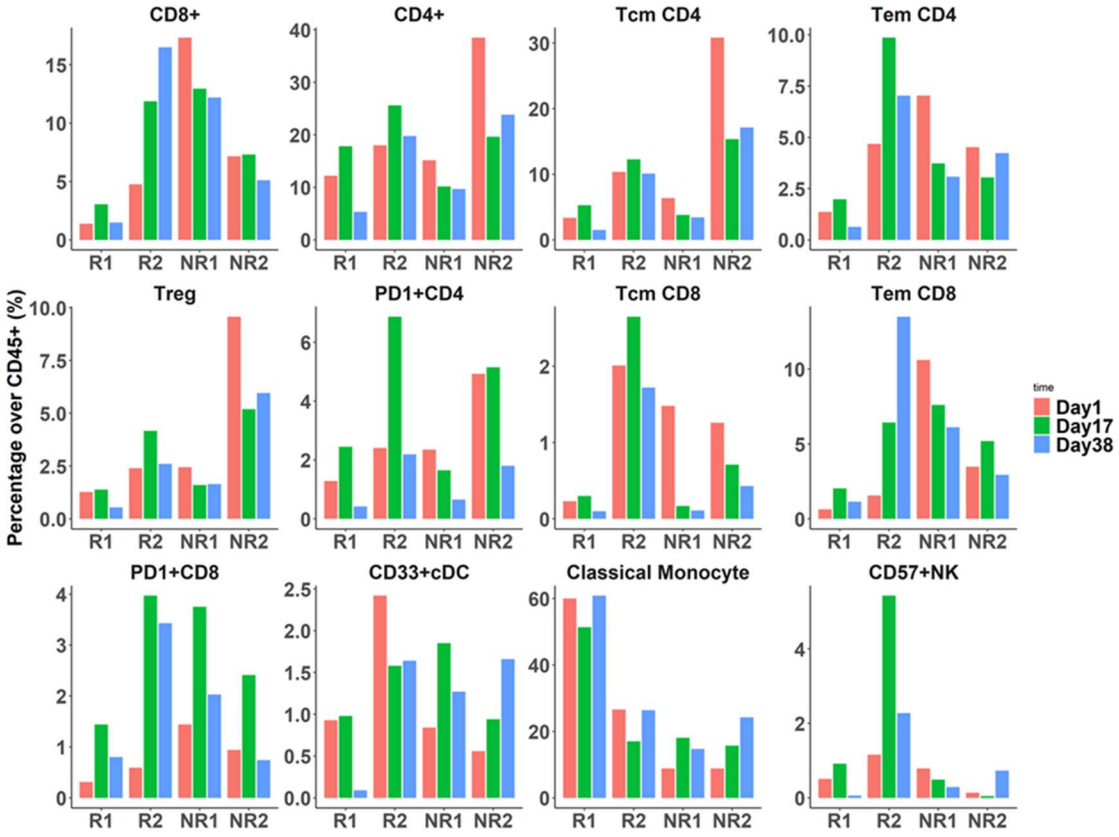

Figure 3-9. CyTOF analysis on peripheral blood mononuclear cells from RP2D patients.

Two responder patients and two non-responder patients' baseline, day 17 and day 38 peripheral blood mononuclear cells were analyzed by CyTOF for cell percentage over CD45+ population. Cell percentage data is shown for all four patients at indicated time points.

To visualize the differences, we observed by tSNE plots an increase in CD8 effector memory cells in responder patients and an increase in myeloid cells in non-responder patients throughout therapy (**Fig. 3-8B**).

3.3.8. Tissue imaging mass cytometry

After assessing differences in PBMCs between the two groups, we next investigated intratumor immune profiling. To identify tumor immune cell infiltration, we performed imaging mass cytometry (IMC) analysis on 35 cell surface markers comparing baseline (BL) to end of treatment (EOT) breast cancer tissue from three responders vs. three non-responders. We first visualized the represented metacluster IMC data from all six patients by tSNE (**Fig. 3-10**).

Metacluster	Celltype
1	Tumor
2	Stroma
3	M2
4	M1
5	M0
6	CD4 T
7	CD8 T
8	B cell
9	Neutrophil
10	NK
11	Other Immune Cells
12	Others
13	Surface-

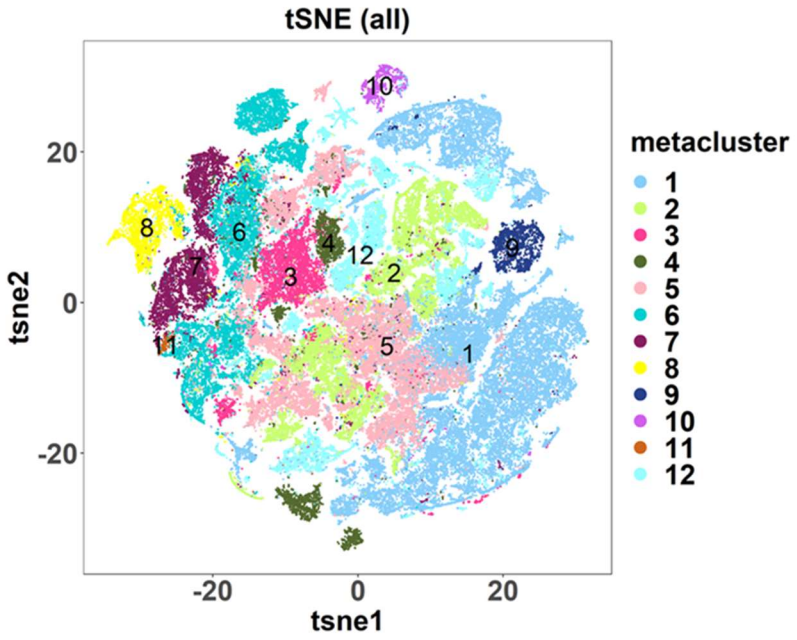

Figure 3-10. IMC analysis on tissue from RP2D patients.

Three responder patients and three non-responder patients' paired baseline (BL) and end of treatment (EOT) tissue sections were analyzed by Imaging Mass Cytometry (IMC). Shown are tSNE plots for indicated metaclusters from all six patients.

Two-way ANOVA from the IMC showed that the non-responders had a significantly increased M2 macrophage, while responders had significantly increased CD15+ granulocyte population at EOT (**Fig. 3-8C**). Metacluster images from non-responder and responder are shown as representation from group analysis (**Fig. 3-8D**). CD15 is a pan-granulocyte marker (*18*). As neutrophils represent 70% of all white blood cells (*19*), we investigated for a neutrophil-specific marker, myeloperoxidase (MPO) (*20*) by immunohistochemical staining in paired IMC patients. Due to insufficient tissue at EOT from the third IMC responder in post-treatment tissue, two

additional responders were substituted for a total of four responders in MPO+ neutrophils analysis. MPO staining aligned with our IMC results showing no significant changes of CD15 granulocytes at EOT in non-responders (**Fig. 3-11A**), but a significant increase of CD15 granulocytes in two matched responders (**Fig. 3-11B**, two patients left side).

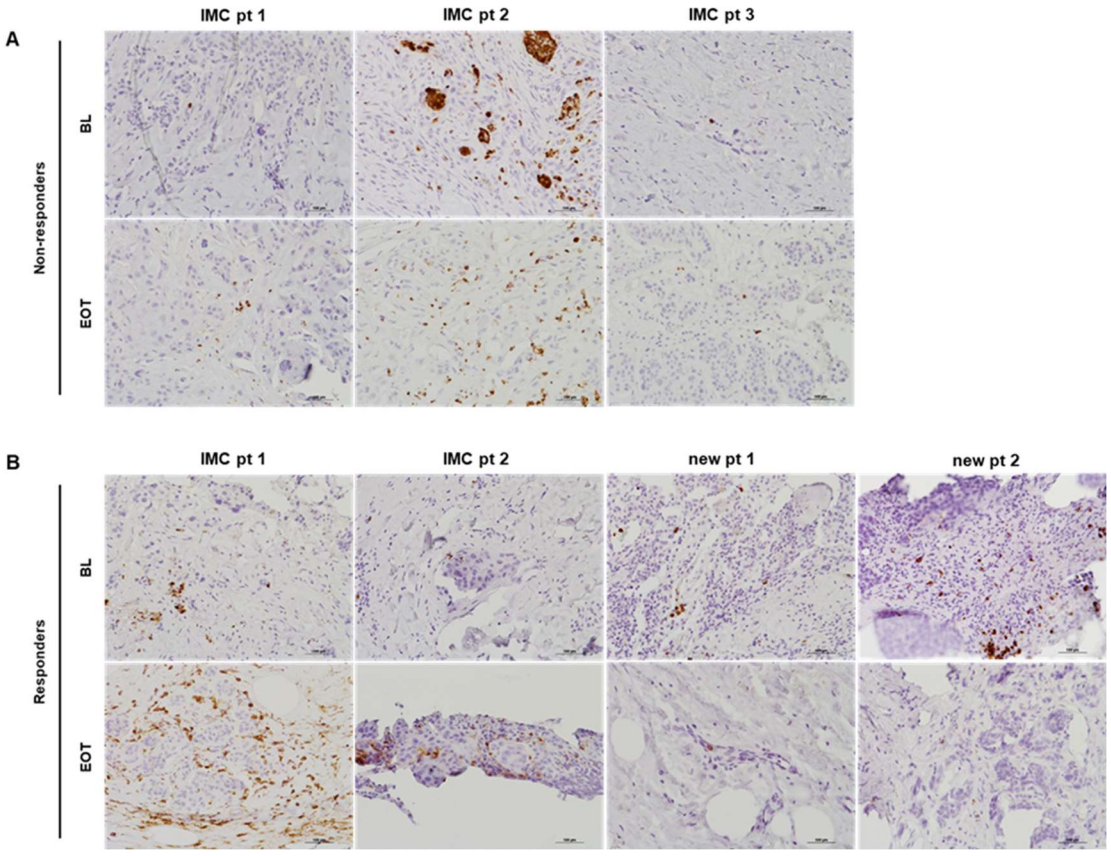

Figure 3-11. Immunohistochemistry staining for MPO in RP2D patients.
Shown are 10X IHC staining images for myeloperoxidase from **(A)** three non-responder patients and **(B)** four responder patients. Scale bar represents 100 μm.

While the other two responders did not mirror this increase of CD15 granulocytes at EOT (**Fig. 3-11B**, two patients' right side), our data suggest that some responders may have an influx of neutrophils at EOT, an observation that is not apparent in non-responders.

Next, to determine the functional relevance of changes in neutrophils over time in responders, we performed immunofluorescence (IF) staining on the above-mentioned tissues. There is growing evidence that neutrophils can be polarized into different activation states (*21-24*). N1 neutrophils have anti-tumor characteristics and low levels of arginase, while N2 neutrophils are immunosuppressive, supporting a pro-tumor microenvironment with high levels of arginase. The arginase expression-dependent neutrophil polarization plays a critical function in anti-tumor immunity as deprivation of arginine leads to loss of T cell function and proliferation (*22, 25*). Therefore, we investigated double IF labeling for MPO (neutrophil marker) and arginase as a potential marker to distinguish between N1 and N2 neutrophils in patient tissues.

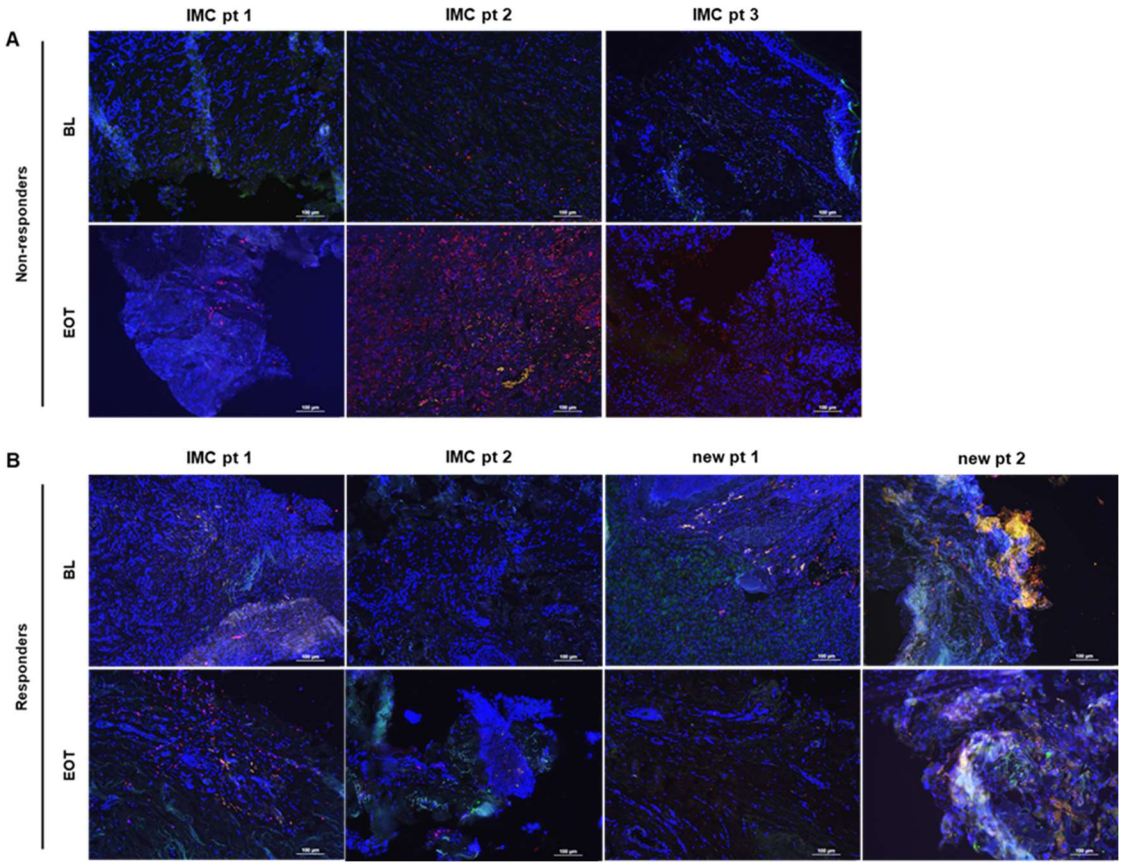

Figure 3-12. Immunofluorescent staining in RP2D patients.
Shown are 10X IMF staining for myeloperoxidase (red), arginase (green), and merged (yellow) from **(A)** three non-responder patients and **(B)** four responder patients. Scale bar represents 100 μm.

We observed that co-localized expression of MPO and arginase did not change in non-responders, whereas co-localized expression of MPO and arginase decreased in responders at EOT (**Fig. 3-12A and 3-12B**). These data support that the influx of neutrophils in responders may represent a shift from pro-tumor N2 neutrophils into anti-tumor N1 neutrophils.

3.4. Discussion

This phase 1/2 clinical study builds on robust published work and is the first-in-class clinical study of iNOS inhibition in cancer patients. Additionally, immuno-modulation of the tumor microenvironment and the potential mechanistic basis by which iNOS inhibition enhances chemotherapy response is described.

Previously, by isolating the subpopulation with chemo-resistant stem-like properties (*4, 26, 27*), we identified two putative candidate genes, *RPL39* and *MLF2,* which were associated with treatment resistance. In *RPL39* and *MLF2* knockdown experiments in TNBC PDXs, tumor shrinkage together with the reduction in lung metastases was observed (*4*). Through a series of bioinformatic analyses, iNOS signaling was determined to be the primary pathway common to both genes. Further analysis revealed that *RPL39* and/or *MLF2* overexpression and knockdown increased and decreased iNOS protein levels, respectively (*4*). iNOS has been described to be a mediator of metastasis in different cancer types (*28-30*) and elevated iNOS expression has been linked to poor survival in breast cancer (*31, 32*). We recently reported that increased iNOS expression correlates with poor survival and metastasis in TNBC patients (*8*). The pan-NOS inhibitor L-NMMA was evaluated in TNBC PDX preclinical studies (*8, 33*). We demonstrated the efficacy of L-NMMA in combination with chemotherapy in four PDX models. In all four models, the addition of L-NMMA significantly reduced tumor volume compared to docetaxel alone. The clinical study was designed based on these published studies.

In this study, the overall response rate was 45.8% for the whole cohort, with 16.7% achieving CR. In metastatic TNBC, the response rate of 15.4% and clinical benefit rate of 53.8% were noteworthy for heavily pretreated patients who had a median of five prior lines of chemotherapy. (*34, 35*) In the chemorefractory LABC cohort, the response rate was impressive at 81.8%, with 36.4% achieving CR. Of note, 27.3% of the anthracycline refractory LABC

patients achieved pCR at the surgery where the expected response based on historic published results is expected to be less than 5% (*36*).

The regimen was well tolerated and only 21% had grade ≥ 3 toxicity, with none of the ≥Grade 3 toxicity attributed to L-NMMA. The anticipated blood pressure elevation was manageable with the addition of oral amlodipine, in this regimen.

Imaging mass cytometry (IMC) is a highly multiplexed single-cell protein detection system. IMC technology can simultaneously interrogate 35 protein markers in a single 5-micron tissue section of formalin-fixed paraffin-embedded (FFPE) tissue while preserving tissue architecture and cellular morphology to uncover biomarker correlations and immune-cancer cell interactions. Our combined IMC and blood analysis data suggest that non-responders to L-NMMA and taxane may have a cumulative M2 macrophage signature. Firstly, our PBMC analysis of responders vs. non-responders by CyTOF showed a trend of increased circulating monocytes in non-responders (**Fig. 3-8A and 3-8B**). The CyTOF data consistently showed high expression of M2 macrophage markers CD163+ and PPARγ+ in circulating PBMCs from non-responder patients compared to inconsistent trends in responder patients during therapy (*37, 38*). As a correlate, we also observed increased circulating CD8s in responders compared to inconsistent CD8 changes in non-responders with therapy. Our data is suggestive that higher circulating M2 macrophages in non-responders may repress cell-mediated immunity given that responders have higher circulating CD4 and CD8 populations with lower circulating CD163+ and PPARγ+ cells. Moreover, our IMC results further showed that non-responder patients had a significant increase in intra-tumor M2 macrophages at end of therapy (**Fig. 3-8C, and 3-8D**). In addition, we found IL-10 expression was significantly higher in non-responders (**Fig. 3-6C**). IL-10 is an immunosuppressive cytokine produced by M2 macrophages (*39, 40*) and has a high correlation with poor prognosis in various cancers (*41-43*). Furthermore, non-responders had

significantly higher levels of IL-6 (**Fig. 3-6C**) and IL-6 can promote induction of M2 macrophages (*44-46*). Furthermore, IL-6 is an inducer of STAT3 signaling and the IL-6/STAT3 axis is a well-established pathway for cancer metastasis, proliferation, and stem cell induction (*47-49*). There is growing evidence that IL-1A may drive IL-6 induction in breast cancer (*50*). Similarly, tumor-derived GM-CSF modulates the tumor microenvironment to favor pro-tumor immunity (*51-53*). The significance of elevated IL-1A, IL-6, IL-10, and GM-CSF in non-responders may potentially serve as a predictor to L-NMMA efficacy and have biological context for poor outcome.

Tumor-associated neutrophils (TANs) have been reported to have a strong correlation with poor patient outcomes in various cancers (*24*). Our previous studies have demonstrated that TNBCs utilize iNOS to resist chemotherapy (*8, 33*). Given that neutrophils express iNOS constitutively (*54*), we hypothesized that L-NMMA may target TANs in the microenvironment of chemorefractory TNBC patients. Surprisingly, we noted that responders had increased tumor neutrophils (**Fig. 3-8C**) at end of treatment. There is growing literature that neutrophils may undergo differential polarization into an N1 anti-tumor or N2 pro-tumor state in murine models (*55*), which may be distinct from humans (*23*). However, by using arginase as a marker of N2 neutrophils (*22, 25*), we observed decreased arginase expression at EOT in responders (**Fig. 3-12B**), suggesting that responders to L-NMMA therapy may have reprogrammed N1 neutrophils to assist in effective anti-tumor immunity.

L-NMMA in combination with taxanes was well tolerated with a notable response rate in heavily pretreated metastatic TNBC patients who were refractory to multiple lines of chemotherapy and in chemorefractory locally advanced TNBC patients leading to unexpected pathologic complete responses. Immunomodulation of the tumor microenvironment with increased neutrophils at the tumor site in responders, while having M2 macrophages at end of

therapy in non-responders were observed. This combination warrants further investigation in larger studies along with correlative biomarker evaluation.

3.5. Materials and Methods

3.5.1. Patients

Female patients >18 years of age with pathologically determined chemorefractory locally advanced TNBC or metastatic TNBC. TNBC is defined as estrogen receptor-negative and progesterone receptor-negative (<10% staining by immunohistochemistry (IHC) for estrogen and progesterone receptor) and HER2 negative (status as defined by the current American Society of Clinical Oncology and College of American Pathologists (*56*)) were eligible for the trial. The study was approved by the Institutional Review Board at the Houston Methodist Hospital and written informed consent was obtained from all patients before sample and data collection. The trial was registered at Clinicaltrials.gov (NCT02834403). All patients had an Eastern Cooperative Oncology Group (ECOG) performance status of ≤ 2 and a cardiac ejection fraction of ≥ 45%. Exclusion criteria included history of poorly controlled hypertension (defined as systolic BP> 150 mm Hg at baseline), use of docetaxel within the past 12 months, New York Heart Association class III or greater cardiac disease, history of myocardial infarction, stroke, ventricular arrhythmia or symptomatic conduction abnormality within the past 12 months, history of congenital QT prolongation or absolute correct QT interval of >480 msec and symptomatic central nervous system metastases.

3.5.2. Clinical Study Design

The Phase 1 portion of the study (**Fig. 3-1**) was designed to investigate the combination at two dose levels of docetaxel (75 and 100 mg/m^2) and seven dose levels of L-NMMA (5, 7.5,

10, 12.5, 15, 17.5, and 20 mg/kg). The starting dose for L-NMMA was at 7.5 mg/kg and docetaxel at 75 mg/m^2. L-NMMA was given Day 1-5 IV every three weeks and docetaxel was given IV after L-NMMA on Day 1 every 3 weeks; therefore, one cycle is defined as each 3-week regimen. A standard Bayesian model averaging continual reassessment method (CRM) approach was used to determine recommended phase 2 L-NMMA dose (RP2D). In the phase 2 portion of the study, patients were treated with the L-NMMA combination at the RP2D and taxane at standard chemotherapy doses. Patients treated at the RP2D in the phase I portion of the study were included in the phase 2 portion of the trial. Patients received a maximum of six (21-day) cycles of the L-NMMA combination. L-NMMA was administered as a 2-hour intravenous (IV) infusion on Days 1-5 of each cycle. To prevent L-NMMA-induced hypertension, amlodipine (10 mg) was administered for 6 days at each cycle, starting 24 hours before the first dose of L-NMMA. Enteric-coated low-dose aspirin (81 mg) was orally administered once daily during the six 21-day cycles, as thromboembolic prophylaxis. The phase 2 portion of the trial was conducted using Simon's optimal two-stage design. Patients with amenable tumors had biopsies performed at two time points, at baseline and end of treatment. Patients during study enrollment were recommended to follow a low nitrate diet. Blood pressure was monitored on the day of treatment for each dose of L-NMMA. Computed tomography (CT) scan of the chest, abdomen, and pelvis was performed at baseline and the end of Cycles 2, 4, and 6. The response was assessed using the RECIST 1.1. Patients with chemorefractory locally advanced breast cancer had ultrasound measurements at the end of Cycles 2, 4, or 6 (chemorefractory locally advanced breast cancer patients received 4 or 6 cycles). Pathologic responses, in particular, pathologic complete response defined as no residual disease in the breast, were recorded. Toxicities in the phase 2 trial were described as per Common Terminology Criteria for Adverse Events (CTCAE) v4.03. All radiological assessments (NG, LV) and all surgical pathology (MS) were independently assessed and confirmed.

3.5.3. Pharmacodynamics and pharmacokinetics assays

Serum was analyzed for the effect of L-NMMA on lowering systemic iNOS by measuring nitric oxide metabolites, namely serum nitrites, and nitrates. In brief, serum samples were purified through 10 kDa molecular weight Ultra-0.5 Centrifugal Filters (Amicon, Millipore) to remove hemoglobin and the purified samples were then assayed for circulating nitrites and nitrates using a commercially available fluorometric assay (Cayman Chemicals #780051). To measure the clearance of docetaxel and L-NMMA, pharmacokinetic assays were done described by previously validated methods (*57-59*).

3.5.4. Circulating cytokines assays

Systemic levels of cytokines and other soluble immune mediators were determined by Luminex multiplex cytokine analysis (Human Cytokine/Chemokine Magnetic Bead Panel, Millipore HCYTMAG-60K-PX41) for 38 analytes: epidermal growth factor (EGF), fibroblast growth factor basic (FGF-2), eotaxin, transforming growth factor-alpha (TGF-a), granulocyte-colony stimulating factor (G-CSF), FMS-like tyrosine kinase 3 ligand (FIt-3L), granulocyte-macrophage colony-stimulating factor (GM-CSF), fractalkine, interferon-a2 (IFN-a2), interferon-γ (IFN-γ), GRO, CXCL10, macrophage-derived chemokine (MDC), soluble CD40L, IL-1a, IL-1β, IL-1 receptor antagonist, IL-2, IL-3, IL-4, IL-5, IL-6, IL-7, IL-8, IL-9, IL-10, IL-12p70, IL-12p40, IL-13, IL-15, IL-17, monocyte chemoattractant protein-1 (MCP-1), MCP-3, macrophage inflammatory protein (MIP)-1α, MIP-1β, TNF-α, TNF-b, and VEGF. All patient serum samples were assayed according to the manufacturer's instructions, and plates were analyzed by Millipore's Luminex 200.

3.5.5. CyTOF

PBMCs were isolated from peripheral blood and frozen until all time points were collected. On the day of CyTOF staining, PBMC from the same patients at different time points were thawed and recovered. Single cell suspension was stained with metal-tag viability dye for 5min and wash with Cell staining buffer (Fluidigm), followed by staining of surface markers and intracellular markers separately, according to the Foxp3 staining kit (eBioscience). Cells were then stained with Cell ID Intercalator Ir (Fluidigm) at 4C overnight. The next day, cells were washed and prepared for acquisition with Helios (Fluidigm). The data was analyzed by Cytofbank. Briefly, data were normalized, gated out beads and dead cells, and gated on singlet and CD45+ cell population, which was selected to perform a tSNE analysis. The tSNE plot is gated according to display the cell populations with different colors. The ratio of the different cell populations within CD45+ cells was quantified by Cytobank. Log2 fold change was calculated of Day 17 vs. Day 1, and Day 38 vs. Day 1 for different cell populations (percentage of CD45+) and plotted by heatmap. To plot tSNE, we used the Barnes-Hut t-SNE implementation in Rtsne package. Data were 99th-percentile normalized before the analysis, and we used the default t-SNE parameters (initial dimensions,110; perplexity,30; theta,0.5). The random seed is recorded for reproducibility.

3.5.6. Tissue biopsies- Imaging mass cytometry

The Hyperion Imaging System (Fluidigm), CyTOF technology together with imaging capability was used on 12 biopsy samples from 6 patients (3 responders, and 3 with progressive disease) recruited to the phase 2 study to determine the profile of circulating suppressor and effector immunocytes. The 35 markers are listed under **Table 3-4**. A detailed description of Imaging Mass Cytometry (IMC) was done as previously described (*60*).

Table 3-4. List of IMC marker antibodies.

GzmB
CD20
CD3
CD206
CD4
CD8a
a-SMA
Pan-CK
CD31
PD-L1
PD-1
CD163
CD80
Foxp3
pSTAT1
CD45
E-cadherin
CD68
CD14
RORgt
HER2
pSTAT3
CD15
p-S6
pNF-kB
Ki67
PR
Collagen
CD1c
ER
Gata3
Tbet
HLA-DR
CD86
CD56

3.5.7. Immunohistochemistry

Baseline (BL) and end of therapy (EOT) tissue from seven RP2D patients (three non-responders and four responders) were evaluated by IHC for myeloperoxidase (MPO). In brief, 5 μm sections of FFPE tissue were prepared on slides. After xylene deparaffinization and ethanol rehydration, antigen retrieval (Tris-Cl, pH 9.0) was performed followed by hydrogen peroxide

fixation. After blocking with Avidin/Biotin Blocking kit (Vector Labs), the primary antibody for MPO (diluted 1:200) was incubated for 1 hour at room temperature. Next, HRP conjugated anti-rabbit secondary antibody (Dako) was incubated for 30 minutes at room temperature. Then chromogens were produced by DAB reaction (Dako). After counterstaining with hematoxylin, slides were mounted and imaged under bright field microscopy. MPO antibody was from ThermoFisher Scientific (cat# PA5-16672).

3.5.8. Immunofluorescence

BL and EOT tissue from the same seven patients as MPO IHC went through the same deparaffinization and antigen retrieval as previously described with no hydrogen peroxide fixation. Followed by 1 hour blocking with 10% normal goat serum at room temperature, primary antibodies (Arginase 1:50 and MPO 1:200) were dually incubated for 1 hour at room temperature. Next, secondary antibodies (Alexa 488 anti-mouse and Alexa 594 anti-rabbit, both 1:200) were dually incubated for 1 hour at room temperature. Slides were mounted with Vectashield (Vector Labs H-1200) and sealed with coverslips. Images were acquired within one week. Arginase antibody was from Abcam (cat# ab212522). Alexa anti-mouse 488 (cat# A-11001) and Alexa anti-rabbit 594 (cat# A-11012) are both from ThermoFisher Scientific.

3.5.9. Statistical analysis

The following statistical analyses were performed for each respective assay.

Pharmacodynamics: Friedman's test for a randomized block design based on the intra-patient ranked data was performed to determine significant effect due to day measurements of total nitrates/nitrites measured in sera.

Luminex heat map: For normalization of each cytokine, pg/ml data was standardized to set the highest measured value as 100 by a constant. Next, each unique constant was multiplied to

respective cytokines to normalize the expression scale from zero to 100. Next, paired t-test was performed comparing Days 2 or 5 to respective Day 1 for each cycle. Finally, normalized data of 21 cytokines with significant changes on Days 2 or 5 were graphed by heat map.

Luminex PCA: For an individual day, PCA was conducted on the cytokines data for all patients across both responders and non-responders. The top 3 principal components which account for the maximum variance in the data are plotted for each patient in one figure. In the 3-dimensional PCA space, Permutational multivariate analysis of variance (PERMANOVA, number of permutations=9999) was used to test the null hypothesis that the centroids and dispersion of the two groups of patients (responders and non-responders) are equivalent for all groups. A rejection of the null hypothesis means that either the centroids and/or the distribution are different between the groups.

Luminex significance by group effect: Significance was determined with pairwise analysis by Wilcoxon Ranked-Sum test.

IMC significance by group effect: Two-way ANOVA was performed for three responders vs. three non-responders comparing BL versus EOT tissues.

Significance of blood pressure change: Significant changes in systolic and diastolic blood pressure comparing baseline to after 2 cycles of therapy were determined by paired t-test and signed-rank.

3.6. References

1. K. R. Bauer, M. Brown, R. D. Cress, C. A. Parise, V. Caggiano, Descriptive analysis of estrogen receptor (ER)-negative, progesterone receptor (PR)-negative, and HER2-negative invasive breast cancer, the so-called triple-negative phenotype: a population-based study from the California cancer Registry. *Cancer* **109**, 1721-1728 (2007).

2. R. Dent, M. Trudeau, K. I. Pritchard, W. M. Hanna, H. K. Kahn, C. A. Sawka, L. A. Lickley, E. Rawlinson, P. Sun, S. A. Narod, Triple-negative breast cancer: clinical features and patterns of recurrence. *Clinical cancer research* **13**, 4429-4434 (2007).

3. C. J. Creighton, X. Li, M. Landis, J. M. Dixon, V. M. Neumeister, A. Sjolund, D. L. Rimm, H. Wong, A. Rodriguez, J. I. Herschkowitz, Residual breast cancers after conventional therapy display mesenchymal as well as tumor-initiating features. *Proceedings of the National Academy of Sciences* **106**, 13820-13825 (2009).

4. B. Dave, S. Granados-Principal, R. Zhu, S. Benz, S. Rabizadeh, P. Soon-Shiong, K. D. Yu, Z. Shao, X. Li, M. Gilcrease, Z. Lai, Y. Chen, T. H. Huang, H. Shen, X. Liu, M. Ferrari, M. Zhan, S. T. Wong, M. Kumaraswami, V. Mittal, X. Chen, S. S. Gross, J. C. Chang, Targeting RPL39 and MLF2 reduces tumor initiation and metastasis in breast cancer by inhibiting nitric oxide synthase signaling. *Proc Natl Acad Sci U S A* **111**, 8838-8843 (2014).

5. C. N. Chen, F. J. Hsieh, Y. M. Cheng, K. J. Chang, P. H. Lee, Expression of inducible nitric oxide synthase and cyclooxygenase-2 in angiogenesis and clinical outcome of human gastric cancer. *Journal of surgical oncology* **94**, 226-233 (2006).

6. P. Garrido, A. Shalaby, E. M. Walsh, N. Keane, M. Webber, M. M. Keane, F. J. Sullivan, M. J. Kerin, G. Callagy, A. E. Ryan, Impact of inducible nitric oxide synthase (iNOS) expression on triple negative breast cancer outcome and activation of EGFR and ERK signaling pathways. *Oncotarget* **8**, 80568 (2017).

7. E. Lopez-Rivera, P. Jayaraman, F. Parikh, M. A. Davies, S. Ekmekcioglu, S. Izadmehr, D. R. Milton, J. E. Chipuk, E. A. Grimm, Y. Estrada, Inducible nitric oxide synthase

drives mTOR pathway activation and proliferation of human melanoma by reversible nitrosylation of TSC2. *Cancer research* **74**, 1067-1078 (2014).

8. S. Granados-Principal, Y. Liu, M. L. Guevara, E. Blanco, D. S. Choi, W. Qian, T. Patel, A. A. Rodriguez, J. Cusimano, H. L. Weiss, H. Zhao, M. D. Landis, B. Dave, S. S. Gross, J. C. Chang, Inhibition of iNOS as a novel effective targeted therapy against triple-negative breast cancer. *Breast Cancer Res* **17**, 25 (2015).

9. J. H. Alexander, H. R. Reynolds, A. L. Stebbins, V. Dzavik, R. A. Harrington, F. Van de Werf, J. S. Hochman, T. investigators, Effect of tilarginine acetate in patients with acute myocardial infarction and cardiogenic shock: the TRIUMPH randomized controlled trial. *Jama* **297**, 1657-1666 (2007).

10. M. Kelm, Nitric oxide metabolism and breakdown. *Biochimica et Biophysica Acta (BBA)-Bioenergetics* **1411**, 273-289 (1999).

11. H. Kenmotsu, Y. Tanigawara, Pharmacokinetics, dynamics and toxicity of docetaxel: why the Japanese dose differs from the Western dose. *Cancer Science* **106**, 497-504 (2015).

12. B. X. Mayer, C. Mensik, S. Krishnaswami, H. Derendorf, H. G. Eichler, L. Schmetterer, M. Wolzt, Pharmacokinetic-pharmacodynamic profile of systemic nitric oxide-synthase inhibition with L-NMMA in humans. *British journal of clinical pharmacology* **47**, 539-544 (1999).

13. T. Eyob, T. Ng, R. Chan, A. Chan, Impact of chemotherapy on cancer-related fatigue and cytokines in 1312 patients: a systematic review of quantitative studies. *Current Opinion in Supportive and Palliative Care* **10**, 165-179 (2016).

14. K. Mahon, H.-M. Lin, L. Castillo, B. Y. Lee, M. Lee-Ng, M. D. Chatfield, K. Chiam, S. N. Breit, D. A. Brown, M. P. Molloy, Cytokine profiling of docetaxel-resistant castration-resistant prostate cancer. *British journal of cancer* **112**, 1340-1348 (2015).

15. P. Mathew, S. Wen, S. Morita, P. F. Thall, Placental growth factor and soluble c-kit receptor dynamics characterize the cytokine signature of imatinib in prostate cancer and bone metastases. *Journal of Interferon & Cytokine Research* **31**, 539-544 (2011).

16. L. Pusztai, T. R. Mendoza, J. M. Reuben, M. M. Martinez, J. S. Willey, J. Lara, A. Syed, H. A. Fritsche, E. Bruera, D. Booser, Changes in plasma levels of inflammatory cytokines in response to paclitaxel chemotherapy. *Cytokine* **25**, 94-102 (2004).

17. F. Tas, S. Karabulut, M. Serilmez, M. Karabulut, D. Duranyildiz, Elevated circulating monocyte chemoattractant protein 1 (MCP-1/CCL-2) level may be an unfavorable predictive factor to platinum-and taxane-based combination chemotherapy in patients with gastric cancer. *Cancer chemotherapy and pharmacology* **77**, 127-131 (2016).

18. F. Nakayama, S. Nishihara, H. Iwasaki, T. Kudo, R. Okubo, M. Kaneko, M. Nakamura, M. Karube, K. Sasaki, H. Narimatsu, CD15 expression in mature granulocytes is determined by α1, 3-fucosyltransferase IX, but in promyelocytes and monocytes by α1, 3-fucosyltransferase IV. *Journal of Biological Chemistry* **276**, 16100-16106 (2001).

19. C. Rosales, Neutrophil: a cell with many roles in inflammation or several cell types? *Frontiers in physiology* **9**, 113 (2018).

20. Y. Aratani, Myeloperoxidase: its role for host defense, inflammation, and neutrophil function. *Archives of biochemistry and biophysics* **640**, 47-52 (2018).

21. Z. G. Fridlender, J. Sun, S. Kim, V. Kapoor, G. Cheng, L. Ling, G. S. Worthen, S. M. Albelda, Polarization of tumor-associated neutrophil phenotype by TGF-beta: "N1" versus "N2" TAN. *Cancer Cell* **16**, 183-194 (2009).

22. M. A. Giese, L. E. Hind, A. Huttenlocher, Neutrophil plasticity in the tumor microenvironment. *Blood* **133**, 2159-2167 (2019).

23. M. T. Masucci, M. Minopoli, M. V. Carriero, Tumor Associated Neutrophils. Their Role in Tumorigenesis, Metastasis, Prognosis and Therapy. *Front Oncol* **9**, 1146 (2019).

24. M. E. Shaul, Z. G. Fridlender, Tumour-associated neutrophils in patients with cancer. *Nat Rev Clin Oncol* **16**, 601-620 (2019).

25. T. M. Grzywa, A. Sosnowska, P. Matryba, Z. Rydzynska, M. Jasinski, D. Nowis, J. Golab, Myeloid Cell-Derived Arginase in Cancer Immune Response. *Front Immunol* **11**, 938 (2020).

26. B. Dave, D. D. Gonzalez, Z. B. Liu, X. Li, H. Wong, S. Granados, N. E. Ezzedine, D. H. Sieglaff, J. E. Ensor, K. D. Miller, M. Radovich, A. KarinaEtrovic, S. S. Gross, O. Elemento, G. B. Mills, M. Z. Gilcrease, J. C. Chang, Role of RPL39 in Metaplastic Breast Cancer. *J Natl Cancer Inst* **109**, (2017).

27. Z. B. Liu, N. E. Ezzedine, A. K. Eterovic, J. E. Ensor, H. J. Huang, J. Albanell, D. S. Choi, A. Lluch, Y. Liu, F. Rojo, H. Wong, E. Martinez-Duenas, A. Guerrero-Zotano, Z. M. Shao, J. G. Darcourt, G. B. Mills, B. Dave, J. C. Chang, Detection of breast cancer stem cell gene mutations in circulating free DNA during the evolution of metastases. *Breast Cancer Res Treat* **178**, 251-261 (2019).

28. H. Cheng, L. Wang, M. Mollica, A. T. Re, S. Wu, L. Zuo, Nitric oxide in cancer metastasis. *Cancer Lett* **353**, 1-7 (2014).

29. J. Girouard, D. Belgorosky, J. Hamelin-Morrissette, V. Boulanger, E. D'Orio, D. Ramla, R. Perron, L. Charpentier, C. Van Themsche, A. M. Eijan, G. Berube, C. Reyes-Moreno, Molecular therapy with derivatives of amino benzoic acid inhibits tumor growth and metastasis in murine models of bladder cancer through inhibition of TNFalpha/NFKappaB and iNOS/NO pathways. *Biochem Pharmacol* **176**, 113778 (2020).

30. R. Wang, D. A. Geller, D. A. Wink, B. Cheng, T. R. Billiar, NO and hepatocellular cancer. *Br J Pharmacol* **177**, 5459-5466 (2020).

31. Z. Jin, W. Wang, N. Jiang, L. Zhang, Y. Li, X. Xu, S. Cai, L. Wei, X. Liu, G. Chen, Y. Zhou, C. Liu, Z. Li, F. Jin, B. Chen, Clinical Implications of iNOS Levels in Triple-Negative Breast Cancer Responding to Neoadjuvant Chemotherapy. *PLoS One* **10**, e0130286 (2015).

32. E. M. Walsh, M. M. Keane, D. A. Wink, G. Callagy, S. A. Glynn, Review of Triple Negative Breast Cancer and the Impact of Inducible Nitric Oxide Synthase on Tumor Biology and Patient Outcomes. *Crit Rev Oncog* **21**, 333-351 (2016).

33. D. Davila-Gonzalez, D. S. Choi, R. R. Rosato, S. M. Granados-Principal, J. G. Kuhn, W. F. Li, W. Qian, W. Chen, A. J. Kozielski, H. Wong, B. Dave, J. C. Chang, Pharmacological Inhibition of NOS Activates ASK1/JNK Pathway Augmenting Docetaxel-Mediated Apoptosis in Triple-Negative Breast Cancer. *Clin Cancer Res* **24**, 1152-1162 (2018).

34. J. Cortes, J. O'Shaughnessy, D. Loesch, J. L. Blum, L. T. Vahdat, K. Petrakova, P. Chollet, A. Manikas, V. Diéras, T. Delozier, Eribulin monotherapy versus treatment of physician's choice in patients with metastatic breast cancer (EMBRACE): a phase 3 open-label randomised study. *The Lancet* **377**, 914-923 (2011).

35. E. Thomas, J. Tabernero, M. Fornier, P. Conté, P. Fumoleau, A. Lluch, L. T. Vahdat, C. A. Bunnell, H. A. Burris, P. Viens, Phase II clinical trial of ixabepilone (BMS-247550), an epothilone B analog, in patients with taxane-resistant metastatic breast cancer. *Journal of Clinical Oncology* **25**, 3399-3406 (2007).

36. K. Anand, T. Patel, P. Niravath, A. Rodriguez, J. Darcourt, A. Belcheva, T. Boone, J. Ensor, J. Chang, Targeting mTOR and DNA repair pathways in residual triple negative breast cancer post neoadjuvant chemotherapy. *Sci Rep* **11**, 82 (2021).

37. J. M. Hu, K. Liu, J. H. Liu, X. L. Jiang, X. L. Wang, Y. Z. Chen, S. G. Li, H. Zou, L. J. Pang, C. X. Liu, X. B. Cui, L. Yang, J. Zhao, X. H. Shen, J. F. Jiang, W. H. Liang, X. L. Yuan, F. Li, CD163 as a marker of M2 macrophage, contribute to predicte aggressiveness and prognosis of Kazakh esophageal squamous cell carcinoma. *Oncotarget* **8**, 21526-21538 (2017).

38. Q. Yao, J. Liu, Z. Zhang, F. Li, C. Zhang, B. Lai, L. Xiao, N. Wang, Peroxisome proliferator-activated receptor gamma (PPARgamma) induces the gene expression of integrin alphaVbeta5 to promote macrophage M2 polarization. *J Biol Chem* **293**, 16572-16582 (2018).

39. L. Qi, H. Yu, Y. Zhang, D. Zhao, P. Lv, Y. Zhong, Y. Xu, IL-10 secreted by M2 macrophage promoted tumorigenesis through interaction with JAK2 in glioma. *Oncotarget* **7**, 71673 (2016).

40. A. Shapouri-Moghaddam, S. Mohammadian, H. Vazini, M. Taghadosi, S. A. Esmaeili, F. Mardani, B. Seifi, A. Mohammadi, J. T. Afshari, A. Sahebkar, Macrophage plasticity, polarization, and function in health and disease. *Journal of cellular physiology* **233**, 6425-6440 (2018).

41. L. Feng, Q. Qi, P. Wang, H. Chen, Z. Chen, Z. Meng, L. Liu, Serum levels of IL-6, IL-8, and IL-10 are indicators of prognosis in pancreatic cancer. *Journal of International Medical Research* **46**, 5228-5236 (2018).

42. S. K. Mittal, P. A. Roche, Suppression of antigen presentation by IL-10. *Current opinion in immunology* **34**, 22-27 (2015).

43. S. Zhao, D. Wu, P. Wu, Z. Wang, J. Huang, Serum IL-10 predicts worse outcome in cancer patients: a meta-analysis. *PloS one* **10**, e0139598 (2015).

44. J. Braune, U. Weyer, C. Hobusch, J. Mauer, J. C. Bruning, I. Bechmann, M. Gericke, IL-6 Regulates M2 Polarization and Local Proliferation of Adipose Tissue Macrophages in Obesity. *J Immunol* **198**, 2927-2934 (2017).

45. D. Duluc, Y. Delneste, F. Tan, M. P. Moles, L. Grimaud, J. Lenoir, L. Preisser, I. Anegon, L. Catala, N. Ifrah, P. Descamps, E. Gamelin, H. Gascan, M. Hebbar, P. Jeannin, Tumor-associated leukemia inhibitory factor and IL-6 skew monocyte differentiation into tumor-associated macrophage-like cells. *Blood* **110**, 4319-4330 (2007).

46. Q. Wang, Z. He, M. Huang, T. Liu, Y. Wang, H. Xu, H. Duan, P. Ma, L. Zhang, S. S. Zamvil, J. Hidalgo, Z. Zhang, D. M. O'Rourke, N. Dahmane, S. Brem, Y. Mou, Y.

Gong, Y. Fan, Vascular niche IL-6 induces alternative macrophage activation in glioblastoma through HIF-2alpha. *Nat Commun* **9**, 559 (2018).

47. Z. C. Hartman, G. M. Poage, P. den Hollander, A. Tsimelzon, J. Hill, N. Panupinthu, Y. Zhang, A. Mazumdar, S. G. Hilsenbeck, G. B. Mills, P. H. Brown, Growth of triple-negative breast cancer cells relies upon coordinate autocrine expression of the proinflammatory cytokines IL-6 and IL-8. *Cancer Res* **73**, 3470-3480 (2013).

48. D. E. Johnson, R. A. O'Keefe, J. R. Grandis, Targeting the IL-6/JAK/STAT3 signalling axis in cancer. *Nat Rev Clin Oncol* **15**, 234-248 (2018).

49. N. Kumari, B. S. Dwarakanath, A. Das, A. N. Bhatt, Role of interleukin-6 in cancer progression and therapeutic resistance. *Tumour Biol* **37**, 11553-11572 (2016).

50. S. Liu, J. S. Lee, C. Jie, M. H. Park, Y. Iwakura, Y. Patel, M. Soni, D. Reisman, H. Chen, HER2 Overexpression Triggers an IL1alpha Proinflammatory Circuit to Drive Tumorigenesis and Promote Chemotherapy Resistance. *Cancer Res* **78**, 2040-2051 (2018).

51. S. Khanna, S. Graef, F. Mussai, A. Thomas, N. Wali, B. G. Yenidunya, C. Yuan, B. Morrow, J. Zhang, F. Korangy, Tumor-derived GM-CSF promotes granulocyte immunosuppression in mesothelioma patients. *Clinical Cancer Research* **24**, 2859-2872 (2018).

52. T.-t. Wang, Y.-l. Zhao, L.-s. Peng, N. Chen, W. Chen, Y.-p. Lv, F.-y. Mao, J.-y. Zhang, P. Cheng, Y.-s. Teng, Tumour-activated neutrophils in gastric cancer foster immune suppression and disease progression through GM-CSF-PD-L1 pathway. *Gut* **66**, 1900-1911 (2017).

53. W.-L. Yan, K.-Y. Shen, C.-Y. Tien, Y.-A. Chen, S.-J. Liu, Recent progress in GM-CSF-based cancer immunotherapy. *Immunotherapy* **9**, 347-360 (2017).

54. S. Sadaf, A. K. Singh, D. Awasthi, S. Nagarkoti, A. K. Agrahari, R. N. Srivastava, K. Jagavelu, S. Kumar, M. K. Barthwal, M. Dikshit, Augmentation of iNOS expression in myeloid progenitor cells expedites neutrophil differentiation. *J Leukoc Biol* **106**, 397-412 (2019).

55. M. Ohms, S. Moller, T. Laskay, An Attempt to Polarize Human Neutrophils Toward N1 and N2 Phenotypes in vitro. *Front Immunol* **11**, 532 (2020).

56. A. C. Wolff, M. E. H. Hammond, K. H. Allison, B. E. Harvey, P. B. Mangu, J. M. S. Bartlett, M. Bilous, I. O. Ellis, P. Fitzgibbons, W. Hanna, R. B. Jenkins, M. F. Press, P. A. Spears, G. H. Vance, G. Viale, L. M. McShane, M. Dowsett, Human Epidermal Growth Factor Receptor 2 Testing in Breast Cancer: American Society of Clinical Oncology/College of American Pathologists Clinical Practice Guideline Focused Update. *Arch Pathol Lab Med* **142**, 1364-1382 (2018).

57. O. Bilgic, H. C. Altinyazar, H. Baran, A. Unlu, Serum homocysteine, asymmetric dimethyl arginine (ADMA) and other arginine-NO pathway metabolite levels in patients with psoriasis. *Arch Dermatol Res* **307**, 439-444 (2015).

58. I. M. Di Gangi, L. Chiandetti, A. Gucciardi, V. Moret, M. Naturale, G. Giordano, Simultaneous quantitative determination of N(G),N(G)-dimethyl-L-arginine or asymmetric dimethylarginine and related pathway's metabolites in biological fluids by ultrahigh-performance liquid chromatography/electrospray ionization-tandem mass spectrometry. *Anal Chim Acta* **677**, 140-148 (2010).

59. K. A. Mortier, V. Renard, A. G. Verstraete, A. Van Gussem, S. Van Belle, W. E. Lambert, Development and validation of a liquid chromatography-tandem mass spectrometry assay for the quantification of docetaxel and paclitaxel in human plasma and oral fluid. *Anal Chem* **77**, 4677-4683 (2005).

60. H. C. Liu, D. I. Viswanath, F. Pesaresi, Y. Xu, L. Zhang, N. Di Trani, J. Paez-Mayorga, N. Hernandez, Y. Wang, D. R. Erm, J. Ho, A. Susnjar, X. Liu, S. Demaria, S. H. Chen, B. S. Teh, E. B. Butler, C. Y. Xuan Chua, A. Grattoni, Potentiating Antitumor Efficacy Through Radiation and Sustained Intratumoral Delivery of Anti-CD40 and Anti-PDL1. *Int J Radiat Oncol Biol Phys*, (2020).

4. CONCLUSIONS

4.1. Pre-clinical and clinical merits of inhibiting inflammatory mediators in treatment of TNBC

In chapters 2 and 3, we highlighted the pre-clinical and clinical therapeutic merits in treatment of TNBC with tocilizumab and L-NMMA, respectively. Neither anti-inflammatory agents are currently FDA approved in the management of breast cancer, however we provide evidence for additional follow-up studies in large cohort clinical trial studies for potential applications as targeted therapy options for TNBC patients. To the best of our knowledge, there have not yet been any clinical trials investigating the efficacy of using anti-IL-6 targeted therapies in breast cancer. There are however additional pre-clinical studies that have investigated the efficacy of tocilizumab against TNBC. The first study found that tocilizumab in combination with Notch signaling inhibition led to suppression of tumor growth in vivo (*1*). The second study found that tocilizumab decreased the potential induction of breast cancer stem cells (*2*). Furthermore, this study found that tocilizumab treatment promoted anti-tumor M1 macrophage polarization over the pro-tumor M2 macrophage. And furthermore, one study found that tocilizumab synergized with cisplatin therapy in targeting TNBC cell lines (*3*). As an extension to these published studies, we identify a specific cohort of TNBCs highlighted by active MAPK pathway which may be ideal targets for tocilizumab therapy. In chapter 3, we report our findings of the first study reporting the safety and efficacy of iNOS inhibition therapy for TNBC patients. Although no other cancer clinical trials have investigated the efficacy of L-NMMA, there is growing literature evidence that iNOS signaling is utilized by a variety of cancer pathologies (*4, 5*). Given our results that L-NMMA is safe, there may be rationale to

utilize this anti-inflammatory agent in other cancer pathologies that also utilize iNOS as a mechanism for tumor-persistence.

4.2. Rationale for investigating tocilizumab with chemotherapy in TNBC

In chapter 2, we found that the MAPK pathway induction of IL-1Awas the main upstream contributor for exacerbated autocrine IL-6 production in response to chemotherapy. Although we did not find any evidence that MAPK pathway contributed to regulating iNOS in TNBCs, there are additional pathways that can promote iNOS in the TNBC microenvironment (*6*). In order to further rationalize the potential application of tocilizumab for TNBC patients, we re-analyzed the phase Ib/II clinical trial from Experiment 2 with IL-6 expression as a parameter of interest (**Fig. 4-1**).

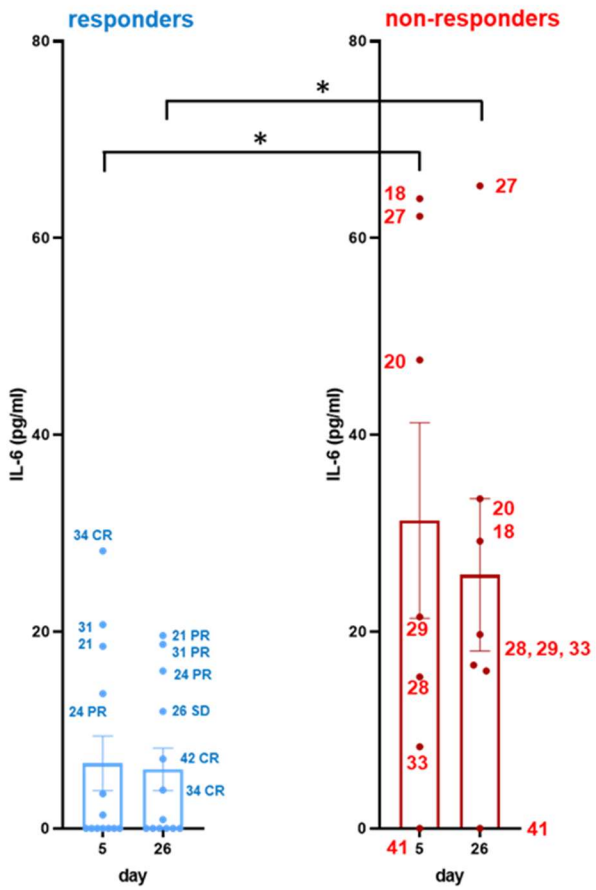

Figure 4-1. L-NMMA patients IL-6 levels comparing responders vs non-responders.

20 patients' sera from indicated time points were analyzed by Luminex for 38 circulating cytokines/chemokines. Shown are the significant differential expression of IL-6 between responders (13) versus non-responders (7). Significance was determined with pairwise analysis by Wilcoxon Ranked-Sum test. * $p < 0.05$.

In chapter 3, we previously established there was differential upregulation of IL-6 comparing the two cohorts on day 5 of both cycles. It is noteworthy that of non-responders to L-NMMA therapy, the same six patients (85.7%, 6/7) maintained detectable levels of circulating IL-6 during the first two cycles of therapy. And only 1/7 non-responder patients had no

detectable levels of IL-6. In contrast, responder patients either had consistent low to no detectable levels of IL-6 and in one case, a stark decrease of IL-6 during the progression of L-NMMA therapy (patient 34, complete responder).

In order to evaluate any prognostic significance of IL-6, we re-analyzed the ORR of the patients with expression level of IL-6 as the parameter of interest (**Fig. 4-2**).

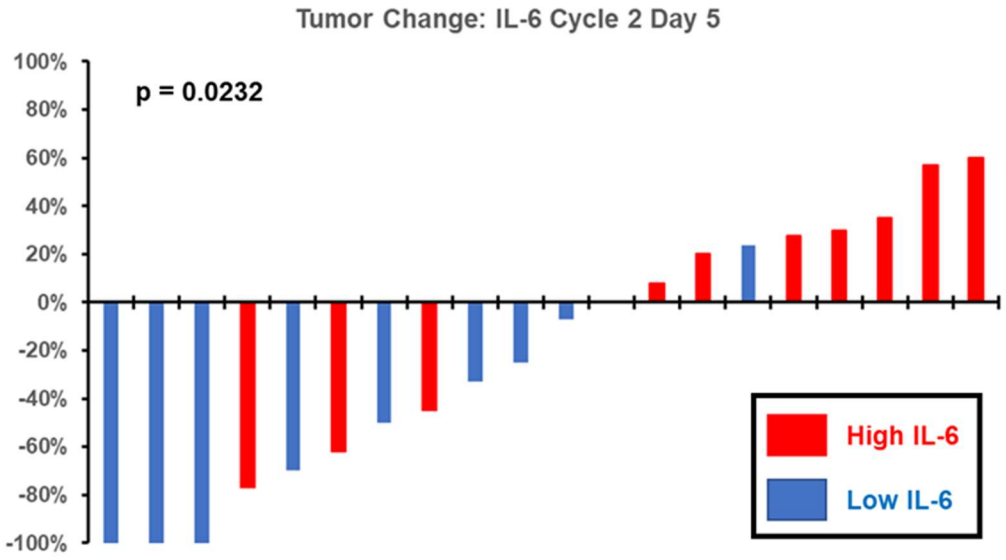

Figure 4-2. L-NMMA patients tumor change based on IL-6 expression.
Shown are tumor changes from the same 20 L-NMMA RP2D patients analyzed by Luminex from experiment 2 (Figure 4) with group assignment based on circulating IL-6 levels during cycle 2 day 5 of therapy. Patients with > 10 pg/ml of IL-6 were grouped as High IL-6 and patients with < 10 pg/ml of IL-6 were grouped as Low IL-6. Wilcoxon rank-sum test was performed to determine percent change between the two cohorts.

The two cohorts of patients comparing high IL-6 patients to low IL-6 patients were analyzed to determine whether the percent change of tumor volume differed based on IL-6 expression during cycle 2 day 5. We determined that the results were significant ($p < 0.0.5$) and that IL-6 expression may correlate with tumor decrease and efficacy to L-NMMA therapy in

TNBC patients. These results are encouraging and may potentially provide non-responders to L-NMMA therapy another inflammatory mediator targeting option with the inclusion of tocilizumab therapy.

4.3. Limitations

The chief limitation of chapter 2 was the absence of immune cells for in vivo efficacy of tocilizumab. As IL-6 is an immune mediator, it has a multi-faceted role in regulating immune cells. However, this limitation was difficult to overcome in chapter 2 due to lack of knowledge on the MSL vs BL1 subtype of murine TNBC cell lines which made syngeneic models problematic. However, our results from chapter 2 still provide clear evidence that MAPK active tumor cells produce autocrine IL-6 as a chemo-resistance mechanism and tocilizumab neutralizes this pathway. Given that tocilizumab will neutralize IL-6R activity, it will not necessarily matter whether there are additional cells in the tumor microenvironment which also produce paracrine IL-6 for tumor cells. Furthermore, there is evidence that tocilizumab therapy will promote skewing of anti-tumor M1 macrophages which is in alignment with previous studies indicating IL-6 is a M2 macrophage polarizing cytokine (*7, 8*). Therefore, this may indicate that tocilizumab will have a twofold effect by preventing M2 macrophage induction and neutralizing IL-6 mediated resistance pathways on TNBCs.

4.4. Translation of tocilizumab to patient therapy

Although **Figures 4-1 and 4-2** highlight the potential combination of chemotherapy with tocilizumab and L-NMMA for TNBC patients, the lab will need to investigate the benefit of tocilizumab and chemotherapy regimen first (as done with L-NMMA in chapter 3). Although previous anti-IL-6 biologic therapy trials against various other cancers failed to provide benefit, we hypothesize in our proposed clinical trial rationale that not all TNBC patients will have IL-6 dependent tumors for chemo-resistance. Rather, the objective will be to evaluate whether

patients with evidence of either MAPK active tumors or rising levels of IL-6 during chemotherapy are ideal candidates to tocilizumab therapy. If confirmed that tocilizumab provides efficacy for TNBC patients with MAPK active tumors or persistent circulating levels of IL-6, we may then one day evaluate the relevance of combining tocilizumab with L-NMMA.

4.5. References

1. D. Wang, J. Xu, B. Liu, X. He, L. Zhou, X. Hu, F. Qiao, A. Zhang, X. Xu, H. Zhang, M. S. Wicha, L. Zhang, Z. M. Shao, S. Liu, IL6 blockade potentiates the anti-tumor effects of gamma-secretase inhibitors in Notch3-expressing breast cancer. *Cell Death Differ* **25**, 330-339 (2018).
2. Y. S. Weng, H. Y. Tseng, Y. A. Chen, P. C. Shen, A. T. Al Haq, L. M. Chen, Y. C. Tung, H. L. Hsu, MCT-1/miR-34a/IL-6/IL-6R signaling axis promotes EMT progression, cancer stemness and M2 macrophage polarization in triple-negative breast cancer. *Mol Cancer* **18**, 42 (2019).
3. N. N. Alraouji, F. H. Al-Mohanna, H. Ghebeh, M. Arafah, R. Almeer, T. Al-Tweigeri, A. Aboussekhra, Tocilizumab potentiates cisplatin cytotoxicity and targets cancer stem cells in triple-negative breast cancer. *Mol Carcinog* **59**, 1041-1051 (2020).
4. C. N. Chen, F. J. Hsieh, Y. M. Cheng, K. J. Chang, P. H. Lee, Expression of inducible nitric oxide synthase and cyclooxygenase-2 in angiogenesis and clinical outcome of human gastric cancer. *J Surg Oncol* **94**, 226-233 (2006).
5. E. Lopez-Rivera, P. Jayaraman, F. Parikh, M. A. Davies, S. Ekmekcioglu, S. Izadmehr, D. R. Milton, J. E. Chipuk, E. A. Grimm, Y. Estrada, J. Aguirre-Ghiso, A. G. Sikora, Inducible nitric oxide synthase drives mTOR pathway activation and proliferation of human melanoma by reversible nitrosylation of TSC2. *Cancer Res* **74**, 1067-1078 (2014).

6. D. Basudhar, S. A. Glynn, M. Greer, V. Somasundaram, J. H. No, D. A. Scheiblin, P. Garrido, W. F. Heinz, A. E. Ryan, J. M. Weiss, R. Y. S. Cheng, L. A. Ridnour, S. J. Lockett, D. W. McVicar, S. Ambs, D. A. Wink, Coexpression of NOS2 and COX2 accelerates tumor growth and reduces survival in estrogen receptor-negative breast cancer. *Proc Natl Acad Sci U S A* **114**, 13030-13035 (2017).

7. D. Duluc, Y. Delneste, F. Tan, M. P. Moles, L. Grimaud, J. Lenoir, L. Preisser, I. Anegon, L. Catala, N. Ifrah, P. Descamps, E. Gamelin, H. Gascan, M. Hebbar, P. Jeannin, Tumor-associated leukemia inhibitory factor and IL-6 skew monocyte differentiation into tumor-associated macrophage-like cells. *Blood* **110**, 4319-4330 (2007).

8. Q. Wang, Z. He, M. Huang, T. Liu, Y. Wang, H. Xu, H. Duan, P. Ma, L. Zhang, S. S. Zamvil, J. Hidalgo, Z. Zhang, D. M. O'Rourke, N. Dahmane, S. Brem, Y. Mou, Y. Gong, Y. Fan, Vascular niche IL-6 induces alternative macrophage activation in glioblastoma through HIF-2alpha. *Nat Commun* **9**, 559 (2018).